

DESIGN, DEVELOPMENT AND EVALUATION OF TRACTOR OPERATED SPADING MACHINE

Dissertation

**Submitted to the Punjab Agricultural University
in partial fulfillment of the requirements
for the degree of**

**DOCTOR OF PHILOSOPHY
in
FARM MACHINERY & POWER ENGINEERING
(Minor Subject: Computer Science & Engineering)**

By

**Nitin Karwasra
(L-2014-AE-134-D)**

**Department of Farm Machinery & Power Engineering
College of Agricultural Engineering & Technology
© PUNJAB AGRICULTURAL UNIVERSITY
LUDHIANA-141004**

2020

CERTIFICATE – I

This is to certify that the thesis entitled, “**Design, Development and Evaluation of Tractor Operated Spading Machine**” submitted for the degree of **Ph.D.** in the subject of **Farm Machinery and Power Engineering** (Minor subject: **Computer Science and Engineering**) of the Punjab Agricultural University, Ludhiana, is a bonafide research work carried out by **Nitin Karwasra (Admission No. L-2014-AE-134D)** under my supervision and no part of this dissertation has been submitted for any other degree.

The assistance and help received during the course of investigations have been fully acknowledged.

Dr. Baldev Dogra (Major Advisor)
Principal Scientist
Deptt. of Farm Machinery & Power Engineering,
Punjab Agricultural University,
Ludhiana-141004

CERTIFICATE – II

This is to certify that the thesis entitled, “**Design, Development and Evaluation of Tractor Operated Spading Machine**” submitted by **Nitin Karwasra (Admission No. L-2014-AE-134-D)** to the Punjab Agricultural University, Ludhiana in partial fulfillment of the requirements for the degree of **Ph.D.** in the subject of **Farm Machinery and Power Engineering** (Minor subject: **Computer Science and Engineering**) has been approved by the Student’s Advisory Committee alongwith the External Examiner after an oral examination on the same.

(Dr. Baldev Dogra)
Major Advisor

(Dr. Vijaya Rani)
External Examiner
Head of department
Deptt. of Farm Machinery & Power
Engineering, CCS HAU, Hisar

(Dr. Manjeet Singh)
Head of the Department

(Dr. Gurinder Kaur Sangha)
Dean, Post-Graduate Studies

ACKNOWLEDGEMENT

First of all, I offer my reverence to "Almighty God" as its all by his grace that I have been able to complete this work.

*I am thankful to **Dr. Baldev Dogra**, Principal Scientist, my Major Advisor for encouraging during research and helpful at every stage during the study. Each meeting with him added priceless aspects to the execution and expanded my perspective. He has guided me with his precious suggestions, lightened up the way in my darkest times and encouraged me a lot in the academic life. It was an immense indulgence for me to have an opportunity of working with him.*

*My deep sense of acknowledgement is due to the member of my Advisory Committee viz **Dr. M. K. Narang**, Principal Extension Scientist, Department of Farm Machinery and Power Engineering, **Dr. Derminder Singh**, Professor, Department of Electrical Engineering and Information Technology, **Dr. Mohammad Javed**, Professor, Department of Mathematics, Statistics and Physics and **Dr. Rohinish Khurana**, Professor, Department of Farm Machinery and Power Engineering for their constant help, valuable guidance and kind cooperation throughout the course of study, selfless attitude, constant motivation, encouragement, professional and creative suggestions which helped me in completing the degree.*

*I duly acknowledge **Dr. Manjeet Singh**, Head, Department of Farm Machinery and Power Engineering for providing me the necessary research facilities in the department.*

*I owe my heartiest gratitude to **Er. Arshdeep Singh**, **Dr. Santosh Kumar**, **Dr Shiv Kumar Lohan**, **Dr. Aseem Verma** and **Er. Apoorva Prakash**, for guiding me and helping me on every step of my research.*

*I am thankful to all my seniors **Dr. Anand Gautam**, **Dr. P. K. Mishra**, **Er. Bharat Patel**, **Dr. Angam Ralenge**, **Dr. Sandeep Panday**, **Dr. Devesh Kumar** and my friends **Dr. Kanishk Verma**, **Dr. Shiva Bhambota**, **Dr. Nitin Kumar**, **Dr. Arun Attkan**, **Dr. Ankit Sharma** also my junior, **Dr. Parmar Raghuvirsinh P.**, **Dr. Mudasir Ali**, **Dr. Modi Rajesh Uttreshwar**, **Dr. Sunil Kumar**, **Hasan Mirzakhani**, **Neeraj Kumar Singh**, **Vinay**, **Jaideep**, **Parveen**, **Akshay**, **Avesh**, **Dr. Prasad Chavan**, **Pankaj Sharma** for their unconditional help, encouragement, moral support and constant concern for my welfare and made my degree days as remarkable one. The atmosphere of friendliness and deep association created by my friends which helped me a lot to accomplish this task with earnest effort and kept me bloomed even during ups and downs of my life.*

*Finally, I dedicate my dissertation work to my parent's **Dr. Jagdish Chander Karwasra** and **Smt. Saroj Karwasra** who encouraged and helped me at every stage of my personal and academic life, and longed to see this achievement come true. No words can suffice my feelings of gratitude to the love, deep concern for my progress and persistent encouragement received from you. Thank you for giving me strength to reach stars and chase my dreams.*

*I am also thankful to my elder sister **Neetika Karwasra Sihag** and brother-in-law **Major Ankit Sihag** for their moral support, encouragement, inspiration and affections.*

*Sincere thanks are extended to **Sh. Jagmohan Singh, Sh. Devi Lal, Sh. Harman, Sh. Avtar Singh,** and **Simran** for their involvement and help in execution of the experimental work,*

*Special thanks are due to **Mr. Kanav Aggawal**, Owner of Jaycee Jaycee Strips & Fasteners P. Ltd., **Mr. Charandeep Singh, Mr. Karan Sharma** and **Mr. Tejvir** for their help for making the machine.*

At the end of my thesis I would like to thank all those people who made this thesis possible and an unforgettable experience for me. It is a pleasant task to express my thanks to all those who contributed in many ways to the success of this study and made it an unforgettable experience for me. I would never have been able to finish my dissertation without the guidance of my committee members, help from friends, and support from my family. I will always appreciate what all they have done.

I feel proud to be a part of PAV, Ludhiana where I learnt a lot and spent unforgettable moments of my life. None can be forgotten, but all may not have been mentioned.

Place:

Date:

(Nitin Karwasra)

Title of Dissertation : Design, development and evaluation of tractor operated spading machine
 Name of Student : Nitin Karwasra
 Admission No. : L-2014-AE-134-D
 Major Subject : Farm Machinery & Power Engineering
 Minor Subject : Computer Science & Engineering
 Name and Designation : Dr. Baldev Dogra
 of Major Advisor : Principal Scientist
 Degree to be Awarded : Ph.D.
 Year of Award of Degree : 2018
 Total pages in Dissertation : 78 + Appendices + VITA
 Name of the University : Punjab Agricultural University, Ludhiana-141004

One of the most important operation in farming is tillage that handles the breaking of soil. Soil tilth needs to be managed by best management practice in order to reduce energy consumption. Primary advantage of spading machine as compared to the other ploughing methods is that it does not over-pulverize and create compact layer at the bottom of tilled soil. The present study was conducted to design, develop and evaluate a tractor operated indigenous spading machine. A crank-rocker type motion of four-bar mechanism was selected to simulate the spading action. Analytical analysis of four-bar mechanism was conducted and the link lengths were optimized using simulation software. The gearbox was developed assuming 50hp tractor to be used for operating the machine and its 3D model was developed in CAD software. The machine was fabricated and assembled with the help of a manufacturer. Field evaluation of the developed spading machine was conducted at three levels of forward speed ($S_1 = 2.26$, $S_2 = 3.37$ and $S_3 = 4.92$ km/h), three levels of depth of operation ($D_1 = 20$, $D_2 = 25$ and $D_3 = 30$ cm) and three levels of angle of attack ($A_1 = 30^\circ$, $A_2 = 35^\circ$ and $A_3 = 40^\circ$). The performance was analyzed on selected dependent variables i.e. bulk density, PTO torque, pulverization index and cone index. Statistical analysis revealed that forward speed (S) and depth of operation (D) had significant effect at 5% level of significance, while no significant effect observed for angle of attack (A) on bulk density of tilled soil. Maximum and minimum mean bulk density was observed at S3D3A3 (1.54 Mg/m^3) and S1D1A1 (1.17 Mg/m^3), respectively. PTO torque was affected significantly by forward speed and depth of operation, while angle of attack had no significant effect at 5% level of significance. Maximum and minimum mean PTO torque was observed at S3D3A1 (550.78 Nm) and S1D1A3 (327.66 Nm), respectively. Pulverization index was affected significantly by forward speed and depth of operation, while angle of attack had no significant effect at 5% level of significance. Maximum and minimum mean pulverization index was observed at S3D3A1 (18.20 mm) and S1D1A3 (3.68 mm), respectively. Effect of forward speed and depth of operation was statistically significant while angle of attack had no significant effect at 5% level of significance for cone index. Maximum and minimum cone index was found at S3D3A1 (1888.09 kPa) and S1D1A3 (624.27 kPa), respectively.

Keywords: tillage, spading machine, crank-rocker, evaluation

Signature of Major Advisor

Signature of Student

ਖੋਜ ਦਾ ਸਿਰਲੇਖ	: ਟਰੈਕਟਰ ਨਾਲ ਚੱਲਣ ਵਾਲੀ ਸਪੇਡਿੰਗ ਮਸ਼ੀਨ ਦਾ ਡਿਜ਼ਾਈਨ, ਨਿਰਮਾਣ ਅਤੇ ਮੁਲਾਂਕਣ
ਵਿਦਿਆਰਥੀ ਦਾ ਨਾਮ ਅਤੇ ਦਾਖਲਾ ਕ੍ਰਮਾਂਕ	: ਨਿਤਿਨ ਕਰਵਾਸਰਾ ਐਲ-2014-ਏ.ਈ.-134-ਡੀ
ਪ੍ਰਮੁੱਖ ਵਿਸ਼ਾ	: ਫਾਰਮ ਪਾਵਰ ਅਤੇ ਮਸ਼ੀਨਰੀ
ਸਹਿਯੋਗੀ ਵਿਸ਼ਾ	: ਕੰਪਿਊਟਰ ਸਾਇੰਸ ਅਤੇ ਇੰਜੀਨੀਅਰਿੰਗ
ਮੁੱਖ ਸਲਾਹਕਾਰ ਦਾ ਨਾਮ ਅਤੇ ਅਹੁਦਾ	: ਡਾ. ਬਲਦੇਵ ਡੋਗਰਾ ਸੀਨੀਅਰ ਰਿਸਚਰਚ ਇੰਜੀਨੀਅਰ
ਡਿਗਰੀ	: ਪੀ.ਐਚ.ਡੀ.
ਡਿਗਰੀ ਮਿਲਣ ਦਾ ਸਾਲ	: 2020
ਖੋਜ ਪੱਤਰ ਵਿੱਚ ਕੁੱਲ ਪੰਨੇ	: 78 + ਅੰਤਿਕਾਵਾਂ + ਵੀਟਾ
ਯੂਨੀਵਰਸਿਟੀ ਦਾ ਨਾਮ	: ਪੰਜਾਬ ਖੇਤੀਬਾੜੀ ਯੂਨੀਵਰਸਿਟੀ, ਲੁਧਿਆਣਾ - 141 004, ਪੰਜਾਬ, ਭਾਰਤ

ਸਾਰ-ਅੰਸ਼

ਖੇਤੀ ਦੌਰਾਨ ਖੇਤ ਦੀ ਜੁਤਾਈ ਕਰਨਾ ਇੱਕ ਬਹੁਤ ਹੀ ਮਹੱਤਵਪੂਰਨ ਕੰਮ ਹੈ ਜਿਸ ਦੌਰਾਨ ਮਿੱਟੀ ਨੂੰ ਭੋਰਿਆ ਜਾਂਦਾ ਹੈ। ਖੇਤ ਦੀ ਜੁਤਾਈ ਦਾ ਕੰਮ ਵਧੀਆ ਤਕਨੀਕਾਂ ਦੀ ਵਰਤੋਂ ਕਰਕੇ ਇਸ ਤਰੀਕੇ ਨਾਲ ਕਰਨਾ ਚਾਹੀਦਾ ਹੈ ਕਿ ਉਰਜਾ ਦੀ ਖਪਤ ਘੱਟ ਤੋਂ ਘੱਟ ਹੋਵੇ। ਖੇਤ ਵਾਹੁਣ ਦੀਆਂ ਬਾਕੀ ਵਿਧੀਆਂ ਦੇ ਮੁਕਾਬਲੇ ਸਪੇਡਿੰਗ ਮਸ਼ੀਨ ਦਾ ਪ੍ਰਮੁੱਖ ਲਾਭ ਇਹ ਹੈ ਕਿ ਇਹ ਮਿੱਟੀ ਨੂੰ ਲੋੜ ਤੋਂ ਜ਼ਿਆਦਾ ਨਹੀਂ ਤੋੜਦੀ ਅਤੇ ਇਸਦੀ ਵਰਤੋਂ ਨਾਲ ਮਿੱਟੀ ਦੇ ਹੇਠਾਂ ਠੋਸ ਪਰਤ ਨਹੀਂ ਬਣਦੀ। ਰੋਟਾਵੇਟਰ ਦੇ ਮੁਕਾਬਲੇ ਇਸਦੀ ਟਿਲਿੰਗ ਪਿੱਛ ਵਧੇਰੇ ਅਤੇ ਰਗੜ ਪ੍ਰਤੀਰੋਧਕਤਾ ਘੱਟ ਹੁੰਦੀ ਹੈ। ਮੌਜੂਦਾ ਅਧਿਐਨ ਦੌਰਾਨ ਟਰੈਕਟਰ ਨਾਲ ਚੱਲਣ ਵਾਲੀ ਸਵਦੇਸ਼ੀ ਸਪੇਡਿੰਗ ਮਸ਼ੀਨ ਦਾ ਡਿਜ਼ਾਈਨ, ਨਿਰਮਾਣ ਅਤੇ ਇਸਦਾ ਮੁਲਾਂਕਣ ਕੀਤਾ ਗਿਆ। ਸਪੇਡਿੰਗ ਐਕਸ਼ਨ ਦੇ ਅਨੁਕਰਣ ਲਈ ਚਾਰ-ਬਾਰਾਂ ਵਾਲੀ ਪ੍ਰਣਾਲੀ ਦੇ ਕਰੈਂਕ ਰਾਕਰ ਵਾਲੀ ਵਿਧੀ ਨੂੰ ਚੁਣਿਆ ਗਿਆ। ਚਾਰ-ਬਾਰਾਂ ਵਾਲੀ ਪ੍ਰਣਾਲੀ ਦਾ ਵਿਸ਼ਲੇਸ਼ਣ ਕੀਤਾ ਗਿਆ ਅਤੇ ਸਿਮੂਲੇਸ਼ਨ ਸਾਫਟਵੇਅਰ ਦੀ ਵਰਤੋਂ ਕਰਕੇ ਲਿੰਕ ਲੰਬਾਈਆਂ ਦਾ ਅਨੁਕੂਲਨ ਕੀਤਾ ਗਿਆ। ਇਹ ਮੰਨ ਕੇ ਕਿ ਇਸ ਮਸ਼ੀਨ ਨੂੰ 50 hp ਟਰੈਕਟਰ ਨਾਲ ਚਲਾਇਆ ਜਾਵੇਗਾ, ਇੱਕ ਗੇਅਰਬਾਕਸ ਦਾ ਨਿਰਮਾਣ ਕੀਤਾ ਗਿਆ। ਸਪੇਡਿੰਗ ਮਸ਼ੀਨ ਦਾ ਸਿਧਾਂਤਕ ਡਿਜ਼ਾਈਨ ਬਣਾਇਆ ਗਿਆ ਅਤੇ CAD ਸਾਫਟਵੇਅਰ ਦੀ ਵਰਤੋਂ ਕਰਕੇ ਇਸਦਾ 3D ਮਾਡਲ ਤਿਆਰ ਕੀਤਾ ਗਿਆ। ਨਿਰਮਾਣਕਰਤਾ ਦੀ ਮਦਦ ਨਾਲ ਇਸ ਮਸ਼ੀਨ ਨੂੰ ਨਿਰਮਿਤ ਕੀਤਾ ਗਿਆ ਅਤੇ ਅਸੈਂਬਲ ਕੀਤਾ ਗਿਆ। ਤਿੰਨ ਅਗਾਂਹ ਗਤੀਆਂ ($S1=2.26$, $S2=3.37$ ਅਤੇ $S3=4.92$ km/h), ਤਿੰਨ ਡੂੰਘਾਈ ਪੱਧਰਾਂ ($D1=20$, $D2=25$ ਅਤੇ $D3=30$ cm) ਅਤੇ ਮਿੱਟੀ ਭੇਦਨ ਦੇ ਤਿੰਨ ਕੋਣਾਂ ($A1=30^\circ$, $A2=35^\circ$ ਅਤੇ $A3=40^\circ$) ਉੱਤੇ ਖੇਤ ਵਿੱਚ ਇਸ ਮਸ਼ੀਨ ਦਾ ਮੁਲਾਂਕਣ ਕੀਤਾ ਗਿਆ। ਚੋਣਵੇਂ ਪਰਿਵਰਤਨਸ਼ੀਲਾਂ ਜਿਵੇਂ ਕਿ ਥੋਕ ਘਣਤਾ, PTO ਟਾਰਕ, ਮਿੱਟੀ ਦੇ ਢੇਲਿਆਂ ਦਾ ਸੂਚਕਾਂਕ ਅਤੇ ਕੋਨ ਸੂਚਕਾਂਕ ਦੇ ਅਧਾਰ ਤੇ ਮਸ਼ੀਨ ਦੀ ਕਾਰਜ ਸਮਰੱਥਾ ਦਾ ਮੁਲਾਂਕਣ ਕੀਤਾ ਗਿਆ। ਆਂਕੜਾ ਮੁਲਾਂਕਣ ਤੋਂ ਪਤਾ ਚੱਲਿਆ ਕਿ ਤੋੜੀ ਗਈ ਮਿੱਟੀ ਦੀ ਥੋਕ ਘਣਤਾ ਉਪਰ, ਅਰਥਪੂਰਨਤਾ ਦੇ 5% ਪੱਧਰ ਉਪਰ, ਅਗਾਂਹ ਗਤੀ (S) ਅਤੇ ਡੂੰਘਾਈ (D) ਦਾ ਅਰਥਪੂਰਨ ਪ੍ਰਭਾਵ ਸੀ ਜਦੋਂਕਿ ਮਿੱਟੀ ਨੂੰ ਭੇਦਨ ਦੇ ਕੋਣ (A) ਦਾ ਗੈਰ ਅਰਥਪੂਰਨ ਪ੍ਰਭਾਵ ਸੀ। ਅਗਾਂਹ ਗਤੀ ਅਤੇ ਡੂੰਘਾਈ ਵਿੱਚ ਵਾਧਾ ਹੋਣ ਨਾਲ ਥੋਕ ਘਣਤਾ ਵਿੱਚ ਵਾਧੇ ਦਾ ਰੁਝਾਨ ਦੇਖਿਆ ਗਿਆ। S3D3A3 ਅਤੇ S1D1A1 ਪੱਧਰਾਂ ਉਪਰ ਥੋਕ ਘਣਤਾ ਸਭ ਤੋਂ ਵਧੇਰੇ ਅਤੇ ਸਭ ਤੋਂ ਘੱਟ ਦਰਜ ਕੀਤੀ ਗਈ ਜੋ ਕਿ ਕ੍ਰਮਵਾਰ 1.54 g/cc ਅਤੇ 1.17 g/cc ਸੀ। ਅਰਥਪੂਰਨਤਾ ਦੇ 5% ਪੱਧਰ ਉਪਰ PTO ਟਾਰਕ ਉਪਰ ਅਗਾਂਹ ਗਤੀ ਅਤੇ ਡੂੰਘਾਈ ਦਾ ਅਰਥਪੂਰਨ ਪ੍ਰਭਾਵ ਪਿਆ, ਜਦੋਂਕਿ ਮਿੱਟੀ ਭੇਦਨ ਦੇ ਕੋਣ ਦਾ ਇਸ ਉਪਰ ਕੋਈ ਵੀ ਅਰਥਪੂਰਨ ਪ੍ਰਭਾਵ ਵੇਖਣ ਨੂੰ ਨਹੀਂ ਮਿਲਿਆ। S3D3A1 ਅਤੇ S1D1A3 ਪੱਧਰਾਂ ਉਪਰ ਸਭ ਤੋਂ ਜ਼ਿਆਦਾ ਅਤੇ ਸਭ ਤੋਂ ਘੱਟ ਔਸਤਨ PTO ਟਾਰਕ ਦਰਜ ਕੀਤੀ ਗਈ ਜੋ ਕਿ ਕ੍ਰਮਵਾਰ 550.78 Nm ਅਤੇ 327.66 Nm ਸੀ। ਅਰਥਪੂਰਨਤਾ ਦੇ 5% ਪੱਧਰ ਉਪਰ ਮਿੱਟੀ ਦੇ ਢੇਲਿਆਂ ਦੇ ਸੂਚਕਾਂਕ ਉਪਰ ਸਾਰੇ ਦੇ ਸਾਰੇ ਅਜ਼ਾਦ ਮਾਪਦੰਡਾਂ ਦਾ ਅਰਥਪੂਰਨ ਪ੍ਰਭਾਵ ਵੇਖਣ ਨੂੰ ਮਿਲਿਆ। S3D3A1 ਅਤੇ S1D1A3 ਪੱਧਰਾਂ ਉਪਰ ਢੇਲਿਆਂ ਦੇ ਸੂਚਕਾਂਕ ਦੀਆਂ ਮਿਕਦਾਰਾਂ ਸਭ ਤੋਂ ਵਧੇਰੇ ਅਤੇ ਸਭ ਤੋਂ ਘੱਟ ਸਨ ਜੋ ਕਿ ਕ੍ਰਮਵਾਰ 18.20 mm ਅਤੇ 3.68 mm ਸਨ। ਅਰਥਪੂਰਨਤਾ ਦੇ 5% ਪੱਧਰ ਉਪਰ ਕੋਨ ਸੂਚਕਾਂਕ ਉਪਰ ਸਾਰੀਆਂ ਅਗਾਂਹ ਗਤੀਆਂ ਅਤੇ ਡੂੰਘਾਈਆਂ ਦਾ ਪ੍ਰਭਾਵ ਅਰਥਪੂਰਨ ਸੀ ਜਦੋਂਕਿ ਮਿੱਟੀ ਭੇਦਨ ਦੇ ਕੋਣ ਦਾ ਗੈਰ ਅਰਥਪੂਰਨ ਪ੍ਰਭਾਵ ਵੇਖਣ ਨੂੰ ਮਿਲਿਆ। S3D3A1 ਅਤੇ S1D1A3 ਪੱਧਰਾਂ ਉਪਰ ਕੋਣ ਸੂਚਕਾਂਕ ਸਭ ਤੋਂ ਵਧੇਰੇ (1888.09 kPa) ਅਤੇ ਸਭ ਤੋਂ ਘੱਟ (624.27 kPa) ਦਰਜ ਕੀਤਾ ਗਿਆ।

ਮੁੱਖ ਸ਼ਬਦ: ਜੁਤਾਈ, ਸਪੇਡਿੰਗ ਮਸ਼ੀਨ, ਕਰੈਂਕ ਰਾਕਟ, ਮੁਲਾਂਕਣ

CONTENTS

CHAPTER NO.	TITLE	PAGE NO.
	LIST OF TABLES	
	LIST OF FIGURES	
	LIST OF ABBRIVATIONS	
I.	INTRODUCTION	1-3
II.	REVIEW OF LITERATURE	4-16
2.1	Soil tool interaction under different tillage system	4
2.2	Effect of different tillage practices on soil properties	6
2.3	Soil compaction caused by different tillage systems	8
2.4	Work done on spading machine	11
III.	MATERIALS AND METHODS	17-46
3.1	Study of Soil Failure Action of Spading Machine	17
3.1.1	Four Bar Mechanism	17
3.1.2	Crank-rocker linkage optimization	20
3.2	Kinematic analysis of crank-rocker mechanism	22
3.2.1	Mobility	22
3.2.2	Analytical analysis of crank-rocker mechanism	22
3.2.3	Velocity and Acceleration Analysis	24
3.3	Design of spading machine	25
3.1.1	Design and selection of gearbox	25
3.3.2	Design of shaft for bevel gears	26
3.3.3	Selection of blade	27
3.3.4	Trochoidal path tracing of spading machine blade	28
3.4	Computer aided design and development of spading machine	29
3.4.1	Frame of spading machine	29

3.4.2	Gearbox of spading machine	30
3.4.3	Spade arm of spading machine	30
3.4.4	Crank of spading machine	33
3.4.5	Depth adjuster of spading machine	33
3.5	Field evaluation of developed spading machine	39
3.5.1	Independent parameters of the study	39
3.5.2	Forward speed	40
3.5.2.1	Depth of operation	40
3.5.2.2	Angle of attack	40
3.5.2	Dependent parameters of the study	41
3.5.2.1	PTO torque	41
3.5.2.2	Soil bulk density	42
3.5.2.3	Cone index	43
3.6.2.4	Clod size distribution	44
3.5.2.5	Soil moisture	46
3.5.3	Experimental field layout	46
3.5.4	Statistical analysis	46
IV	RESULTS AND DISCUSSION	48-69
4.1	Effect on bulk density	48
4.1.1	Effect of forward speed on bulk density	51
4.1.2	Effect of depth of operation on bulk density	52
4.2	Effect on PTO torque requirement	54
4.2.1	Effect of forward speed on PTO torque	56
4.2.2	Effect of depth of operation on PTO torque	57
4.3	Effect on clod size distribution	59
4.3.1	Effect of forward speed on PI	62

4.3.2	Effect of depth of operation on PI	63
4.4	Effect on soil strength	64
4.4.1	Effect of forward speed on soil strength	66
4.4.2	Effect of depth of operation on soil strength	68
4.5	Operational parameters for best field performance of spading machine	68
V	SUMMARY	69-72
	REFERENCES	74-78
	APPENDICES	i-v

LIST OF TABLES

Table No.	Title	Page No.
3.1	Angle of crank-rocker mechanism for θ_2	23
3.2	Analytical analysis of crank-rocker mechanism using optimized link length values	24
3.3	Specifications of developed spading machine	37
3.4	Specification of Gomadhi spading machine	37
3.5	Physical characteristics of soil at experimental site	39
3.6	Brief specification of tractor used with spading machine for field evaluation	39
3.7	Independent parameters and their levels	40
4.1	ANOVA for effect of forward speed, depth of operation and attack angle on bulk density of soil ploughed by spading machine	51
4.2	Mean values of bulk density at different levels of forward speed	51
4.3	Mean values of bulk density at different levels of depth of operation	52
4.4	Mean values of bulk density for the effect of interaction between forward speed and depth of operation	53
4.5	ANOVA for effect of forward speed, depth of operation and attack angle on PTO torque of spading machine	56
4.6	Mean values of PTO torque at different levels of forward speed	56
4.7	Mean values of PTO torque at different levels of depth of operation	57
4.8	Mean values of PTO torque for the effect of interaction between forward speed and depth of operation	58
4.9	ANOVA for effect of forward speed, depth of operation and attack angle on pulverization index of soil ploughed by spading machine	62
4.10	Mean values of pulverization index at different levels of forward speed	62
4.11	Mean values of pulverization index at different levels of depth of operation of spading machine	63
4.12	Mean values of pulverization index for the effect of interaction between forward speed and depth of operation	64
4.13	ANOVA for effect of forward speed, depth of operation and attack angle on cone index of soil ploughed by spading machine	66
4.14	Mean values of cone index at different levels of forward speed	66
4.15	Mean values of cone index at different levels of depth of operation	68

LIST OF FIGURES

Figure No.	Title	Page No.
3.1	Hand spade tool used by farmer	18
3.2	Four-bar linkage mechanism	18
3.3	Movement of crank-rocker mechanism	19
3.4	Nomenclature of the main parts of the spading	20
3.5	A view of simulation software used for link optimization	21
3.6	Optimization iteration graph	21
3.7	Illustration of crank-rocker bar	23
3.8	Front and side view of selected blade	27
3.9	Von mises stress diagram of blade	28
3.10	Trochoidal curve traced by the blade tip	28
3.11	Solid model of frame of spading machine	29
3.12	Development of frame of spading machine	30
3.13	Developed spade arm of spading machine	30
3.14	Exploded view of gearbox of spading machine	31
3.15	Exploded view of spade arm of spading machine	32
3.16	Solid model of crank of spading machine	33
3.17	CAD drawing of depth adjuster of spading machine	33
3.18	A sketch Front view of tractor operated spading machine	34
3.19	A sketch of side view of tractor operated spading machine	34
3.20	Side view designed spading machine solid model	35
3.21	An isometric view of complete machine assembly solid model	35
3.22	Back view of spading machine solid model	36
3.23	Front view of spading machine solid model	36
3.24	Preliminary trials of developed spading machine in field	38
3.25	Preliminary trials of developed spading machine in field	38
3.26	A view of torque sensor attached to telescopic shaft connecting PTO with machine gearbox	41
3.27	A view of data receiving unit and laptop arranged on tractor to extract Torque data	42

3.28	Core cutter inserted in tilled soil for sample collection	43
3.29	Cone penetrometer used to measure soil strength	44
3.40	Measurement of weight of soil retained on each sieve	45
3.41	Field trial of developed spading machine	47
3.42	Field trial of developed spading machine	47
4.1	Effect of forward speed and depth of operation at 30° angle of attack on bulk density	50
4.2	Effect of forward speed and depth of operation at 35° angle of attack on bulk density	50
4.3	Effect of forward speed and depth of operation at 40° angle of attack on bulk density	50
4.4	Diffogram for the effect of forward speed and depth of operation on bulk density	53
4.5	Effect of forward speed and depth of operation at 30° angle of attack on PTO torque	55
4.6	Effect of forward speed and depth of operation at 35° angle of attack on PTO torque	55
4.7	Effect of forward speed and depth of operation at 40° angle of attack on PTO torque	55
4.8	Diffogram for the effect of forward speed and depth of operation on PTO torque	59
4.9	Effect of forward speed and depth of operation at 30° angle of attack on PI index	61
4.10	Effect of forward speed and depth of operation at 35° angle of attack on PI	61
4.11	Effect of forward speed and depth of operation at 40° angle of attack on PI	61
4.12	Diffogram for the effect of forward speed and depth of operation on PI	65
4.13	Effect of forward speed and depth of operation at 30° angle of attack on CI	67
4.14	Effect of forward speed and depth of operation at 35° angle of attack on CI	67
4.15	Effect of forward speed and depth of operation at 40° angle of attack on CI	67

LIST OF ABBREVIATIONS

%	-	Percentage
CI	-	Cone index
cm	-	Centimeter
d.f.	-	Degree of freedom
Fig.	-	Figure
g	-	Gram
h	-	Hour
hp	-	Horse power
J kg ⁻¹	-	Joules per kilogram
Kg	-	Kilogram
km/h	-	Kilometer per hour
Kn	-	Kilo newton
KPa	-	Kilo pascal
kW	-	Kilowatt
m	-	Meter
m/s	-	Meters per second
Mg/m ³	-	Mega gram per cubic meter
mm	-	Millimeter
MMD	-	Mean mass diameter
MPa	-	Mega pascal
N	-	Newton
Nm	-	Newton meter
°	-	Degree
PI	-	Pulverization index
PTO	-	Power take off
rad/s	-	Radians per sec
rad/sec ²	-	Radians per second square
rpm	-	Revolutions per minute
SS	-	Sum of squares

CHAPTER-I

INTRODUCTION

Tillage is defined as a process aimed at creating a desired final soil condition for seeds from some undesirable initial soil conditions through manipulation of soil (Gill and Vandenberg 1968). Crop growth requires preferred environment of soil by achieving good soil structure and air permeability which is accomplished by tillage operation (Canarache 1991). This can be achieved using several tillage implements. Over last many years, plough is being used for this operation but in recent years to reduce the environmental and economic impact of tillage and to obtain maximum crop production alternate solutions have been developed like minimum or zero tillage. Thus, bringing up alternate machinery, not just plough (Hoffman 1993, Borin *et al* 1997). Tillage practices represent around half of the energy used in agricultural production (Kushwaha and Zhang 1998). Therefore, soil tillage needs to be managed by best management practice in order to reduce energy consumption. In tillage operation the soil failure action mainly depends upon the soil properties, tool geometry and cutting speed. In the real situation, when initial cutting begins, the shear failure develops progressively to a total failure ahead of the tillage tool. During cutting, the configuration of soil ahead of tillage tool and soil-tool interface changes continuously. Over pulverisation is also one of the major problems nowadays as it influences the soil characteristics, because of which the soil results in soft and finely powdered without structure. It causes weak soil structure thus resulted in loss of water holding capacity which greatly affects the soil fertility. Several researchers have sought to optimize the energy consumption of the tillage by reducing the draft force (Shmulevich 2010). This force is related to the mechanical properties of the soil, to the working parameters (depth and speed of plowing) and to the geometry of the soil tillage tool. Therefore, draft and power requirements are important in order to determine the size of the tractor that could be used for a specific implement. The draft and power required for a given implement will also be affected by the soil conditions and the geometry of the tillage implement (Taniguchi *et al* 1999, Naderloo *et al* 2009, Olatunji *et al* 2009).

Optimizing the design of soil tillage tools will not only help in improving the field performance of the machine but also improving the energy efficiency. Accurate modeling of soil-tool interaction is key to this optimization and can eliminate the need for numerous expensive field tests and reduce prototype development and verification time. However, soil-tool interaction is a complex process due to spatial variability of soil, dynamic effects, flow and mixing occurring in the soil as a result of this interaction. The three design factors involved in the design of tillage tools are, shape, manner of movement and the initial soil condition. Of the above three design factors, the designer has complete control only over shape. The user of a

tillage tool may vary the manner of tool movement namely, the depth or speed of operation and may use the tool through a wide range of initial soil conditions. The shape of tillage tools, therefore, has received considerable emphasis since the ideal tillage tool should perform satisfactorily over wide ranges of soil conditions, depths and speeds of operation. Bishnoi (2008) conducted a research on different types of blades of spading machine in soil-bin to evaluate the effect of widths and spade angle. There are many studies done on soil-tool interaction and field performance of various implements mooting various parameters like soil condition before and after treatment, tool shape and speed, draft and power take-off (PTO) requirement of the driven implements (Perdok and Kouwenhoven, 1994).

Spading machine has had a noticeable success in Italy, or more importantly in the Mediterranean areas. Primary advantage of spading machine as compared to the other ploughing methods is that it doesn't create compact layer at the bottom of tilled soil and it has zero draft requirement (Gasparetto 1966). The spading machine is attached to 3-point hitch of tractor and operated with tractor PTO. Study has been done on the performance of different shapes of spades, thus leads to trapezoidal shape spade gave best result in terms of soil bulk density and soil pulverization (Dogra *et al* 2017). The spades are attached on the end of connecting rods which form an articulated quadrilateral mechanism. The spades cut slice of soil and launch it behind the machine thus crumbling it. This deformation of soil in this case can be divided into three stages. The first stage is the cutting stage where the blade simply cuts into the soil. The second stage is where the blade holds the cut soil on its scoop surface called as holding stage. The third stage of deformation in rotary tillage is the no-load stage. In this stage, the blade throws the tilled soil into the air where it ceases to have contact with any materials. Studies have been done to get the most efficient mechanism of spading machine. Gasparetto studied it in 1966 and observed that quadrilateral mechanism found to give best results, by studying the kinematic point of view on several type of spading machines considering both movement paths for different speed and acceleration developed. Spading machine mimic the movement of hand digging tool for better soil aeration, mixing of organic matter and deeper operation. As the spades penetrates the soil at an angle to the soil surface, therefore there was no problem of hardpan of soil. Spading machine also called as crank-type rotavator uses several equal spaced spades represents a slider of a crank–slider mechanism and has a relatively deeper rotavating depth upto 30 cm. Deeper tillage rip the hardpan thus reducing the soil bulk density and soil strength, thereby encouraging deeper rooting of plants, and improving soil infiltration rates and plants' access to water and minerals (Busscher and Bauer 2003). Varsa *et al* 1997, Kim *et al* 2011 and Yoo *et al* 2006 also reported that tillage operation at depths greater than 200 mm is very effective in improving the physical properties of soil as it influences air permeability and moisture content of tilled soil.

Conventional tillage can break up the soil from 10 to 15 cm, but it may be inadequate where soil compaction is a problem. Spading machine gained interest primarily in Italy in 80s and was also the major manufacturer of spading machines at the time (Baraldi and Pezzi 1987). It was also found that energy requirement for spade impact force is reduced by changes in spade angle. Saimbhi (2006) developed a prototype of articulated tillage machine (spading machine) to compare its performance with rotary tillage machine and found that there was 43% of power and 44% of energy saving in soil metal friction resulting in saving in energy requirement but also leave the field with reasonable mechanical impedance for crop production.

Compared to a rotavator, the spading machine has a longer tilling pitch and shorter traction resistance because several tillage blades mounted on a flange continuously rotavate the subsurface soil, when the rotavating depth is increased. Although rotary tillers are known to be best tillage machine for single pass operation but their energy consumption is more than conventional tillage implement. Moreover, the spading machine is also safe from abrasion and breakage of the tillage blades (NIAE, 2004) caused by stones or foreign substances because of the shoveling style of cultivating. The spading machine improves the crop yield by having a good influence on the air permeability and moisture contents of the soil (Varsa *et al* 1997, Kim *et al* 2011, Yoo *et al* 2006). Economic and environmental considerations are forcing farmers to operate soil tillage with an optimum implement configuration to achieve a desirable final soil condition.

Unfortunately, the results above mentioned researches cannot be referred nowadays, because at that time ploughs were characterized by a limited working width, a factor reducing their performance. There was a need to have spading machine design information and its operational parameters. Thus, the aim of this research is to design, develop an indigenous spading machine and evaluate its performance for Indian field condition.

The present study was conducted with the following objectives:

- i) To design a tractor operated spading machine.
- ii) To develop the designed spading machine.
- iii) To evaluate the performance of developed spading machine.

CHAPTER – II

REVIEW OF LITERATURE

Several studies have been carried out on soil tool interaction and their effect on soil during tillage operation. Various researchers have conducted work on effect of different tillage practices on soil physical characteristics and their effect on soil compaction. In this Chapter, review about the studies related to tillage machines carried out by different researchers in India and abroad has been briefly reviewed and compiled. The review has been presented under the following heads:

- 2.1 Soil tool interaction under different tillage system
- 2.2 Effect of different tillage practices on soil properties
- 2.3 Effect of soil compaction caused by different tillage systems
- 2.4 Work done on spading machine (Crank-type rotavator)

2.1 Soil tool interaction under different tillage system

Tillage practices account for about half of the energy used in crop production (Kushwaha and Zhang 1998). Soil tilth needs to be managed by best management practice in order to reduce energy and fertilizer consumption. Economical and environmental considerations are forcing farmers to operate soil tilth with an optimum implement configuration to achieve a desirable final soil condition (Shmulevich *et al* 2007). Modeling soil-tillage interaction is a complex process due to dynamic soil-implement interaction which includes a high rate of plastic deformation and soil failure, characterized by the flow of soil particles.

Shmulevich *et al* (2007) studied interaction between soil and a wide cutting blade using the discrete element method. The wide cutting-blade interaction was modeled using a two-dimensional discrete element method and the soil particles by clumps of two disks with a cohesion force contact model between the particles. Four different blade shapes were analyzed by the discrete element model and experimentally by a soil box filled with sand. A very good correlation was obtained between the discrete element simulation and the experimental results. The simulations indicate an increasing horizontal force applied on the blades during motion, as a result of the piling effect of the soil in front of the blade. It was found that the soil flow beneath the blade tip can affect the vertical force applied on the blade.

The simulation results were also compared with classical soil mechanics theories for straight blades i.e. the McKyes approach (McKyes 1985). A good correlation was obtained between the simulation results and McKyes approach for the horizontal force applied on the

blade. Weaker correlations were obtained in the vertical direction. This finding can be explained by the soil particle flow beneath the blade tip, which the McKyes approach, does not take into consideration. Observation of the simulation revealed that the failure curve could be reasonably described by a straight line, as assumed in the classical theories.

Moeenifar *et al* (2014) investigated the influence of three independent variables including tillage depth (10, 15, 20 cm), angle of attack (60, 75, 90 degrees) and forward speed (0.5, 1, 1.35, 1.7 m/s) on draft force of a thin blade. Chisel plow in this research was constructed in two furrows with a blade width of 3 cm and a maximum depth of 25 cm (the distance between two blades was 1 m). Some changes were made in the chassis of the chisel plow in order to obtain different attack angle of the blade. The experimental work was then complemented with a new theoretical model for predicting the blade force using dimensional analysis method. The final expression for estimating the pull resistance is as a function of several soil engineering properties (soil bulk density, soil adhesion and cohesion coefficients), blade parameters (blade width and blade rake angle) and operational conditions (tillage depth and forward speed). Finally, constants of the model were computed based on obtained experimental data. The proposed model properly estimated the draft force of a thin blade. Results obtained in this study indicate the stronger influence of tillage depth on the pulling force of a thin soil-working blade compared to the penetration angle and forward velocity. The average error for the vertical blade with depth of 20, 15 and 10 cm were obtained equal to 4.5%, 4% and 1.5%, respectively.

Fechete *et al* (2019) evaluated the draft force on a simple tillage tool operating in different conditions in sand. The soil-tool interaction was evaluated in controlled laboratory conditions in a soil bin. A full multi-level factorial experiment was used with one response variable and four experimental factors. The selected design is three tools, three tillage depth, three rake angle, three forward speed with two replications had a total of 243 runs. Influence of four independent variables including tillage depth (15, 20, 25 cm), rake angle (25, 35, 50 degrees), forward speed (0.67, 0.98, 1.39 m/s) and cutting-edge angle of the tool (30, 45 and 60 degrees) on draft force as the dependent variable was assessed.

In the results, the tool depth and the rake angle were determined to have, individually taken, each one more than 60% influence in the variability of tool draft force with an increase effect up to 30% in the case on combining the two. The other two investigated variables have a smaller effect over the dependent investigated variable. The most interesting observation is the positive effect of decrease in draft force encountered in the case of modifying the cutting-edge angle, the tool sharpening angle, in the most unfavourable situations for tillage tools operation respectively at higher rake angle, depth or tool speed.

Daraghmeh *et al* (2019) conducted a research with an aim to improve the knowledge of potential precision tillage practices by characterising the effect of varied tillage intensities on structural properties of a clay loam soil. An experiment with seedbed preparation was conducted using a PTO-driven rotovator equipped to measure torque and angular velocity and with operational speed (OS) and rotational speed (RS) as main factors.

Effects of soil coverage prior to tillage and wheeling directly after tillage were measured at one combination of OS and RS. The soil was sampled at 0–80 mm depth. Under slow OS (2.9 km h⁻¹) compared with fast OS (6.3 km h⁻¹) specific energy input was greater (116 and 52 J kg⁻¹ on average, respectively) and it increased with RS. Wheeling resulted in larger aggregate diameter right after tillage (at T1; 56 mm as geometric mean compared with 9 mm), with 42 times smaller geometric mean of air permeability 45 days after tillage (at T2) and with greater soil dispersibility at T2. Highly significant correlations were observed between soil dispersibility and energy input, specific surface area of aggregates, fractions of small (< 4 mm) and medium (8–16 mm) aggregates and geometric mean diameter. Slow OS combined with fast RS showed significantly greater air permeability than all other treatments. The results suggest that there is a potential for controlling soil structure in seedbed preparation by minimizing compaction from traffic and adapting site-specific control of rotoation intensity.

2.2 Effect of different tillage practices on soil

Crop residues retained on the soil surface supply additional soil organic matter (SOM) to the soil, improving soil structure, root development and plant growth (Dimassia *et al* 2013). Crop residue is the material which usually not taken away but rather left in the field after the crop harvesting which include leaves, straw, stubble and roots stalks. The residue management strategy affects soil structure, organic matter content, nutrient availability, hydraulic properties and crop productivity (Bronick and Lal 2005). The impact of different tillage practices on soil physical properties, specifically infiltration has been well investigated using tension infiltrometer (Logsdon and Kaspar 1995).

Tillage and crop residue management play an important role on soil physical and chemical properties and eventually affects the crop productivity. Singh *et al* (2018) examined the effect of tillage and crop residue management on soil physical properties. Management of soil physical properties such as bulk density, infiltration, porosity, soil organic carbon, saturated hydraulic conductivity and soil temperature, plays an important role in crop productivity. A compatible combination of tillage and crop residue management found an impactful strategy to improve the properties of soil for provision of favourable environment to crop plants. Conservational tillage practices such as zero tillage, minimum tillage and reduced tillage along with retaining crop residues on soil surface have a great advantage over conventional tillage.

Thus, incorporating crop residue with tillage practices have advantage through adding organic matter and carbon to the soil that are preconditions for the better physical, biological as well as for chemical properties. Allowance of crop residue to the soil surface reduces its bulk density and compaction. Infiltration and hydraulic conductivity also reported to be greater under no tillage than in tilled soils because of the larger number of macrospores and increased microbial activity. Crop residue incorporation into the soil also increases infiltration rate, saturated hydraulic conductivity and regulation of soil temperature. Soil organic carbon content and aggregate stability also found increased because of crop residue incorporation.

Khorami *et al* (2018) studied the combined effect of tillage practices and wheat (*Triticum aestivum* L.) genotypes on soil properties as well as crop and water productivity. The experiment was conducted at Zarghan, Fars, Iran during 2014-2016. Experimental treatments were three-tillage practices—conventional tillage (CT), reduced tillage (RT), and no tillage (NT)—and four wheat genotypes were randomized in the main and subplots, respectively using split-plot randomized complete block design with three replications. Results showed NT had higher soil bulk density at surface soil, thereby lower cumulative water infiltration. The lowest soil organic carbon and total nitrogen were obtained under CT that led to the highest C:N ratio. Reduced tillage produced higher wheat yield and maize (*Zea mays* L.) biomass. Maximum irrigation water was applied under CT, which leads to lower water productivity. It was also suggested that the findings are based on short-term results, but it is important to evaluate medium and long-term effects on soil properties, crop yields and water use in future.

Numerous factors affect tillage operations. During tillage operations, the selection of a working machine (tool) depends on the soil conditions as well as the type of tillage operation to be performed (Naderloo *et al* 2009).

Okyere *et al* (2018) studied the effects of varying working machine parameters of a compact disc harrow on tillage operations under various soil moisture content (SMC) conditions. The working machine parameters were the disc spacing and machine speed. The tillage parameters under investigation were the soil inversion ratio (SIR), tillage cutting depth (TCD) and soil clod breakage ratio (SCB). To determine the SIR, the areas of the white regions before and after tillage were obtained. The ratio of the difference of the areas of the white regions before and after tillage to the area of the white regions before tillage was considered as the SIR. The SCB was obtained as the ratio of the weight of soil clods after sieving with a mesh size of <0.02 m to the total weight of the soil clods before sieving. The soil TCD was measured using a tape measure at random points after the tillage operation. The resulting data were then statistically analysed in a one-way analysis of variance.

The highest soil inversion was achieved when the machine speed was 0.2 m/s with the disc spaced at 0.2 m in the 16.5% SMC. At a 0.4-m/s machine speed and 0.3-m disc spacing the highest soil breakage was achieved in the 26.5% SMC. The highest TCD was achieved at a 0.2-m/s machine speed and 0.2-m disc spacing in the 16.5% SMC. Thus, the research concluded that varying the working machine parameters, such as the disc spacing and machine speed, could significantly affect the soil inversion and soil clod breakage; however, it had no significant impact on the TCD.

Tillage practice and residue management play important roles in nitrogen pool in soils. Ye *et al* (2019) determined the impacts of tillage practice and residue management on crop yield. They also investigated the distribution, fractionation and stratification of N at soil at depths ranging from 0 to 60 cm under wheat–maize cropping systems. Three treatments were established in 2009; no-tillage with straw removal for winter wheat and summer maize (NT), no-tillage with straw mulching for winter wheat and summer maize (NTS), no-tillage with straw mulching for summer maize and plow tillage with straw incorporation for winter wheat (NPTS). After 8 years, soil total nitrogen (TN) content in NTS was greater than in NT, but only in 0–10 cm layer. NPTS treatment increased TN content over NT and NTS in 10–20 cm layer by 18.0% and 13.9%, and by 16.8% and 18.1% in 20–30 cm layer, respectively. Particulate organic N, microbial biomass N and water-extractable organic N levels were the greatest in 0–10 cm layer under NTS treatment and in 10–30 cm layer; the corresponding values were the highest under NPTS treatment. NPTS treatment could immobilize the mineral N in 10–30 cm layer, and reduced leaching losses into deeper soil layers (40–60 cm). Furthermore, total yield increased by 14.7% and 8.5% in NPTS treatment compared to NT and NTS treatments, respectively. These results indicate that NPTS is an effective and sustainable management practice, which will improve soil fertility, sustainable crop production and environmental quality in low-productivity soils in central China.

2.3 Effect of soil compaction caused by different tillage systems

Singh *et al* (2015) studied the soil compaction resulted due to mechanization of farm operations, intensive agriculture and continuous use of farm machinery. Soil compaction affects soil physical properties, plant growth, root growth and yield of crops. It increases bulk density and penetration resistance, decreases porosity, infiltration rate and hydraulic conductivity. It was found that vehicular traffic and puddling resulted in formation of compacted subsoil layer in the root zone at 10–40 cm depth that restricted the root growth and root density of plants. The reduction in root growth and density further decreased nutrient uptake and ultimately crop yield. The review showed the need of conservation agriculture to reduce traffic on the soil and subsoiling/ chiseling to remove hardpan developed due to traffic and puddling.

When soil conditions are poor for machine operations, the rate of operation is affected; forward speed must usually be reduced. This condition will improve field efficiency but it is not, of course, a desirable operating condition (Alnahas 2003). Measures of agricultural machine performance are the rate and quality at which the operations are accomplished (Hunt, 2013). According to Belel and Dahab (1997), tillage operations are soil-related procedures; soil type and condition are cardinal factors affecting the field performance of a tractor through their effects on the powered implement and tractor traction.

The soil physical characteristics which affect crop production and tillage requirements, are hard to be studied or assessed directly; these involve size, shape, arrangement of solids, continuous voids and forces relevant to physical soil characteristics. Structural stability is usually assessed in terms of different properties including total porosity, pore size distribution, available water content and bulk density (Lal 1995).

Oduma *et al* (2018) conducted research at the demonstration farms of Michael Okpara University of Agriculture, Umudike, Abia State and Veterinary School, Ezzangbo, Ebonyi State in 2017 to assess the effect of soil physical properties on the performance of some selected agricultural field machineries in the tropical region of Nigeria. Results of the effect of the soil textural type on implement performances revealed that the average efficiency of the implements was highest on sandy-clay soil with average efficiency of 87.35% and the least was loamy-sandy soil that gave an average efficiency of 86.21%. It was observed from the results that the highest average moisture content of 17.7% was recorded for all the soils before tillage, but after tillage; ploughing recorded 16.3% moisture content. Harrowing, ridging, pulverization and planting had 15.45%, 14.70%, 14.23% and 14.12% moisture content, respectively. The reduction in moisture content during the field operations promoted workability of the soils. The highest moisture contents are observed for the plough as compared to other implements was attributed to high compaction associated with ploughing operation which decelerates infiltration rate.

Results further showed that the bulk density of the soils reduced with the application of the implements. Prior to the field operations, the average bulk density of the soil was 1.62 Mg/m³, but when the implements were applied there was shortfall in the bulk densities in ploughing harrowing, ridging, rotovator and planter which is 1.49 Mg/m³, 1.40 Mg/m³, 1.33 Mg/m³, 1.29 Mg/m³ and 1.35 Mg/m³, respectively. The reduction in the bulk density of the soil enhances the field performances of the implements by reducing the resistance to the penetration of the implements and also improves the soil for proper root penetration. The effect of porosity on the implement performance followed opposite trend as bulk density. The lowest porosity was observed in untilled soil with average porosity of 48.30%. On the application of the field machineries, the porosity of the soils increased to 49.68% after ploughing, 53.43% after

harrowing, 54.11% after pulverization, 54.14% after ridging and 53.67% after planting. The increase in porosity of the soil during operation provided it was within the acceptable limit for machine operation which improved the workability of the soils, enhanced the water infiltration rate and implemented penetration to the soil. Finally, the statistical analysis (ANOVA) conducted on the effect of soil physical properties on the implement performances showed significant difference at 5% level of significance.

Land use intensification typically amplifies temporal changes in soil physical properties. These changes can affect a range of biogeochemical processes, which may in turn affect soil health and ecosystem services such as water storage and supply and crop production (Bunemann *et al* 2018). Soil compaction is an important impact of agricultural intensification, owing to increases in machinery wheel loads and livestock grazing intensity that pose a growing threat to many key soil functions (Drewry *et al* 2008; Lamandé and Schjønning 2018). Few, if any, studies have focused on the interactions between tillage and compaction and the recovery of soil physical properties with time.

Keeping in mind the above problems Hu *et al* (2018) investigated short-term dynamics of soil physical properties as affected by tillage and compaction in a silt loam soil. After establishment of an autumn-sown forage oat (*Avena sativa* L.) crop with either no-till (NT) or intensive tillage (IT), five degrees of livestock compaction (0–261 kPa) were applied in winter using a cow treading implement. A barley (*Hordeum vulgare* L.) crop was then sown following shallow cultivation of the soil in spring. After two years of sheep-grazed pasture, tillage significantly improved the soil physical quality in the 0 - 0.2 m layer. Compaction significantly deteriorated soil physical quality for example, decreasing macroporosity, available water content and saturated hydraulic conductivity.

Compared with IT and the top 0.1 m soil layer, soil physical properties in NT and the subsurface 0.1-0.2 m layer were more resistant to compaction. Irrespective of tillage, the topsoil (0-0.1 m) was more susceptible to physical degradation than the subsurface soil (0.1-0.2 m). Compaction and tillage effects on soil physical quality declined with time because of natural recovery and the shallow tillage used to establish the subsequent barley crop. This study demonstrated that using NT to establish an autumn-sown forage crop can mitigate the adverse impacts of livestock treading on soil physical quality during subsequent grazing. Although tillage and compaction effects were short lived, soil physical properties were significantly different between every two adjacent measurement times.

Kumar (2017) evaluated the soil compaction caused by different tillage practices. The independent parameters for the study were two soil types (sandy loam, S1 and silty loam, S2), six different tillage practices (conventional tillage practice as P1, P2, rotavator practices as P3,

P4 and spading machine as P5, P6), two forward velocity ranges (V1 and V2) and two operation depth ranges (D1 and D2). Replicated (three) trials in factorial in RBD were adopted for the study. Soil bulk density and cone index values were taken at selected sampling depths for determining the initial soil compaction i.e. before tillage treatments. Effect of irrigation on soil compaction was also noted at optimum moisture level after irrigation but before tillage treatments.

The results showed cone indices of both types of soil were found lesser, after irrigation, than that of before irrigation conditions. Bulk density of soil S1 was higher after irrigation, whereas of soil S2, it was lower than that of before irrigation, before tillage conditions. Cone indices in both types of soils were observed lesser than that of initial compaction, in top 10 cm of soil, after different tillage treatments. Cone indices, at sub-soil depths (at 15 cm and beyond) of both soil types, in P3, P4, P5 and P6 tillage practices were found to be comparatively more than that of initial soil compaction for most of the treatments. Bulk density was observed lower than that of initial soil compaction for all the treatments in both soil types. Mean weight diameter of soil clods formed were minimum whereas fuel consumption (l/h) values were maximum in case of rotavator among all the treatment values.

2.4 Work done on spading machine (Crank-type rotavator)

Two studies were conducted in the department of Farm Machinery & Power Engineering, PAU, Ludhiana on spading machine. One is “Computer aided design and field evaluation of articulated tillage machine” carried out in department by Dr. V. S. Saimbhi and other is “Development and evaluation of blades for spading machine” conducted by Dr. Ritu Bishnoi is reviewed below:

Saimbhi (2006) used computer aided kinematic synthesis and linkage design optimization approach for path generation of four bar linkage mechanism, to manipulate the soil similar to that with spade or by hand shovel. Coordinate transformation approach was used to simulate the mechanism blade interaction with uncut soil. The simulated computer prototype cuts the soil in regular bites and fractured it. However, the blade surface did not interact with uncut soil. Interference of the rear surface of the blade with the soil caused soil compaction and soil metal friction vis-à-vis excessive energy requirement, which had been minimized. The blade trajectory, blade shape, its orientation and width, clearance and cutting angle of blade had been some of the important factors. A laboratory prototype was developed using commercially available crank shaft and connection rods. A soil bin study was performed to ascertain power and energy requirement in different levels of soil-tool interaction. Soil-tool interaction at different combinations of blade attack angle (-15° , 0° , 15° with vertical plane along the line of motion) and bite length (4, 8, 12, 16 cm) were studied. The blade attack angle of 15° and 8cm of

bite length gave maximum specific work. A tractor mounted articulated tillage machine (ATM) prototype was developed on AutoCad and fabricated accordingly and comparative evaluation of prototype was carried out with a commercially available rotary tillage machine (RTM). Mathematical model functions were evaluated for indirect evaluation of tractor engine performance. The ATM takes less amount of power and energy in comparison with RTM and output soil structure was statistically similar. There was 43% of power and 44% of energy saving in soil metal friction resulting in saving in energy requirement but also leave the field with reasonable mechanical impedance for crop production.

Bishnoi (2008) carried out a soil bin study on cultivable soil to ascertain the effect of spading machine blade parameters (spade angle, radius of curvature and blade width) on specific soil resistance, energy consumed per unit volume of soil moved, weighted mean clod size, soil bulk density, soil cone index and cone index ratio (ratio of initial to final cone index) at different levels of spading frequency. Two laboratory models of spading machine were developed for this purpose. Four levels of spading frequency (1.85, 2.31, 3.08 and 4.62 cycles/sec), three levels of spade angle (0, 15 and 30 degrees), three levels of radius of curvature (0, 15 and 30 cm; 0, 0.33 and 0.68 radians at 10 cm blade width & 0, 0.51 and 1.05 radians at 15cm blade width) and two levels of blade width (10 and 15 cm) were studied.

It was found that the specific soil resistance and energy consumed per unit volume decreased with increase in spading frequency and spade angle, but it increased with radius of curvature and blade width. Cone index ratio increased with increase in spading frequency, spade angle and radius of curvature, but it decreased with increase in blade width. Soil bulk density, soil cone index and weighted mean clod size decreased with increase in spading frequency, spade angle and radius of curvature. However, it increased with increase with blade width. Based on the results obtained the optimal combination of spading blade was identified on the basis of soil pulverisation and force/ energy requirement for tillage.

Brzozko and Murawski (2007) studied the effect of loosening depth on power requirement for driving a spading machine on cultivated site at three tractor engine speeds and two gears. It was reported that increase in soil loosening depth resulted in increased power requirement, which also depended on the type of surface being cultivated and tractor engine speed.

In double digging, a 30 cm deep trench was dug across the width of the bed with a flat spade and the soil from that first trench was set aside. The 30 cm below the trench was loosened with a spading fork (Jeavons 2001). When the next trench was dug, that soil was dropped into the empty space of the first trench and the lower layer was again loosened with a spading fork. This process was repeated along the full length of the bed. The final trench was filled with the

soil that was removed from the first trench. The result was a bed that has been tilled to a depth of 60 cm. The soil of the double dug bed had a greater drainage and aeration, which allowed the roots to go deeper and reach the nutrients. During subsequent seasons, it was surface cultivated 5 cm to 10 cm deep. Mohler et al (2006) described the critical depth phenomenon that might not be captured by averaging coarser depth interval.

Nam *et al* (2012) analysed the motion of tillage blades for estimation of tillage characteristics of crank-type and rotary-type rotavator. The inter-relation between tillage traces from motion analysis and field test results including rotavating depth, pulverizing ratio and inversion ratio at the same work conditions were analysed for both crank-type and rotary-type rotavators.

To analyse motion, joint conditions of the main connecting component were specified considering the actual working mechanism of rotavator. In the result, motion analysis and field test results show significant correlations. It was found that further study is needed for applying motion analysis to estimate the accurate tillage related parameters such as rotavating depth, the soil pulverizing ratio and inversion ratio, it could be used to compare the tillage characteristics of various rotavators quickly.

Nam *et al* (2012) conducted research to understand the work performance of crank-type rotavators and compare them with those of rotary-type rotavators in Korean farmland conditions. Tillage operations were carried out using both rotavators with the same nominal rotavating width and rated power. During the operations, PTO speed, torque, actual work speed, rotavating width and depth were measured. To evaluate work performance, pulverizing ratio, inversion ratio and specific volumetric tilled soil were calculated and compared for each rotavator.

It was found that crank-type rotavator has deeper rotavating depth than rotary-type rotavator. PTO power and torque fluctuation during rotavating were larger in the crank-type rotavator. This may be from the unique operational characteristics of the crank-type rotavator. Average PTO torque, however, was smaller in the crank-type rotavator in the practical gear ranges. In both the rotavators, the actual field capacity increased as the actual working speed increased, while the volume of tilled soil changed irregularly according to the rotavating depth, rotavating width and actual working speed, resulting in larger values in the crank-type rotavator at the same gear condition and at the most commonly used gear ranges. The specific volumetric tilled soil was also larger in crank-type rotavators. The pulverizing ratio was better in the rotary-type rotavator while inversion ratio didn't show meaningful differences between both rotavators. The crank-type rotavator is good in the aspect of low power consumption and deep tillage available even though the pulverizing effect is not good but they are acceptable. Thus,

crank-type and rotary type rotavator have different properties each other in several work performances. It's important, therefore, to choose a suitable type of rotavator that satisfy the farmer's requirements in accordance with the condition of field and the purpose of tillage operation

Kim *et al* (2013) investigated the effects of tillage blade shape on tillage and power consumption characteristics for a crank-type rotavator. Three types of tillage blades were applied, i.e. standard blade, end sloped blade and narrow blade for the purpose of the study. Tillage operations were carried out using each blade with the same prime mover tractor and rotavator platforms in two different soil and Power Take Off (PTO) speed conditions. During the operations, PTO speed and torque, soil pulverizing ratio and inversion ratio, actual work speed and rotavating width and depth were measured and the required power of the PTO shaft, field capacity and flow of tilled soil were calculated to compare the characteristics according to the tillage blade shape. Experimental results show that the rotavating width, actual work speed, field capacity, flow of tilled soil and soil inversion ratio were independent of the blade shape, whereas the rotavating depth and soil pulverizing ratio were influenced by the blade shape according to the soil condition. In the most commonly used tractor gear conditions of L2 and L3, the PTO power of the end-sloped blade and narrow blade were almost the same as each other and significantly lower than the standard blade in the paddy field, whereas there were no significant differences among blades in the dry field. It was concluded that if an adequate blade shape suitable for specific soil conditions is applied to the crank-type rotavator, power efficiency and good tillage performance operation can be achieved at the same time. They suggested further research to be needed to determine the optimal shape of tillage blade with certain soil properties.

Kwon *et al* (2014) did feasibility study to evaluate crank-type walking cultivators for weeding in furrowed upland. A crank type walking cultivator was developed and assessed on the factors of working speed (S), depth of cultivator (CD) and weed performance (WP). The field evaluation was conducted in upland field in Korea in month of July and August of 2012. To know more about the design improvements, kinematic analysis was also performed. Working speed in flat, uphill and downhill was about 0.11 m/s, 0.11 m/s and 0.13 m/s, respectively and had low relevance with the user conditions. Cultivator depth was range from 35 - 40 mm which was satisfied with the RDS (Rural Development Administration, South Korea) guide for weeding machine.

Depending upon the growth stages of weed and field conditions a wide variation was observed. The weeding performance of the cultivator was satisfactory for weeds in early growth stage but it showed difficulties in handling on up-slope and in entering up-land. Specifically, the weight of the cultivator was judged as overweight for female workers. Thus, the crank-hoe

type cultivator was judged as unsuitable for small walking type machine due to weight of the four-bar linkage system. Kinematic analysis revealed that the ratio of crank speed to the ground speed must be 850 rpm s m⁻¹ (255 rpm based on 0.3 ms⁻¹) or greater to avoid uncultivated area. Selection of forward speed is a decisive factor in designing the weeding cultivator.

Kim *et al* (2015) used a dynamic analysis program called Recurdyn to predict the fatigue life of a crank-type rotavator evaluated on the uplands and paddy fields in Korea. Torque on PTO shaft was also recorded during the experiment. An S-N curve (plot of the magnitude of an alternating stress versus the number of cycles to failure for a given material) for prediction of fatigue life of the crank-type rotavator was constructed according to the GL (Germanischer Lloyd Wind Energie GmbH, Hamburg, Germany) guideline based on the experimental and analytical results.

The torques experienced by the PTO shaft in the paddy soil and the uplands were in the range of 472 to 797 Nm and 313 to 430 Nm, respectively, for every condition. In case of load condition, the peak torques (846 Nm, 770 Nm) were measured for severe conditions, resulting in a maximum (von Mises) stress of 75 MPa at the crank arm. Fatigue life of the crank-type rotavator was predicted to be 1167 h that satisfies the target value of 1,110 h by substituting the analysis results into an S-N curve of crank arm. Thus, fatigue life of the crank-type rotavator was within the target life for the studied soil conditions; however, it was also stated that further field experiments for various soil conditions would be required to verify the prediction results.

Giordano *et al* (2015) conducted a research to compare a traditional ploughing and a spading (performed at different travelling and rotor speeds) in a paddy field. In this study both technical and agronomic parameters (working time, power required, fuel consumption, pulling force, efficiency of crop residues incorporation, etc.) were considered. They found that traditional ploughing indicated 51% higher effective tillage capacity and reduced in fuel consumption ranging between 20.8 to 44.1% per surface unit. On the other hand, spading machine witnessed no or minimum pulling force, thus making it easier to use adverse conditions such as in wet soil.

Spading machine also demonstrates advantages such as not making hardpan at the bottom of the working depth, which helps in deeper root penetration of crops and does not allow the capillary circulation of the solution into the soil. Surely having a compact layer in paddy field helps in reduced water consumption, so it is not considered a problem to be solved. The spading machine also showed better inversion characteristics thus mixing the organic matter completely with tilled layer of soil.

Dhiman (2016) carried out a study to evaluate the field performance of spading machine and to suggest suitable operational parameters. The research was carried out in

department of Farm Machinery & Power Engineering, PAU, Ludhiana. The 5-spades spading machine used in the study was manufactured by an Italian company 'Selvatici'. The study involved soil type different soil types (S1: sandy loam and S2: silty clay loam), forward speed (two levels: F1: 2.26 km/h and F2: 3.37 km/h), and depth of cut (three levels: D1: 20 cm, D2: 24 cm and D3: 28 cm) as independent parameters. Their effects were studied on dependent parameters like soil bulk density, PTO torque, soil strength (cone index) and pulverization index (weighted mean clod diameter). Bulk density was found to be significantly higher in sandy loam (S1) than silty clay loam (S2). Bulk density was significantly lower in case of lower forward speed (F1) than higher forward speed (F2). Bulk density increased significantly with increase in depth of cut. PTO torque was significantly lower in sandy loam (S1) than silty clay loam (S2). PTO torque was significantly lower for lower forward speed (F1) than higher forward speed (F2). PTO torque increased significantly with increase in depth of cut. Soil strength was significantly lower in sandy loam (S1) than silty clay loam (S2). Soil strength increased significantly with increase in forward speed. Soil strength increased significantly with increase in depth of cut. Pulverisation index (MMD) was significantly lower in sandy loam (S1) than silty clay loam (S2). MMD increased significantly with increase in forward speed in both sandy loam and silty clay loam. MMD increased with increase in depth of cut non-significantly in sandy loam and significantly in silty clay loam. The best operational parameters for this machine were found to be lower forward speed (F1: 2.26 km/h) and lowest depth of cut (C1: 20 cm) in sandy loam.

It can be concluded from the review of literature that:

- Spading machine does not compact the sub soil surface while operation.
- The power and energy requirement of the spading machine is less or comparable to rotary tillage machine depending on soil condition.
- It can also work under wet soil condition.
- It does not demand draft force as compared to conventional tillage implements.
- It is capable of penetrating soil to much deeper than conventional rotary tillage.
- Blades enter the soil one at a time, thereby reducing overall power requirement.

Literature reviewed showed that there is limited knowledge on design and operational parameter of spading machine for Indian condition.

CHAPTER – III

MATERIALS AND METHODS

Tillage consumes large amount of energy thus our goal was to make the machine as efficient as possible and also give satisfactory output thus provide good soil structure and tilth for good plant growth. To achieve this objective, one must have the functional requirement of the spading machine and how soil force react during its operation. This Chapter deals with the design, development and evaluation of tractor operated spading. The machine was designed empirically and using CAD software. It was developed and assembled with the help of local manufacturer.

The field evaluation was carried out at departmental research farms of Farm Machinery and Power Engineering, PAU, Ludhiana. The machine is evaluated on selected machine variables and parameters which are need to describe the soil condition before and after the tillage operation being performed were considered. The design parameters, variables studied, equipment's and instruments used, experimental procedure and statistical design followed have been discussed in this chapter as under following sub-heads:

- 3.1 Study of soil failure action of spading machine
- 3.2 Kinematic analysis of crank-rocker mechanism
- 3.3 Design of spading machine
- 3.4 Computer aided design and development of spading machine
- 3.5 Field evaluation of developed spading machine

3.1 Study of Soil Failure Action of Spading Machine

In former times when mankind learned to grow food to feed themselves, they developed basic tool to make things easier. The simplest tool invented was spade which can be used for many operations such as field preparation, inter-culture operation, bund forming. Nowadays spade is used by small farmers for farming operation because its action proved to be less energy consuming as reported by Saimbhi (2006) and provide good amount of tilth to soil.

3.1.1 Four Bar Mechanism

A four-bar linkage has four binary links (a link is defined as a rigid body having two or more pairing elements which connect it to other bodies for the purpose of transmitting force or motion) and four revolute joints (Figure 3.2). This means that only one input is required to make the linkage move. Because of its simplicity and perhaps also because of the rapid increase in design complexity suffered by linkages with more than four-bars.



Fig 3.1 Hand spade tool used by farmer

A mechanism is one in which one of the links of a kinematic chain is fixed. Different mechanisms can be obtained by fixing different links of the same kinematic chain. These are called as inversions of the mechanism. By changing the fixed link, the number of mechanisms which can be obtained is equal to the number of links. Excepting the original mechanism, all other mechanisms will be known as inversions of original mechanism. The inversion of a mechanism does not change the motion of its links relative to each other.

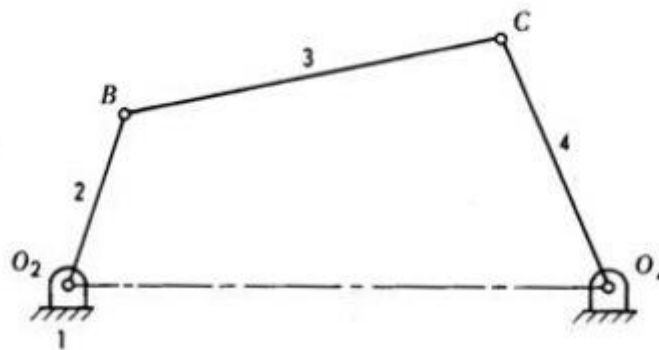


Fig. 3.2 Four-bar linkage mechanism (Myszka 2012)

In four-bar mechanism, when the sum of shortest and longest rod is less than or equal to the sum of other two rods, the mechanism exists crank. During this when the crank link is the shortest link, the mechanism is known as crank-rocker mechanism. It is one of the most useful and most common type of four-bar mechanism (Figure 3.3). In this mechanism, the link which can make complete rotation is known as crank (link 2). The link which oscillates is known as rocker or lever (link 4). The link connecting these two is known as coupler (link 3). Link 1 is the frame.

As shown in Fig 3.3, in the crank-rocker mechanism OABC, the mechanism mainly composed by crank (OA), connecting rod (AB), rocker (BC) and frame (OC). Where O, A, B and C are each link point. Rocker swing angle $\angle B_1CB_2 = \Psi$, pole position angle $\angle B_1OB_2 = \theta$, thus the travel velocity ratio coefficient can be obtained $K = (180^\circ + \theta) / (180^\circ - \theta)$.

In this mechanism, crank (OA) rotates completely and rocker (BC) oscillates from B_1 to B_4 . It shows that rocker mechanism as OA have full 360° rotation. $\angle A_3B_3C$ and $\angle A_4B_4C$ are the minimum angle δ_{\min} and maximum angle δ_{\max} between the connecting rod and rocker, respectively. Regardless of the friction influence, the transmission angle γ_{\min} of crank-rocker mechanism is the smallest values of δ_{\min} or $180^\circ - \delta_{\min}$ (when $\delta_{\min} > 90^\circ$).

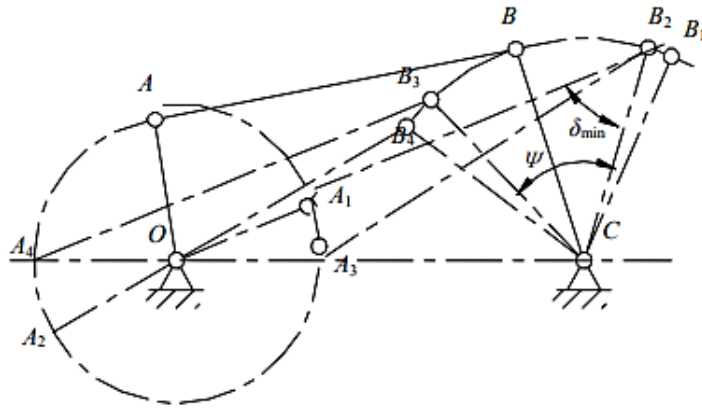


Fig. 3.3 Movement of crank-rocker mechanism (Jian 2015)

To have the same action or movement of spade in a tractor operated machine can be achieved by using the four-bar linkage mechanism. From the above study it was found that crank-rocker mechanism of four bar linkage will perfectly mimic the motion of hand spade in tractor operated spading machine.

Figure 3.4 show the nomenclature of main parts of spading machine using the crank-rocker linkage mechanism. Its main parts are crank (which take full 360° rotation), rod (which is called as coupler to transmit motion to rocker), rocker arm (it is called rocker because it oscillates and does not take full rotation) and spades which are attached to the overextending coupler to penetrate into soil and breaks it.

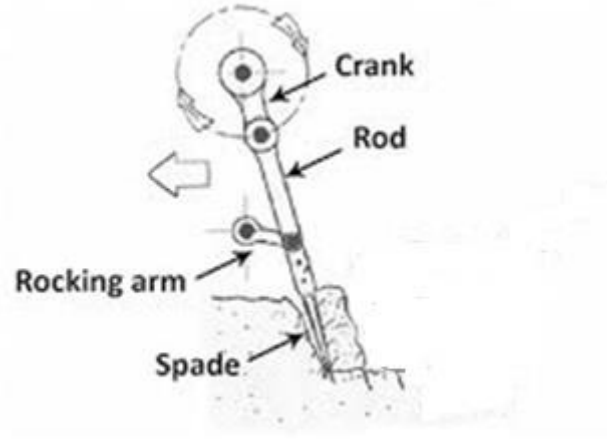


Fig. 3.4 Nomenclature of the main parts of the spading (Giordano *et al* 2015)

3.1.2 Crank-rocker linkage optimization

The motion characteristics of crank rocker mechanism were analyzed and the parameterization model of crank-rocker mechanism has been established by motion simulation software for data analysis and optimization of the transmission angle. Transmission angle is an important parameter in the crank rocker mechanical design and denotes the quality of motion transmission in a mechanism. The greater the transmission angle of mechanism, the higher the transmission efficiency. A measurement of angle parameter has been arranged between the connecting rod and rocker, then taken the maximum of this measurement as the objective function. Gravity constraints are applied to the entire mechanism, rotation constraints are added between two members of the crank and the earth, the crank and the connecting rod, the connecting rod and the rocker, the rocker and the earth. The drive is applied on the crank, and the angular velocity is initially set to 1 rad/s and increased to 20 rad/sec.

According to system model, the mechanical dynamics analysis could automatically establish Lagrange equation based on the dynamic theory of multi-body system. Assuming the crank as the active component to do constant velocity rotation and rocker as the follower to swing back and forth. The crank has strictly had to be the shortest link among all other links of the mechanism. Other constraint functions are expressed as follows so as to have crank-rocker mechanism (Jian 2015).

$$G_1 = L_1 + L_2 - L_3 - L_4 \leq 0$$

$$G_2 = L_1^2 + L_2^2 - L_3^2 - L_4^2 \leq 0$$

$$G_3 = L_1 - L_2 \leq 0$$

$$G_4 = L_1 - L_3 \leq 0$$

$$G_5 = L_1 - L_4 \leq 0$$

Where,

G1, G2, G3, G4 and G5 are the constrain function for crank-rocker mechanism

L1, L2, L3 and L4 are the length of crank, connecting link, rocker and frame, respectively

Assuming the swing angle of the crank rocker mechanism of $\Psi=60^\circ$, the length of rocker $L_3=279$, the work scope of the crank rocker mechanism model is $120 \text{ mm} \leq L_1 \leq 170 \text{ mm}$, $350 \text{ mm} \leq L_2 \leq 400 \text{ mm}$ and $400 \text{ mm} \leq L_4 \leq 450 \text{ mm}$ (50 mm range is provided for optimization of all linkages). Figure 3.5 shows the view of simulation software used for the optimization of crank-rocker mechanism.

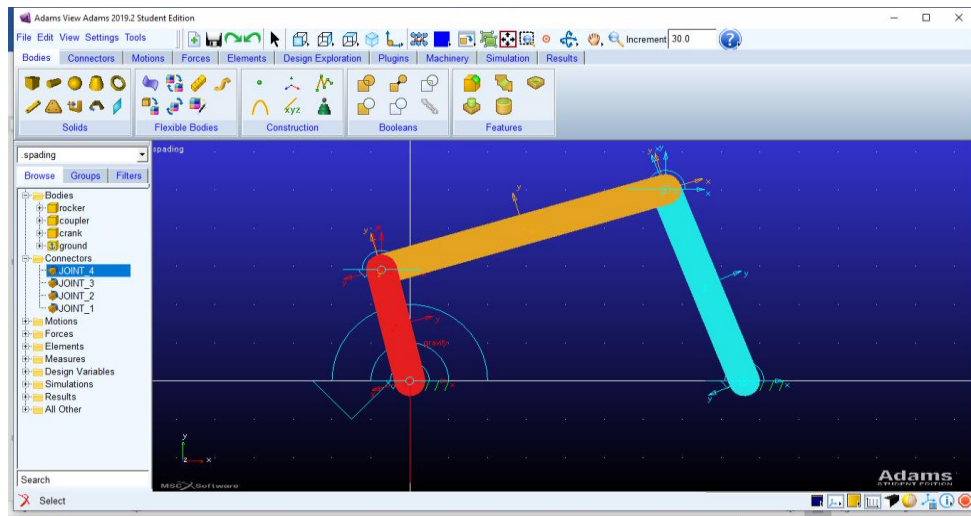


Fig. 3.5 A view of simulation software used for link optimization

The curve for each iteration value of the objective function is shown in figure 3.6, as it can be seen the optimized value of the mechanism comes out to be 45.7° after eight iteration.

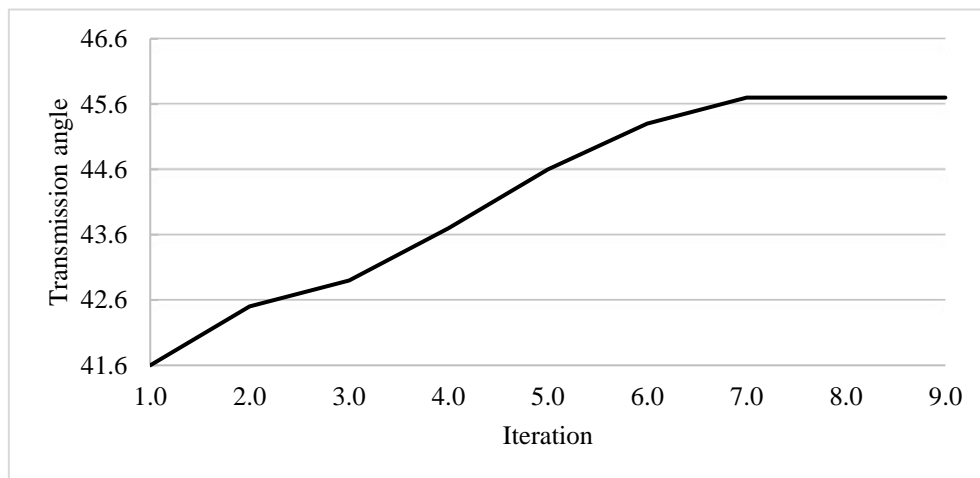


Figure 3.6 Optimization iteration graph

The optimized length of each links are $L_1 = 150 \text{ mm}$, $L_2 = 388 \text{ mm}$, $L_3 = 279 \text{ mm}$ and $L_4 = 436 \text{ mm}$.

3.2 Kinematic analysis of crank-rocker mechanism

3.2.1 Mobility

Mobility defines the linkage degrees of freedom, which is the number of actuators needed to operate the mechanism. The symbol of mobility (M) and it could be calculated through the Gruebler's equation:

$$M = 3 \times (N - 1) - 2j_p - j_h \quad (3.1)$$

Where,

M – degrees of freedom

N – total number of links, including ground

j_p - total number of primary joints (full joints)

j_h - total number of higher-order joints (half joints)

The mobility of a crank-rocker mechanism was calculated using equation 3.1:

$$M = 3 \times (N - 1) - 2j_p - j_h = 3 \times (4 - 1) - 2(4) - 0 = 1 \quad (3.2)$$

As calculated from equation 3.2, the crank-rocker mechanism has one degree of freedom. This shows that crank-rocker mechanism is fully operated with one driver link.

3.2.2 Analytical analysis of crank-rocker mechanism

The main objective of analyzing a mechanism is to study its motion. Motion proceeds, as the position of links is changed which happened due to the movement in the mechanism configuration by forces. To collect results with a high degree of accuracy, analytical methods in the position analysis is used, as defined by Myszka (2012). During analysis of the mechanisms, triangle method of position analysis is be used. Triangle method includes fitting reference lines within a mechanism and studying the triangles. An angular position, θ , is defined as the angle a line between two points on that link forms with a reference axis.

Angular Position is specified by Rider (2015):

1. As positive, if the angle is measured counterclockwise from the reference axis.
2. As negative, if the angle is measured as clockwise from the reference axis.

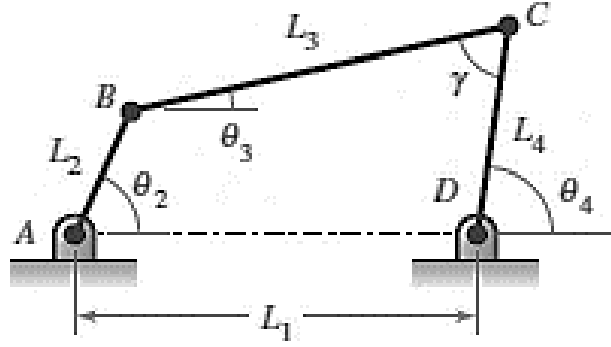


Fig. 3.7 Illustration of crank-rocker bar (Myszka, 2012)

Where,

θ_2 = certain crank angle

$\theta_3, \theta_4, \gamma$ = interior joint angles

L_1, L_2, L_3, L_4 = links

$$BD = \sqrt{L_1^2 + L_2^2 - 2 \cdot L_1 \cdot L_2 \cos \theta_2} \quad , \text{ mm} \quad (3.3)$$

$$\gamma = \cos^{-1} \left[\frac{L_3^2 + L_4^2 - (BD)^2}{2 \cdot L_3 \cdot L_4} \right] \quad (3.4)$$

$$\theta_3 = 2 \tan^{-1} \left[\frac{-L_2 \cdot \sin \theta_2 + L_4 \cdot \sin \gamma}{L_1 + L_3 - L_2 \cdot \cos \theta_2 - L_4 \cdot \cos \gamma} \right] \quad (3.5)$$

$$\theta_4 = 2 \tan^{-1} \left[\frac{L_2 \cdot \sin \theta_2 - L_3 \cdot \sin \gamma}{L_2 \cdot \cos \theta_2 + L_4 - L_1 - L_3 \cdot \cos \gamma} \right] \quad (3.6)$$

Crank angle is taken from 0-360° (at 30° interval) as crank takes full 360° rotation. The optimized link lengths were considered during the calculation as obtained in section 3.1.2.

Table 3.1 Angle of crank-rocker mechanism for θ_2 (0-360° at 30° interval)

θ_2 , degree	BD, mm	γ , degree	θ_3 , degree	θ_4 , degree
0	286.00	47.38	45.88	93.27
30	315.15	53.41	31.53	84.94
60	383.66	67.98	22.60	90.57
90	461.08	85.82	18.14	103.95
120	527.25	103.25	16.74	119.99
150	570.85	116.76	18.32	135.09
180	586.00	122.09	23.79	145.88
210	570.85	116.76	33.42	150.19
240	527.25	103.25	45.27	148.51
270	461.08	85.82	56.11	141.92
300	383.66	67.98	62.18	130.15
330	315.15	53.41	59.07	112.47
360	286.00	47.38	45.88	93.27

3.2.3 Velocity and Acceleration Analysis

Using the Myszka's theory of position equations for a four-bar linkage, velocity and acceleration calculations of crank-rocker mechanism using the calculated link length and angles are used and the velocity and acceleration of links were determined.

$$\omega_3 = -\omega_2 \left[\frac{L_2 \cdot \sin(\theta_4 - \theta_2)}{L_3 \cdot \sin \gamma} \right] \text{ [rad/s]} \quad (3.7)$$

$$\omega_4 = -\omega_2 \left[\frac{L_2 \cdot \sin(\theta_3 - \theta_2)}{L_4 \cdot \sin \gamma} \right] \text{ [rad/s]} \quad (3.8)$$

$$\alpha_3 = \left[\frac{\alpha_2 L_2 \cdot \sin(\theta_2 - \theta_4) + \omega_2^2 L_2 \cdot \cos(\theta_2 - \theta_4) - \omega_4^2 L_4 + \omega_3^2 L_3 \cdot \cos(\theta_4 - \theta_3)}{L_3 \cdot \sin(\theta_4 - \theta_3)} \right] \text{ [rad/s}^2\text{]} \quad (3.9)$$

$$\alpha_4 = \left[\frac{\alpha_2 L_2 \cdot \sin(\theta_2 - \theta_3) + \omega_2^2 L_2 \cdot \cos(\theta_2 - \theta_3) - \omega_3^2 L_3 + \omega_4^2 L_4 \cdot \cos(\theta_4 - \theta_3)}{L_4 \cdot \sin(\theta_4 - \theta_3)} \right] \text{ [rad/s}^2\text{]} \quad (3.10)$$

Where,

ω_3 and ω_4 = angular velocity for θ_3 and θ_4

α_3 and α_4 = angular acceleration for θ_3 and θ_4

Analytical analysis of crank-rocker has performed on the optimized length as obtained in section 3.1.2. Table 3.2 shows the values of θ_3 , θ_4 , γ , ω_3 , ω_4 , α_3 and α_4 (in degree, degree/sec and degree/sec²) using the equation 3.3 to 3.10. θ_2 (crank angle) is considered from 0-360° at 30° interval.

Table 3.2 Analytical analysis of crank-rocker mechanism using optimized link length values

θ_2	γ	θ_3	θ_4	ω_3	ω_4	α_3	α_4
0	47.38	45.88	93.27	-31.55	-31.55	-2.88	48.98
30	53.41	31.53	84.94	-23.71	-1.08	24.74	52.00
60	67.98	22.60	90.57	-12.76	21.19	17.75	32.22
90	85.82	18.14	103.95	-5.62	30.82	11.85	11.33
120	103.25	16.74	119.99	0.01	32.34	11.60	-8.00
150	116.76	18.32	135.09	6.70	27.06	15.74	-23.67
180	122.09	23.79	145.88	15.40	15.40	17.75	-27.29
210	116.76	33.42	150.19	22.52	2.16	9.22	-19.72
240	103.25	45.27	148.51	23.89	-8.45	-3.92	-17.17
270	85.82	56.11	141.92	18.36	-18.09	-18.79	-20.49
300	67.98	62.18	130.15	4.42	-29.53	-37.60	-19.14
330	53.41	59.07	112.47	-17.65	-40.28	-45.45	6.07
360	47.38	45.88	93.27	-31.55	-31.55	-2.88	48.98

3.3 Design of spading machine

3.3.1 Design and selection of gearbox

As the power for spading machine comes from PTO shaft of tractor, it had standard 540 rpm as majority of tractor comes with 540 rpm. However, 167 rpm (taken as reference from commercially available spading machines worldwide) were needed at crank for efficient spading action and having a suitable bite length. Hence, the speed reduction was

$$S.R. = 540/167 = 3.2$$

Hence, a gearbox of 1:3.2 speed ratio i.e. bevel gear to pinion ratio of 9:31 was selected and rest all the design was done accordingly.

Gearbox of spading machine was designed for 50 hp tractor (Khurmi and Gupta 2005).

Power at PTO = 90% of tractor hp = 90% of 50 hp = 45 hp or 33.55 kW

Rotational speed of pinion, $N_p = 540$ rpm

Rotational speed of gear, $N_G = 167$ rpm

Number of teeth of pinion, $T_p = 9$

Module, $m = 6$

Pitch circle diameter of pinion, $D_p = m \times T_p = 54$ mm

$$\text{Velocity Ratio, } V.R. = N_p/N_G = 3.23 \quad (3.11)$$

$$\text{Also } V.R. = T_G/T_p = \quad (3.12)$$

$$\text{Thus, } T_G = V.R. \times T_p = 3.23 \times 9 = 31$$

$$V.R. = T_G/T_p = 31/9 = 3.44$$

Pitch diameter of gear, $D_G = m \times T_G = 6 \times 31 = 186$ mm, because for a pair of bevel gears, module has to be same.

$$\text{Pitch line velocity of pinion, } V = \frac{\pi D_p N_p}{60} = \frac{3.14 \times 0.054 \times 540}{60} = 1.52 \text{ m/s} \quad (3.13)$$

Taking Service factor, $C_s = 1.25$ (for 8-10 hours per day with high shock load)

$$\text{Design tangential load, } W_T = \left(\frac{P}{V}\right) \times C_s = 27.425 \text{ kN} \quad (3.14)$$

$$\text{Dynamic load, } W_D = W_T + \frac{21V(b.C + W_T)}{21V + \sqrt{b.C + W_T}} \quad (3.15)$$

$$\text{Where, } b = L/4 \text{ and } L = \sqrt{\left(\frac{D_G}{2}\right)^2 + \left(\frac{D_p}{2}\right)^2}$$

$L = 136.95 \text{ mm}$, thus $b = 34.23 \text{ mm}$

$C = \text{deformation factor} = 456 \text{ N/mm}$ (for 20° full depth involute gears of alloy steel with 0.04mm tooth error in action)

$$\text{So, } W_D = 27425 + \frac{21 \times 1.52 (34.23 \times 456 + 27425)}{21 \times 1.52 + \sqrt{34.23 \times 456 + 27425}} = 27632.44 \text{ N}$$

Beam strength of endurance strength of the tooth, $W_s = f_e \cdot b \cdot p_c \cdot y'$

where, $f_e = 700 \text{ N/mm}^2$ (flexural endurance stress for alloy steel having BHN more than 400),

$$p_c = \pi \cdot m = 3.14 \times 6 = 18.85$$

Tooth form factor, $y' = 0.124 - \frac{0.912}{T_E}$ with $T_E = T \cdot \sec \theta_P$ and $\theta_P = \tan^{-1} \left(\frac{1}{V.R.} \right)$

$$\text{Here, } \theta_P = 16.20, T_E = 11.76 \text{ and } y' = 0.124 - \frac{0.912}{11.76} = 0.76$$

$$\text{So, } W_s = 700 \times 34.23 \times 18.85 \times 0.076 = 34,326.52 \text{ N}$$

Since, W_s is greater than W_D ; $34326.52 > 27632.44$, so, design is safe against breakage if tooth gears in operation. So, alloy steel of Ind. Std./ASP designation of 16NiCr2Mo20 was selected for giving $f_e = 700 \text{ N/mm}^2$ and having BHN more than 400. Suitable gears were procured from local market and assembled.

3.3.2 Design of shaft for bevel gears

The design of shaft is based upon maximum shear stress in torsion as there was no data for bending moments at input shafts of gearbox.

Design load of input shaft, $P = 33.55 \text{ kW}$

$$\text{Thus, torsional moment, } T = \frac{P \times 60}{2 \times \pi \times 540} = \frac{33.55 \times 60}{2 \times \pi \times 540} = 590.162 \text{ Nm}$$

Selected shaft diameter. $D = 35 \text{ mm}$, combined shock

Fatigue factor = $k_t = 1.2$

$$\text{Maximum shear stress in torsion, } f_s = \frac{16(k_t T)}{\pi d^3} = 52.35 \text{ MPa}$$

Adding allowance for keyways or splines, allowable shear stress = $f_s / 0.75 = 68.8 \text{ MPa}$

So, mild steel of Ind. Std./ASP designation of C40 was selected for giving $f_s = 75 \text{ MPa}$ for adequate safety in torsional shear.

3.3.3 Selection of blade

Tillage load is the highest when the blade contacts with the soil surface to enter into the subsoil (Choi and Nahmgung, 2000). The initial contact of blade with the soil surface is made for a brief moment, so it could be considered as an impact load. The load in the blade is generally concentrated in the lower part of the tillage blade (Shmulevich *et al* 2007). As lower part of the spade of spading machine contacts with the soil surface at very first, therefore, it can be assumed that all the impact loads is applied to the lower part of the blade. In practice, for the spading machine used for a long time, the paint of the lower part of the blades has been peeled off first as observed by Dhiman (2016). Thus, the lower part of the blades was set as loading surface. From review and literature, it was found that trapezoidal shaped blade gives better performance than other (Bishnoi 2008). Taking into account the unit draft of heavy soil as 14.71 N/cm^2 (Sharma and Mukesh 2008) and dimensions of spading blade were selected based on the blades used in commercially available machines worldwide.

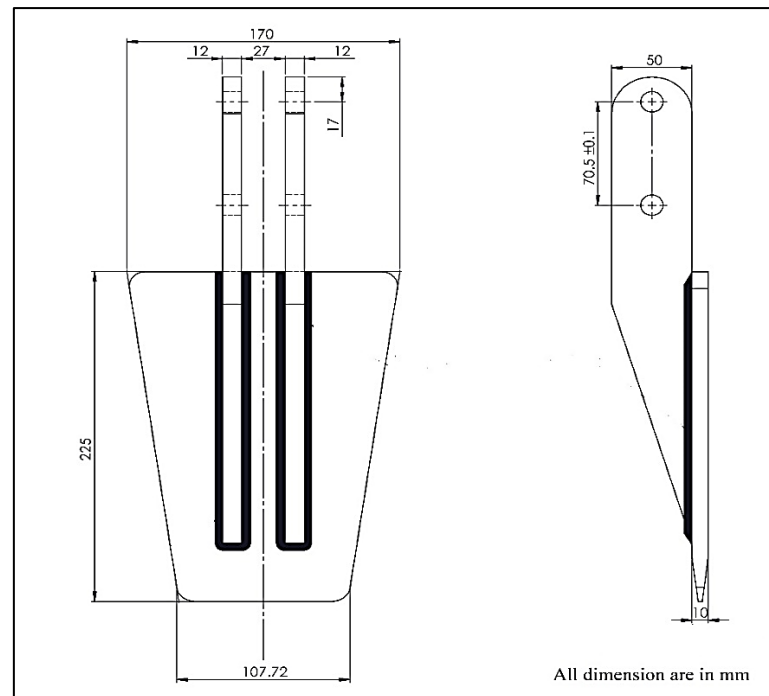


Fig 3.8 Front and side view of selected blade

Dynamic analysis of the selected blade shows the normal force which should be added to the loading surface of tillage blade was 10,247 N. Stress analysis simulation in CAD software shows that maximum equivalent stress on the tillage blade was 424 MPa as evident from figure 3.9 of von mises stress analysis diagram of blade. The tensile yield strength of the nominal tillage blade made with S45C is 490Mpa and safety factor for the 1.15 which is sufficiently safe. Figure 3.8 shows the front and side view of blade selected for spading machine.

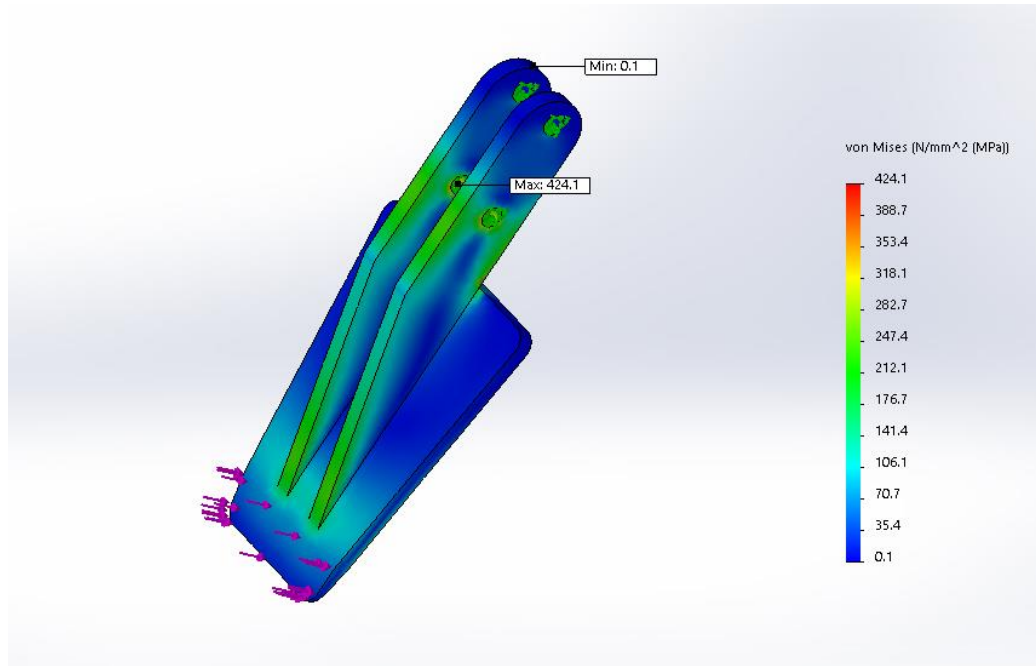


Fig. 3.9 Von mises stress diagram of blade

3.3.4 Trochoidal path tracing of spading machine blade

Trochoidal path is the path followed by a fixed point on a tool. It is one of the most important characteristics in for design and development of a machinery. It helps in understanding the motion followed by the it and how the tool interact when its used. Trochoidal path curve for the blade of spading machine was traced with the help of CAD software. The CAD model of crank-rocker linkage mechanism (using optimized link lengths) was developed and selected blade was attached to the coupler end (called as pen). A point is defined at the tip of blade to trace its motion. The CAD model was given constraints of a four-bar mechanism and forward motion is applied on the model. As crank link begins to rotate along with the forward motion of model, a curve is traced for the selected point in blade. Fig 3.10 show the trochoidal curve traced by CAD software on blade of crank-rocker mechanism model.

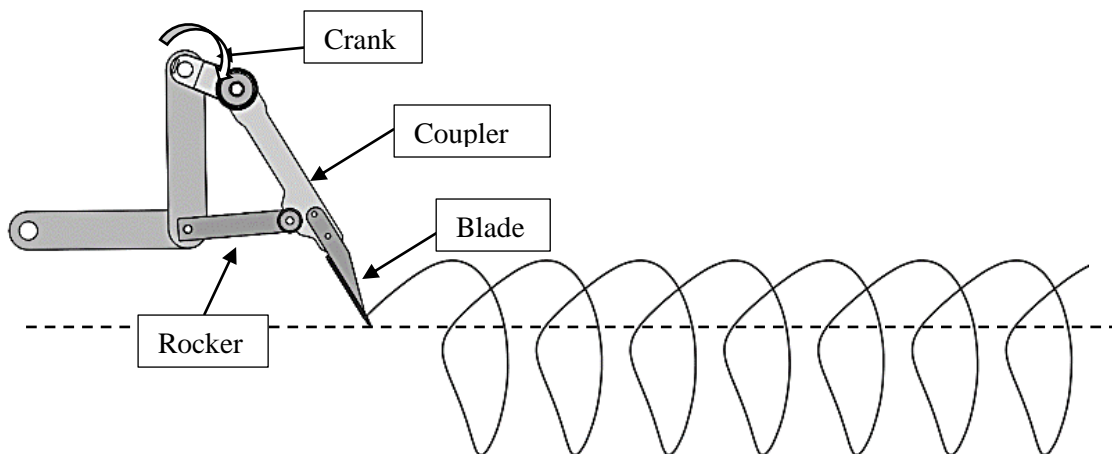


Fig 3.10 Trochoidal curve traced by the blade tip

Trochoidal curve study is useful in selecting the crank rotation rpm. Ratio of forward speed to crank rpm affects the bite length of the machine. The crank-rocker model was tested for different forward speed and crank. The crank speed was changed from 150-170 rpm at forward speed of 2-4 km/h. Too fast crank rpm will result in overlapping (cultivating same spot repeatedly) while too low crank rpm will increase the bite length resulting in untilled spots in the row. Similarly, larger forward speed (keeping crank rpm constant) increased the bite length. Therefore, at 167 rpm of crank, the trochoidal curve show optimum bite length i.e. 6-9 cm.

3.4 Computer aided design and development of spading machine

Computer aided design of spading machine was developed in CAD software. The number of spades in the machine was selected to be eight so that the machine has sufficient width to cover the entire width of tractor which is one of the most important factors determining the field efficiency of the machine. The machine was developed with the help of local manufacturer. The functional requirement of the machine was to cultivate the soil before soil to provide a good tilt for seedbed and proper aeration. The parts of the machine were machined using Computer Numerically Controlled (CNC) machines for accurate fitment and vibrations free working.

3.4.1 Frame of spading machine

A suitable frame was developed such that it should withstand the load coming from the spading machine assembly and forces exerted by the blade during tillage action. Figure 3.11 shows the solid model of frame developed in CAD software. The frame includes crank hub mounting plates, side cover plates, back cover, hitch points and depth adjuster.

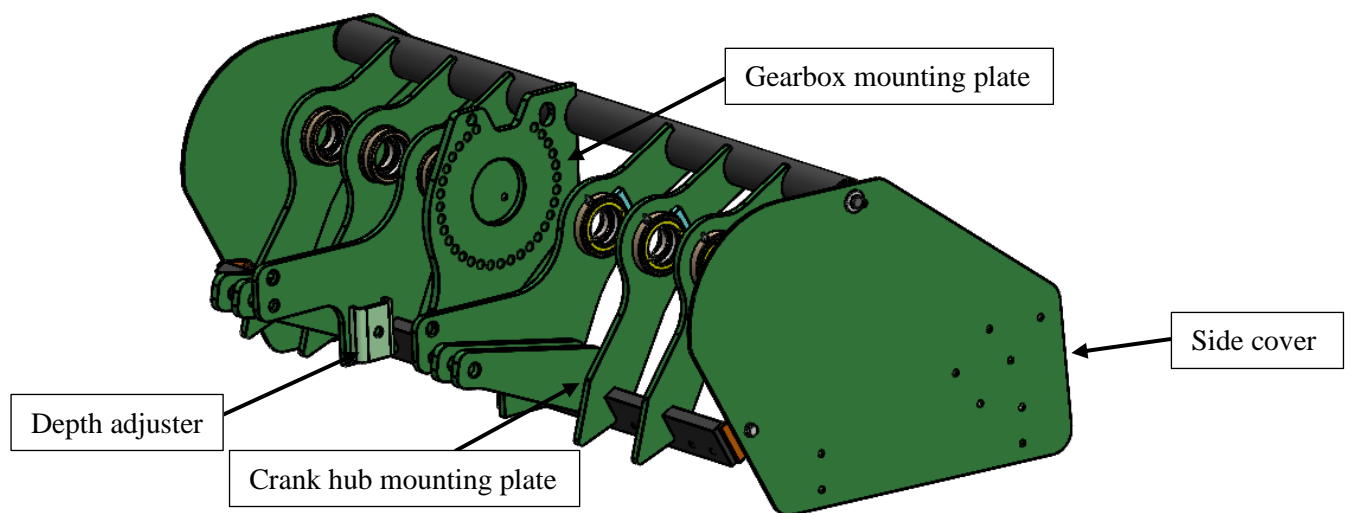


Fig 3.11 Solid model of frame of spading machine



Fig 3.12 Development of frame of spading machine

3.4.2 Gearbox of spading machine

As described in section 3.4.1, gearbox was designed in CAD software. The gearbox has 9:31 gear ratio and total of 16 major components. Input rpm was 540 rpm from tractor PTO which is reduced to 167 rpm for crank of spading machine. The position of gearbox is selected to be in the centre of machine so as to equally distribute the power. Motion was transmitted at 90° angle from both side of gearbox. Figure 3.14 show the exploded view of gearbox with complete assembly. A suitable gearbox housing was developed. It requires 5.6 L of gear oil for good working.

3.4.3 Spade arm of spading machine

Based on the optimized links length, spade arm was developed. The rocker end of coupler arm was extended to attach tillage blade (also called as 'pen'). Fig 3.15 shows the exploded view of spade arm with all major components. A bend is given to four spades to cover up the space left in the centre due to gearbox mounting so that there should be no untilld area left after ploughing. Figure 3.13 shows the developed spade arm after assembly.



Fig. 3.13 Developed spade arm of spading machine

Part No.	Description
1.	Gear box housing
2.	Gasket
3.	Gear box cover
4.	Pinion gear shaft
5.	Taper roller bearing
6.	Oil seal
7.	Spacer bush
8.	Hex head screw
9.	Gear sub assembly
10.	Spacer
11.	Roller bearing
12.	Taper roller bearing
13.	Breather nut
14.	Check nut
15.	Oil seal
16.	Cap

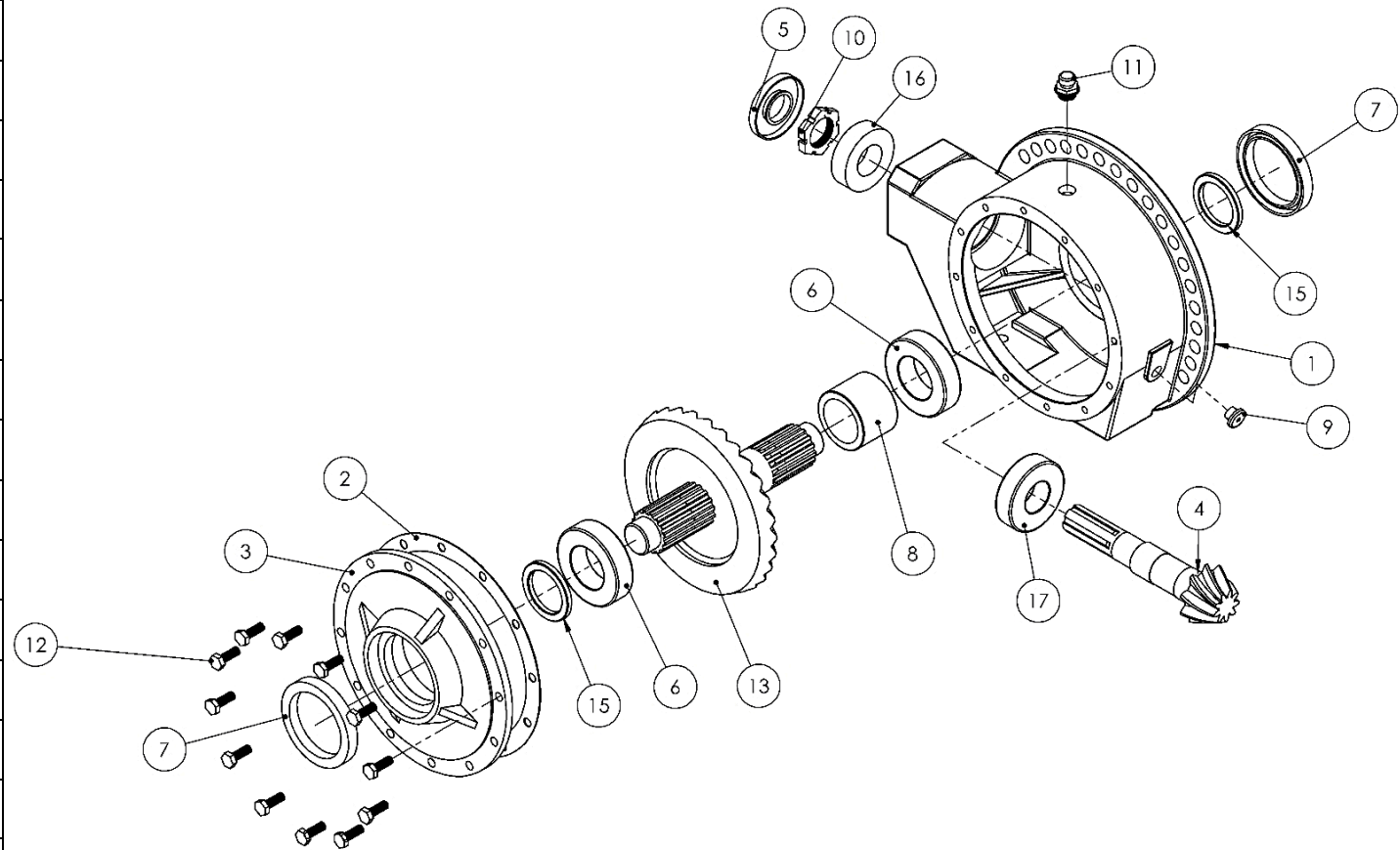


Fig. 3.14 Exploded view of gearbox of spading machine

Part No.	Description
1.	Spade arm
2.	Small cover
3.	Bearing housing cover
4.	Spacer
5.	Oil seal
6.	Oil seal
7.	Small hub spacer
8.	Bearing

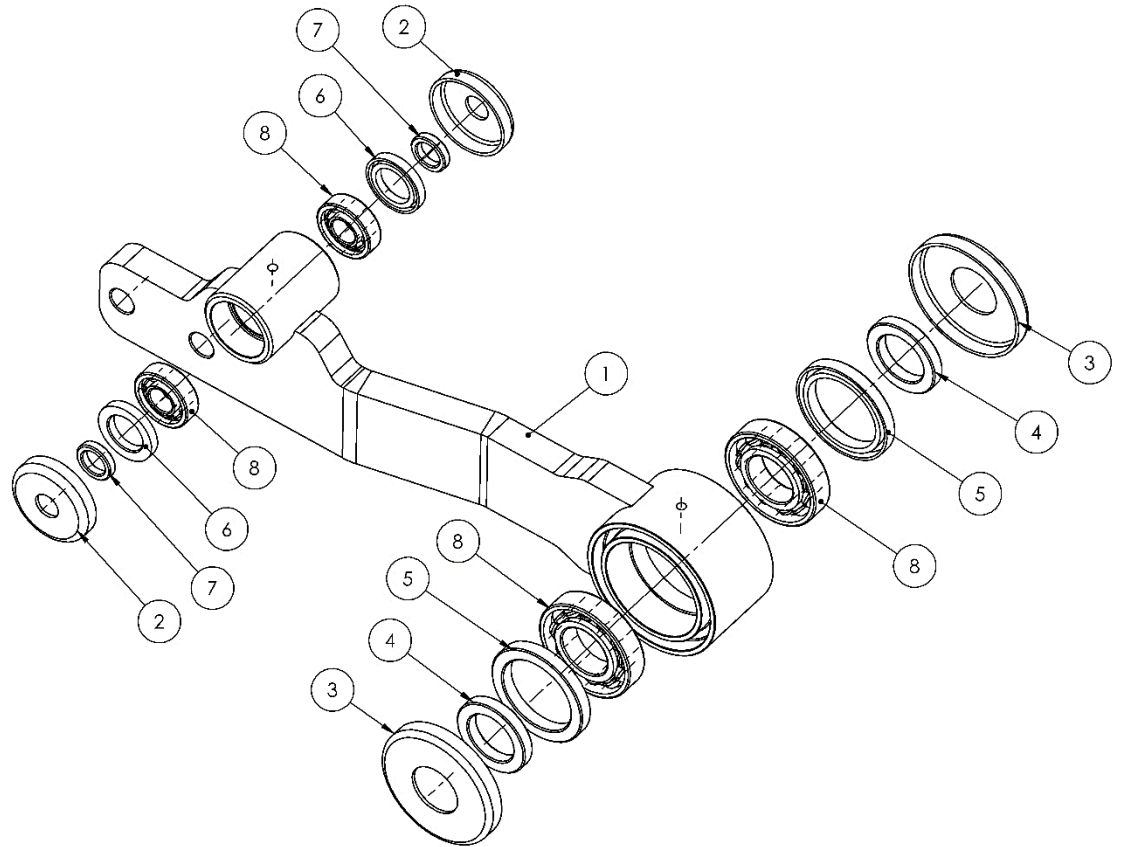


Fig. 3.15 Exploded view of spade arm of spading machine

3.4.4 Crank of spading machine

The crank of optimized length were obtained after link optimization of crank-rocker mechanism is developed. The crank part was casted with steel grade casting so as to with stand load during the machine operation. Figure 3.16 shows solid model of crank having slots made on hub mouting of crank so that key can slide with two crank and both side crank can have motion. The hub of crank hold two crank together and transmit same rotary motion.

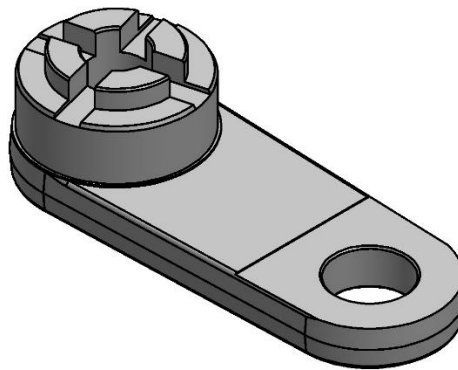


Fig 3.16 Solid model of crank of spading machine

3.4.5 Depth adjuster of spading machine

Spading machine was designed to work upto 30 cm. To adjust the depth of the machine during field operation, depth adjusting mechanism was required. Thus, depth adjusters were developed which can vary height to various levels. The flat plat was having seven holes to adjust the depth at seven different levels as seen in figure 3.17. The bottom sliding plate of the depth adjusted was given 80° bend for smooth operation.

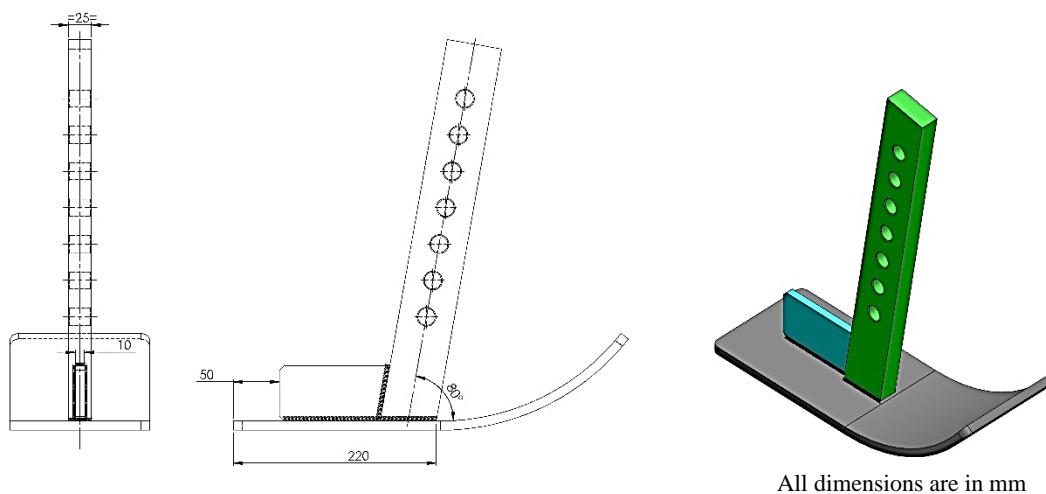


Fig. 3.17 CAD drawing of depth adjuster of spading machine

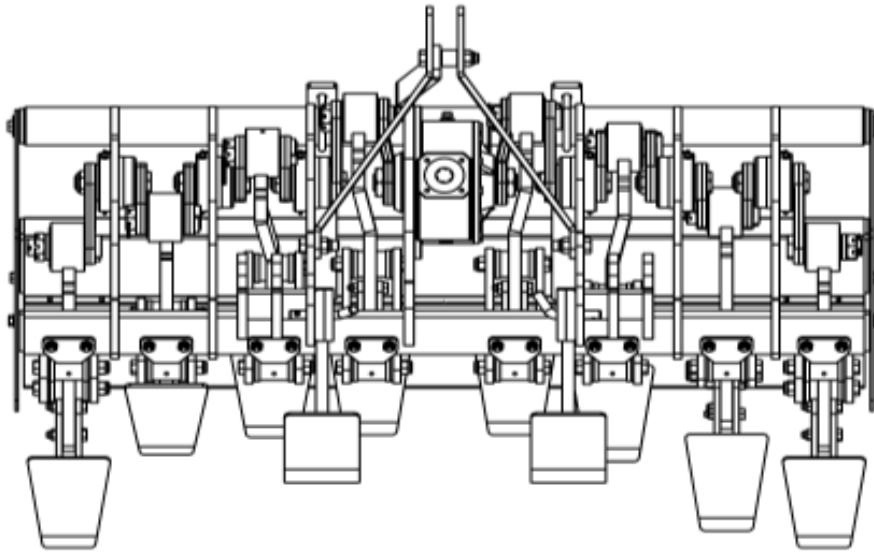


Fig. 3.18 A sketch of front view of tractor operated spading machine

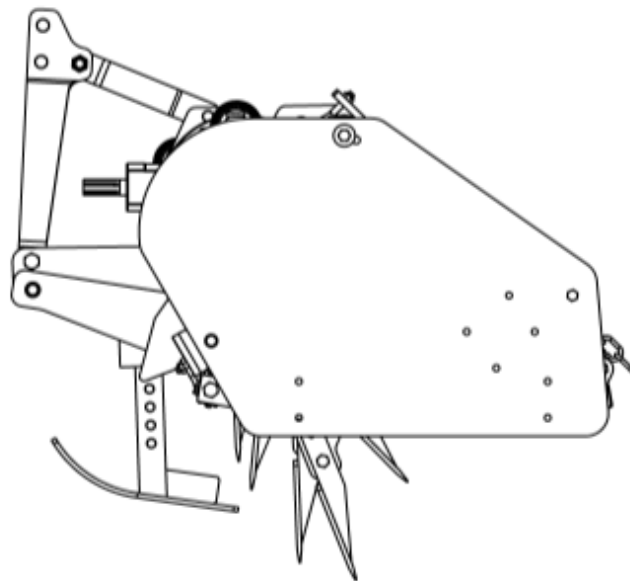


Fig. 3.19 A sketch of side view of tractor operated spading machine

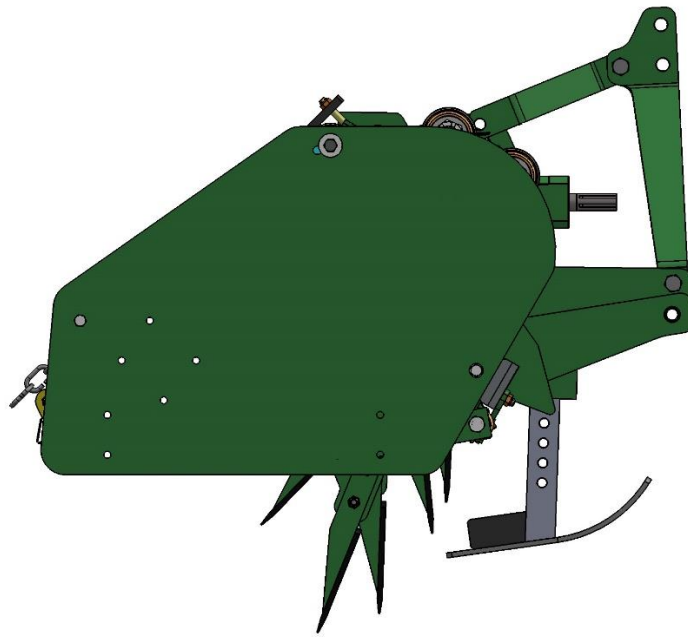


Fig. 3.20 Side view designed spading machine solid model

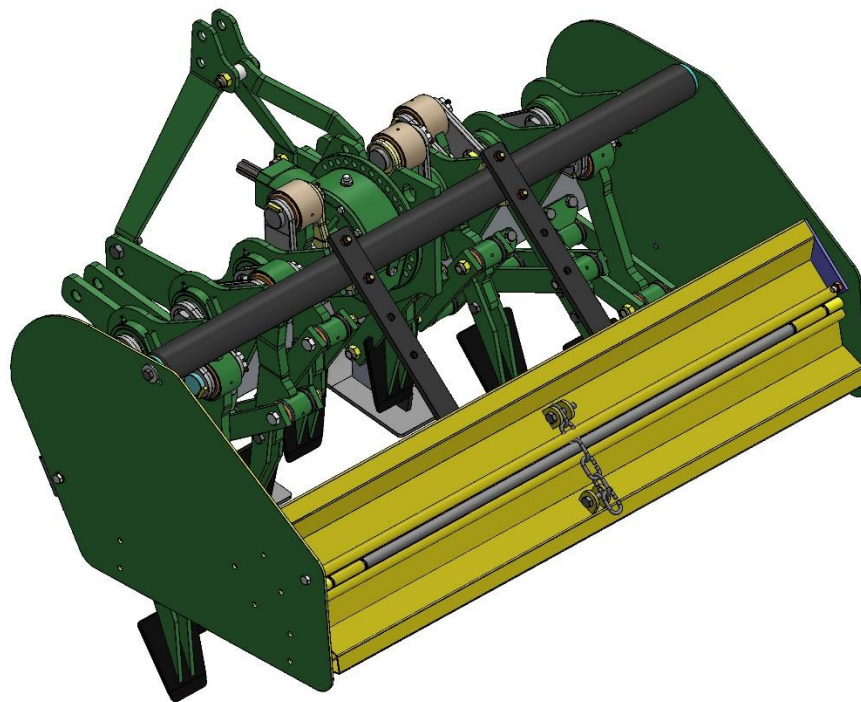


Fig 3.21 An isometric view of complete machine assembly solid model

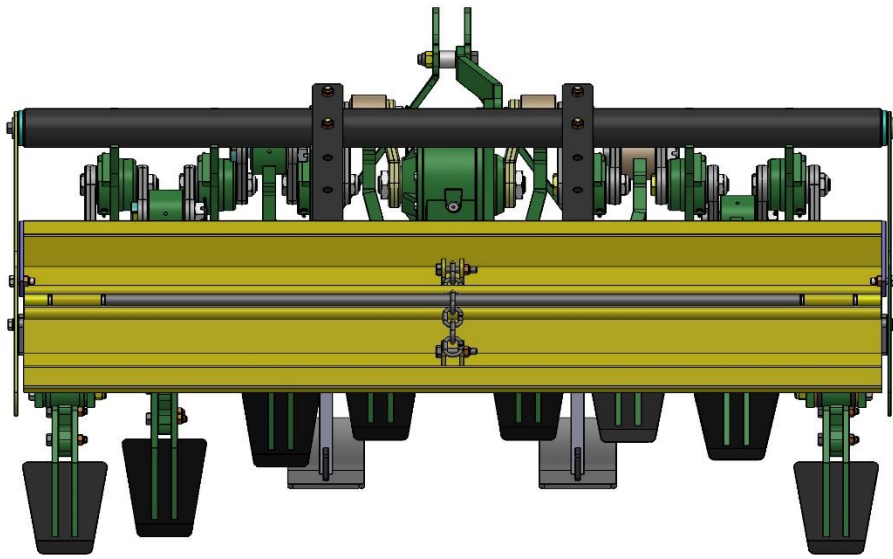


Fig. 3.22 Back view of spading machine solid model

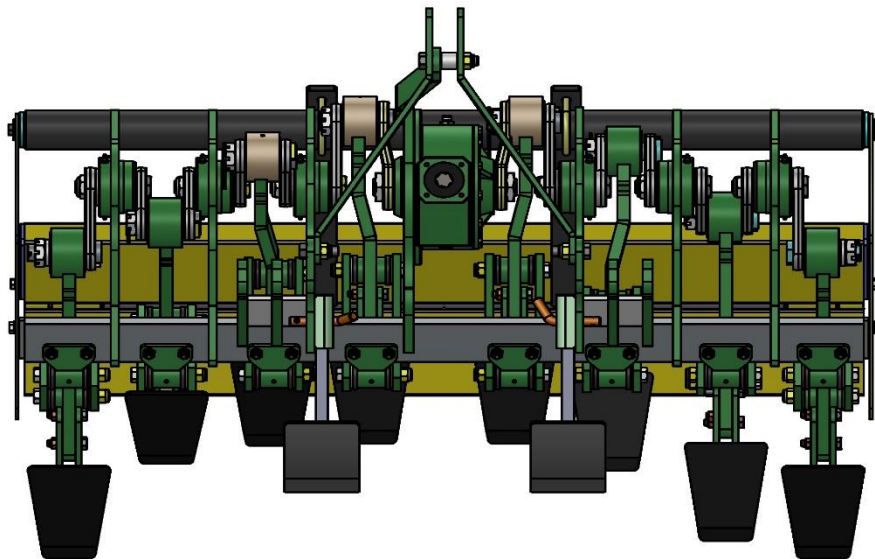


Fig. 3.23 Front view of spading machine solid model

Table 3.3 Specifications of developed spading machine

Sr. No.	Parameter	Specification
1	Type	PTO driven
2	Power source	50 hp
3	Hitch Type	Three point
4	Overall Dimension, mm (L x W x H)	1750 x 1270 x 1090
5	Number of spades	8
6	Shape of blade	Trapezoidal
7	Dimensions of spade, mm (a x b x h)	107 x 170 x 225
8	Gear Ratio	9:31
9	Crank revolution	167 rpm at 540 PTO rpm
10	Working width, mm	1720
11	Depth of operation, mm	200 to 300
12	Depth control mechanism	Two arc shaped skid

Table 3.4 Specification of Gomadhi spading machine

Sr. No.	Parameter	Specification
1	Type	PTO driven
2	Power source	55 hp or above
3	Hitch Type	Three point
4	Overall Dimension, mm (L x W x H)	1810 x 1320 x 1150
5	Number of spades	8
6	Shape of blade	Trapezoidal
7	Dimensions of spade, mm (a x b x h)	106 x 170 x 365
8	Working width, mm	1800
9	Depth of operation, mm	250 to 300 mm



Fig. 3.24 Preliminary trials of developed spading machine in field



Fig. 3.25 Preliminary trials of developed spading machine in field

3.5 Field evaluation of developed spading machine

The developed tractor operated spading machine was evaluated at Research Farm of Department of Farm Machinery & Power Engineering, PAU, Ludhiana. The machine was operated using a John Deere 50hp tractor (brief specification given in Table 3.6). Moisture content was measured at randomly selected locations in the test site using the oven method. The soil texture was classified by using the USDA method.

Table 3.5 Physical characteristics of soil at experimental site

Soil Texture	Percent Content			Bulk Density	Moisture Content	Cone Index
Sandy Loam	Sand	Silt	clay	1.60 Mg/m ³	12-14 %	700 – 2296 kPa
	64	24	12			

Table 3.6 Brief specification of tractor used with spading machine for field evaluation

Sr No.	Parameter	Specification
1	Model	John Deere 5310
2	Total weight	2210 kg
3	Length x Width x Height (mm)	3600 x 1865 x 2320
4	Ground clearance	450 mm
5	Rated Power / speed	41 kW / 2400 rpm
6	PTO speed	540 rpm

3.5.1 Independent parameters of the study

The developed machine was operated at three levels of forward speed, three level of depth of operation and three level of angle of attack. All parameters and their levels are given in Table 3.7. Different independent parameters are discussed as per following sub heads:

3.5.1.1 Forward speed

3.5.1.2 Depth of operation

3.5.1.3 Angle of attack

3.5.1.1 Forward speed

The forward speed at which the machine was intended to be operated was obtained in the preliminary functional testing of the machine. The machine was operated at rated engine rpm and 540 PTO rpm of the tractor. Three different forward speeds described as S1, S2 and S3 viz. 2.26, 3.37 and 4.92 km/h were selected. The speed was maintained in the tractor appropriately by changing gear lever to three different levels viz. A1, A2 and A3.

3.5.1.2 Depth of operation

Depth of operation is an important criterion to study the performance of tillage machinery. Spading machines have been operated upto at depth of 30 cm (Giordano *et al* 2015). Thus, taking 15% variation in the value three different levels were selected described as D1, D2 and D3 (20, 25 and 30cm, respectively) for operating the spading machine. The required depth of operation was maintained by the two depth adjusters on the spading machine. Test runs were conducted for the depth adjustment of machine before actual experimental runs. A steel ruler (30 cm length) was used to measure the depth of operation taking undisturbed surface as a reference.

3.5.1.3 Angle of attack

Angle of attack is defined as the angle (with respect to vertical axis) at which blade penetrates the soil surface. Angle of attack of commercially available machine was 35°. Thus, performance of the machine was evaluated at $\pm 15\%$ of 35° i.e. at 30°, 35° and 40°. These were described as A1, A2 and A3 (30°, 35° and 40°, respectively). The change in angle was managed by changing the three top link rods of different length linking the tractor and machine.

Table 3.7 Independent parameters and their levels

Sr No.	Parameter	Levels		
1	Forward Speed, km/h	3	S1	2.26
			S2	3.37
			S3	4.92
2	Depth of cut, cm	3	D1	20
			D2	25
			D3	30
3	Angle of attack, degree	3	A1	30
			A2	35
			A3	40

3.5.2 Dependent parameters of the study

A brief description of dependent variables to evaluate the performance of developed spading machine and their measurement methods are described in this section under the following heads;

3.6.3.1 PTO Torque

3.6.3.2 Soil Bulk Density

3.6.3.3 Cone Index

3.6.3.4 Clod Size Distribution (Soil Pulverization index)

3.6.3.5 Soil Moisture

3.5.2.1 PTO Torque

Torque was measured to ascertain the power requirement for treatment combination. To measure the torque, a torque transducer was used in the experiment. It consists of a strain gauge mounted on the propeller shaft (as shown in figure 3.26 and specifications given in Appendix B) which includes an amplifying circuit and radio signal transmitter with 9-volt DC battery strapped to it. The strain gauges connected to the wheatstone bridge circuit to measure unknown electrical resistance which corresponds to the twisting moment of the shaft. The strapped unit provide excitation voltage to bridge the strain gauges and received the output, digitized it and transmitted it. The infrared remote control was used to adjust transmitter gain, activate the remote shunt calibration or switch the transmitter to standby power mode. The twisting moment (torque) on the PTO shaft was measured by torque transducer with a given load.



Fig. 3.26 A view of torque sensor attached to propeller shaft

The receiver was switched on and the data logger software was started before running the spading machine. The digitized signal was received by the receiver unit which then convert it into analog output. A direct reading of torque as a function of amplitude verses time graph was displayed on the laptop. The data logger processes the data and stored it in the form of excel sheet. The average torque values stored in the MS Excel sheet was processed for calculations later on. The signals were recorded using the data logger software.



Fig. 3.27 A view of data receiving unit and laptop arranged on tractor to extract Torque data

3.5.2.2 Soil Bulk Density

Soil compaction can be characterized by changes in soil bulk density, which is the weight of the soil per unit volume (Mg/m^3). The core sampler was inserted in the soil to pre-selected depth and samples were drawn without disturbing the soil (Fig 3.28). The samples were weighed using the platform type electronic weighing balance. Core sampler was 30 cm long and of 7 cm in diameter. A steal ring was welded on top of it. It was inserted by slowly hammering matching hood on top of cylindrical core. The soil samples from the core were used for working out the wet bulk density. Standard core sampling technique was used to determine soil bulk density (wet basis) by using the relation given below

$$D_w = \frac{W}{V}$$

Where,

D_w = Bulk density (wet basis) in g/cc,

W = weight of soil taken by sampler in g,

V = volume of core cutter sampler in cc.



Fig. 3.28 Core cutter inserted in tilled soil for sample collection

The soil dry bulk density measurements were taken at field capacity of soil, before and after the treatment at working depth of the experimental field soil. Further, the core samples were placed in a 105 °C hot air oven for 24 hours until thoroughly dried, after which these samples were re-weighed. The resulting weight was used for working out the dry bulk density as per the following formula:

$$\text{Dry bulk density} = \text{Weight of oven dried soil} / \text{volume of soil sampler}$$

3.5.2.3 Cone Index

The soil strength estimated, often referred to as cone index (a composite soil parameter) is strongly influenced by soil type, soil structural state and soil moisture content. The cone penetration resistance has often been used to predict the draft requirement of tillage instruments (Desbiolles *et al* 1999 and Bishnoi 2008). A hand-held digital cone penetrometer (Rimik CP40II) was used to measure soil hardness or penetration resistance. It consisted of a rigid, steel rod, with a cone tip attached to one end, fixed to a force transducer, through the other end (as shown in figure 3.29). The penetrometer was pressed down at uniform rate to measure the penetration resistance acted on the tip of cone. The cone index or penetration resistance, in kPa was measured as an indicator of soil compaction. Cone index was measured at three randomly selected spots in each treatment plot. The value on each insertion were displayed graphically on the display panel of the device mounted above the frame of the digital cone penetrometer.



Fig. 3.29 Cone penetrometer used to measure soil strength

These were saved in the device itself for each insertion for later retrieved by connecting the device with a computer by using Rimik CP40II data extraction software. Detailed specifications given in Appendix C.

3.5.2.4 Clod Size Distribution (Soil Pulverization index)

When tillage force acts on soil, it breaks soil into small aggregates. The mean mass diameter (MMD) of the soil aggregated was considered as index of soil pulverization. The degree of soil pulverization (Pulverization Index) was measured by determining the MMD by using sieve analysis technique. Sieves of appropriate mesh size were selected to assess the degree of pulverization. During the experiments, set of sieves containing 18 sieves in the mesh range of 75 to 0.425 mm and pan were used. The set consisted of 75, 63, 45, 40, 25, 19, 13.2, 8, 6.3, 4.75, 2.80, 2, 1.4, 1, 0.600, 0.500 and 0.425 mm sieve sizes.

The field strip was ploughed for single pass of spading machine and after each treatment, three samples of the soil were drawn from three different locations within the

treatment area randomly, using soil sampler (length 15 cm, width 15 cm and height 30 cm). The soil was shade dried for 24 hours before carrying out the sieve analysis using column of sieves with gradual decrease in mesh size top downwards and mechanical sieve shaker. Thus, mean mass diameter of the soil restrained in different sieves were found to compare with outcome of different treatments. The amount of soil retained by each sieve was determined by weighing with the help of electronic balance as shown in figure 3.30.



Fig. 3.30 Measurement of weight of soil retained on each sieve

The soil mass retained on each sieve was weighed and MMD was calculated as:

$$\text{MMD, mm} = \frac{\sum W_i \times D_i}{W_t}$$

Where,

D_i = average diameter of i & $(i+1)^{\text{th}}$ sieve and $D_i < D_{i+1}$, mm

W_i = Mass of soil retained on the i^{th} sieve, g

W_t = Total mass of soil sample, g

3.5.2.5 Soil Moisture

Soil moisture is the measurement of water held in soil and is determined by measuring the mass of water relative to the mass of dry soil. Soil samples were collected from the field at regular interval. Irrigation is applied in the field so as to maintain same level of moisture content thought out the experiment time period. The wet weight of each sample was recorded. Then the soil samples were kept in the oven set at 105° C for 24 hours. The dried soil samples were again weighed. The soil moisture content (dry basis) in percent was calculated as:

$$S_m = 100 \times \frac{W_w - W_d}{W}$$

where,

S_m = soil moisture content, percent

W_w = wet weight of soil in g

W_d = dry weight of soil in g

3.5.3 Experimental field layout

Experiment in the field was laid out in factorial completely randomized block design. There were three replications for each treatment. Field was divided into 81 equal plots. There were three forward speeds (F1, F2 and F3), three depths of cuts (D1, D2, D3) and three angles of attack (A1, A2 and A3) which were replicated three (R1, R2, R3) times in complete randomization. The layout of the experimental plots is given in Appendix A.

No. of treatments = 3 * 3 * 3 = 27

No. of replications = 3

No. of experiments = 27 * 3 = 81

3.5.4 Statistical analysis

The tests were designed to determine the effect of independent parameters on dependent parameters. Factorial in Completely Randomized Design (CRD) was followed to conduct the experiments and to analyze the effect of study variables. Analysis of variance (ANOVA) was performed to test the significance of independent variables and their interactions on the dependent variables at 5 % level of significance.



Fig. 3.41 Field trial of developed spading machine



Fig. 3.42 Field trial of developed spading machine

CHAPTER – IV

RESULTS AND DISCUSSION

This chapter deals with the results of different experiments conducted on departmental research field for evaluation of developed tractor operated spading machine on field. Soil moisture was maintained from 12-14% (d.b.) during experimentation. To ascertain this soil samples were drawn from experimental plot randomly at regular intervals. Experimental field was divided into smaller fields, which were irrigated at pre-decided intervals before experimentation. Field evaluation was conducted to determine the effect of developed spading machine on the physical characteristics of tilled soil at different forward speed, depth of operation and angle of attack of spading machine. The results have been presented and discussed under the following sub-heads:

4.1 Effect on bulk density

4.2 Effect on PTO torque

4.3 Effect on clod size distribution

4.4 Effect on soil strength

4.5 Operational parameters for best field performance of spading machine

4.1 Effect on bulk density

Bulk density of a soil gives an indication of soil strength which shows the resistance to tillage implements or plant roots as they penetrate the soil. It is an indicator of soil compaction and soil health. Bulk density is dependent on soil organic matter, soil texture, the density of soil mineral (sand, silt, and clay) and their packing arrangement. Bulk density typically increases with soil depth since subsurface layers are more compacted and have less organic matter, less aggregation and less root penetration compared to surface layers, therefore contain less pore space. It affects water infiltration, rooting depth/ restrictions, available water capacity, soil porosity, plant nutrient availability and soil microorganism activity. These influence key soil processes and productivity. A bulk density in a range of 1.4 to 1.6 Mg/m³ was found that severely restricted root growth (Reynolds *et al* 2007, Hunt and Gilkes 1992). Available water capacity is the amount of soil moisture available to plants, varies by texture gets reduced when compaction occurs thus while determining bulk density soil moisture must be determined.

Excessive tillage destroys soil organic matter and weakens the natural stability of soil aggregates making them susceptible to erosion caused by water and wind. When eroded soil particles fill pore space, porosity is reduced and bulk density increases. Tillage and equipment

travel results in compacted soil layers with increased bulk density, most notably a “plow pan or hard pan”. High bulk density is an indicator of low soil porosity and soil compaction as larger the number of pore spaces in soil, lower is the value of bulk density. High bulk density impacts available water capacity, root growth, and movement of air and water through soil. Compaction increases bulk density and reduces crop yields and vegetative cover available to protect soil from erosion.

Mean bulk density at different levels of forward speed (S) and depth of operation (D) at 30°, 35° and 40° angle of attack (A) has been shown in Fig. 4.1, 4.2 and 4.3, respectively. It may be observed from the Fig. 4.1, 4.2 and 4.3 that with increase in forward speed (S) and depth of operation (D) the mean bulk density of the tilled soil increased. This increasing trend of bulk density with forward speed (F) and depth of operation (D) was observed at all three levels (30°, 35° and 40°) of angle of attack (A) of spading machine. The mean bulk density ranged from 1.17 Mg/m³ to 1.51 Mg/m³ for 30° angle of attack, 1.18 Mg/m³ to 1.52 Mg/m³ for 35° angle of attack and 1.20 Mg/m³ to 1.54 Mg/m³ for 40° angle of attack. The minimum mean bulk density of ploughed soil was at S1D1A1 (1.17 Mg/m³) and maximum at S3D3A3 (1.54 Mg/m³). This may be attributed to the fact that with increase in forward speed, bite length of the spading machine increased. As bite length increased, the number of cuts by blade per unit length decreased, thus resulted in more volume of detached soil per bite, resulting in bigger clod sizes in tilled soil. Mean bulk density also increased with increase in depth of operation because as depth of operating increased, more volume of soil is needed to be tilled by the machine leaving bigger clod sizes in ploughed soil. These bigger clods resulted in higher bulk density compared to small sized clods. Bulk density of soil is inversely proportional to porosity.

Analysis of variance (ANOVA) for the effect of independent parameter i.e. forward speed (S), depth of operation (D) and angle of attack (A) and their combinations on bulk density of ploughed soil has been shown in Table 4.1. Statistical analysis revealed that the effect of forward speed (S) and depth of operation (D) on bulk density is highly significant at 5% level of significance. However, effect of angle of attack (A) was not significant at 5% level of significance. Interaction of forward speed and depth of operation (S x D) was significant, while interaction of forward speed with angle of attack (S x A) and depth of operation with angle of attack (D x A) were not significant at 5% level of significance. The combined effect of all independent parameters (S x D x A) had significant effect on the bulk density at 5% level of significance.

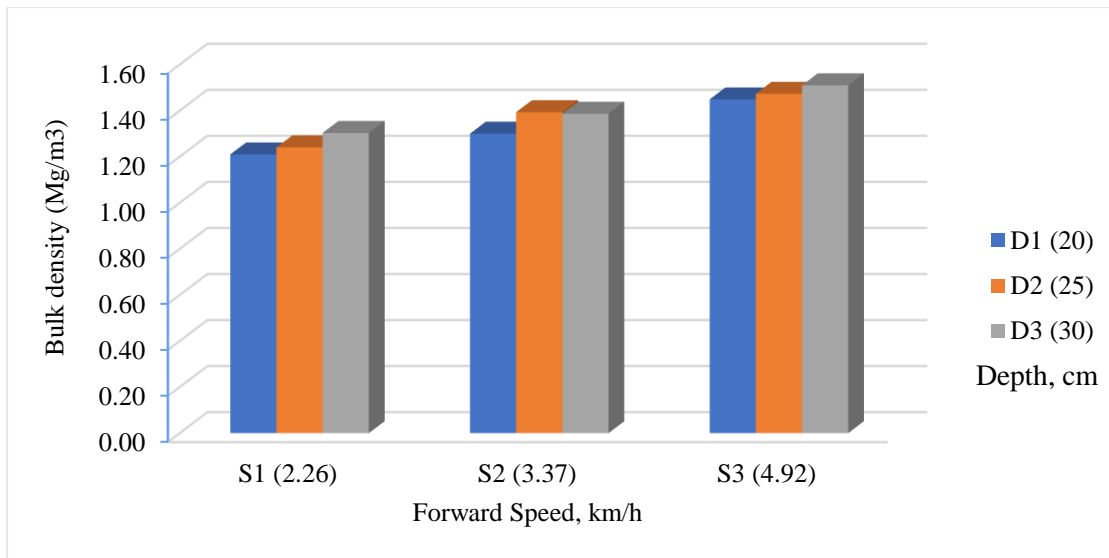


Fig. 4.1 Effect of forward speed and depth of operation at 30° angle of attack on bulk density

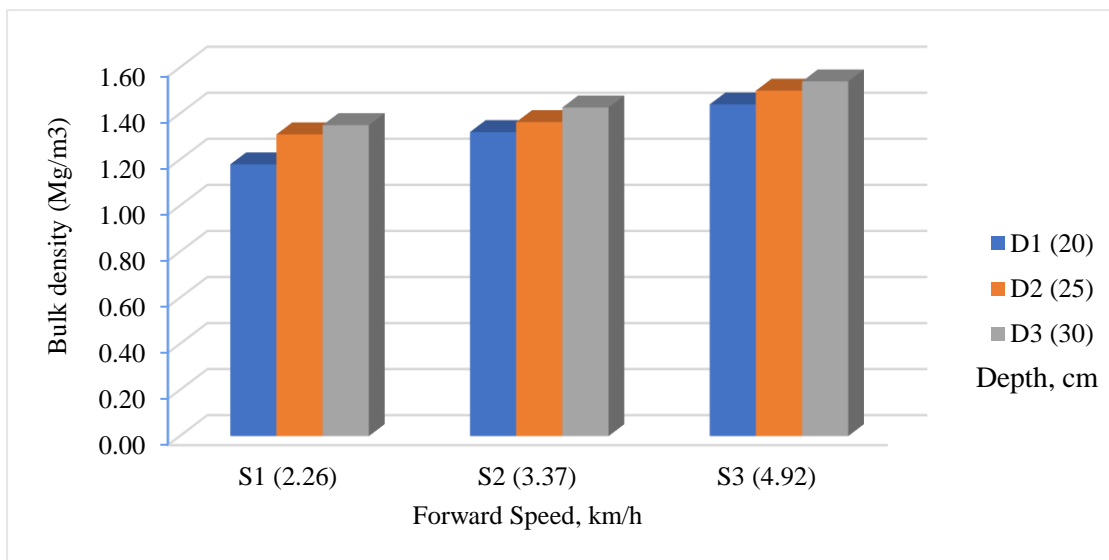


Fig. 4.2 Effect of forward speed and depth of operation at 35° angle of attack on bulk density

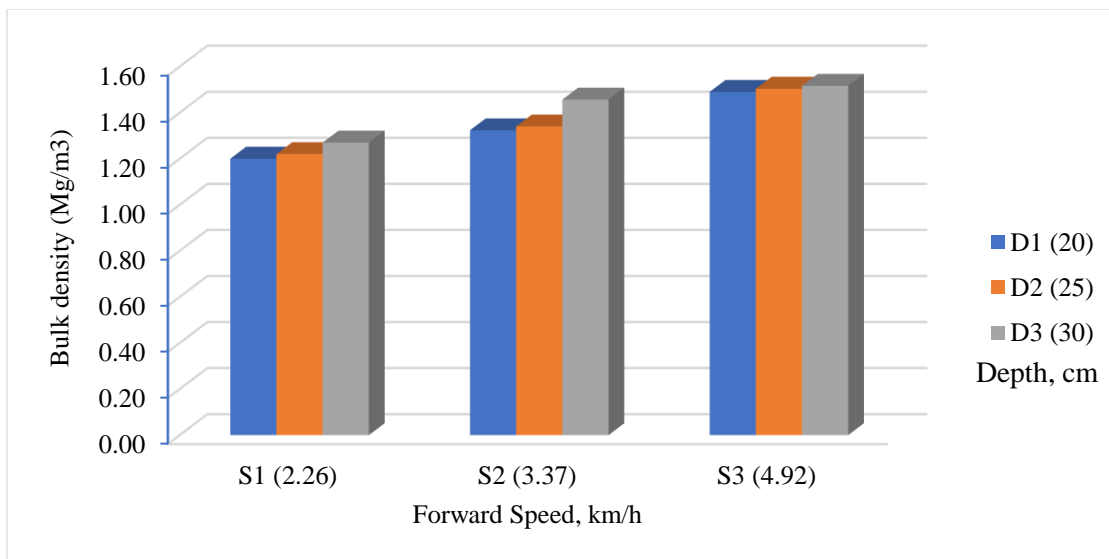


Fig. 4.3 Effect of forward speed and depth of operation at 40° angle of attack on bulk density

Table 4.1 ANOVA for effect of forward speed, depth of operation and attack angle on bulk density of soil ploughed

Source	DF	SS	Mean Square	F Value	Pr > F
Forward Speed (S)	2	0.7756	0.3878	304.93	<.0001 (S)
Depth of operation (D)	2	0.1085	0.0542	42.64	<.0001 (S)
Angle of attack (A)	2	0.0045	0.0022	1.76	0.1821 (NS)
S x D	4	0.0137	0.0034	2.70	0.0404 (S)
S x A	4	0.0095	0.0024	1.87	0.1295(NS)
D x A	4	0.0120	0.0030	2.35	0.0661(NS)
S x D x A	8	0.0249	0.0031	2.45	0.025 (S)

4.1.1 Effect of forward speed on bulk density

Bulk density was affected by the forward speed of the machine. Analysis of variance (Table 4.1) shows that the effect of forward speed on bulk density was significant at 5% level of significance. Mean values of bulk density for three levels of forward speed (S) are presented in Table 4.2.

Table 4.2 Mean values of bulk density at different levels of forward speed

Forward speed	Mean bulk density (Mg/m ³)	Comparison
S3	1.49	A
S2	1.36	B
S1	1.25	C

Note: Mean values with the same letter are not significantly different ($p>0.05$)

The mean bulk density was significant at 5% level of significance at different forward speed as shown in Table 4.1. As evident in Fig. 4.1, Fig. 4.2 and Fig. 4.3, it increased with increase in forward speed (S) of spading machine. Mean bulk density was maximum at forward speed S3 (4.92 km/hr) and minimum for forward speed S1 (2.26 km/hr). This was also observed for all three levels of depth of operation D1, D2 and D3 (20 cm, 25 cm and 30 cm), respectively. It may also be observed from the Fig. 4.1, Fig. 4.2 and Fig 4.3 that the mean bulk density increased with increase with forward speed (S) at all three levels of angle of attacks A1, A2 and A3 (30°, 35° and 40°), respectively. This may be attributed to the fact that as forward speed increased, bite length increased thus increased pulverisation index generating bigger clod of ploughed soil and thus resulted in increased bulk density and also at highest forward speed, some portion of soil might have remained untilled therefore resulted in increased bulk density.

The bulk density of soil is inversely proportional to porosity. Higher the pore space in soil lower is the value of bulk density.

Similar results were reported by Dahab (2011) where tillage implements decreased bulk density and penetration resistance and increased the porosity and aggregate stability of upper soil depth (0-15 cm). Ahaneku and Ogunjirin (2005) while evaluating the effect of tractor forward speed (1.0 to 10.6 km/h) on soil physical parameters, found that in sandy loam fields, the dry bulk density of the soil at different depths for different levels of speed (1.0, 1.3, 6.8, 8.8 and 10.6 km/h) increased with depth but decreased with speed of tillage operation within the 15 cm top layer. Thereafter, the increased speed did not have much impact on bulk density reduction. This might be due to the soil type and other textural properties involved in the study.

4.1.2 Effect of depth of operation on bulk density

Bulk density was affected by the depth of operation of spading machine. Analysis of variance (Table 4.1) also shows that the effect of depth of operation on bulk density was significant at 5% level of significance. Mean values of bulk density for three levels of depth of operation (D) are shown in Table 4.3.

Table 4.3 Mean values of bulk density at different levels of depth of operation

Depth of operation	Mean bulk density (Mg/m ³)	Comparison
D3	1.41	A
D2	1.37	B
D1	1.32	C

Note: Mean values with the same letter are not significantly different ($p>0.05$)

It can be seen from Table 4.3 that mean bulk density with different corresponding alphabets depict that these were significantly different from each other. As evident from Fig. 4.1, Fig. 4.2 and Fig. 4.3 bulk density increased as with increase in depth of operation (D) for all combination of forward speed (S) and angle of attack (A). It may also be observed that mean bulk density was maximum (1.41 Mg/m³) for depth of operation D3 as compared to D2 (1.37 Mg/m³) and least for depth of operation D1 (1.32 Mg/m³). This trend was observed at all three levels of forward speed S1, S2 and S3 (2.26, 3.37 and 4.92 km/hr, respectively) and all three levels of angle of attack A1, A2 and A3 (30°, 35° and 40°, respectively). This may be attributed to the fact that at lower depth of operation, pulverisation of soil was good thus decreased bulk density, further increasing depth resulted in bigger clods sizes thus increased bulk density. First order interactions of forward speed with depth of operation (S x D) was found to be significant

while interaction of forward speed with angle of attack (S x A) and depth of operation with angle of attack (D x A) was found to be non-significant at 5% level of significance.

Table 4.4 Mean values of bulk density for the effect of interaction between forward speed and depth of operation

	S1	S2	S3
D1	1.19 ^f	1.31 ^{cd}	1.47 ^{ab}
D2	1.25 ^e	1.36 ^c	1.49 ^a
D3	1.30 ^d	1.42 ^b	1.51 ^a

Note: Mean values with the same letter are not significantly different ($p > 0.05$)

Various interactions between forward speed (S) and depth of operation (D) in descending order for mean bulk density were: S3 D3, S3 D2, S3 D1, S2 D3, S2 D2, S2 D1, S1 D3, S1 D2 and S1 D1 (Table 4.4 and Fig.4.4). In case of S1D1 bulk density was minimum (1.19 Mg/m³) and significantly different from all other combinations. The highest value bulk density was obtained in S3D3 (1.51 Mg/m³) which doesn't show significant difference with S3D2 (1.49 Mg/m³). The interaction between S3D1 and S2D3 was not significantly different, same is the case with S2D2 and S2D1, S2D1 and S1D3. Bulk density shows decreasing trend with decreasing forward speed and depth of operation which may be attributed to the fact that with increase in forward speed, bite length increased and with increase in depth of operation, the final ploughed soil has bigger sized clods, resulted in poor soil pulverization and thus higher bulk density.

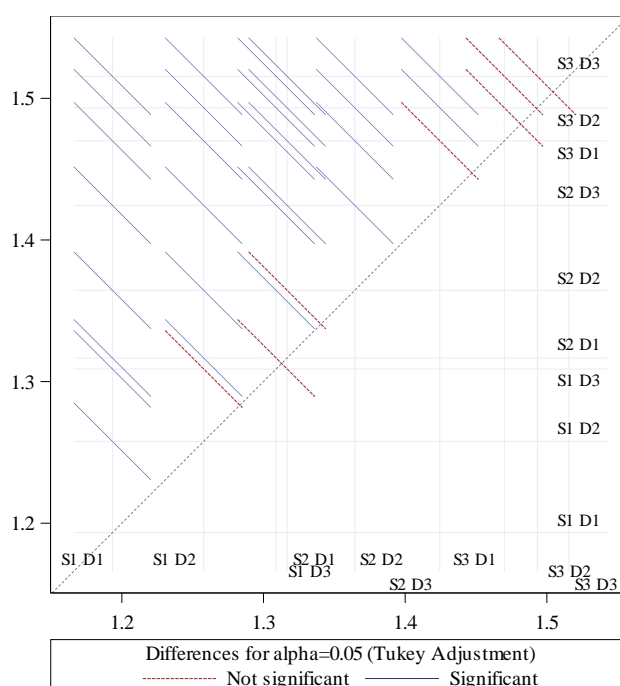


Fig 4.4 Diffogram for the effect of forward speed and depth of operation on bulk density

Least mean bulk density was obtained for S1D1. This was due to the reason that S1 and D1 gives small clod size thus result in better pulverisation of soil and least bulk density as higher the pore space in soil lower the value of bulk density.

4.2 Effect on PTO torque requirement

Spading machine have equally spaced several spades as tillage blades that represents a rocker of a crank-rocker mechanism. Spade operations of spading machine make it possible for the spades to penetrate deeply into the soil and easily override obstacles in the field, resulting in better air permeability and drainage of tilled soil. The energy use in field operation is of great concern for farmer, thus the concept of reduced power requirement, therefore, has become of increased importance.

PTO torque of the spading machine during field evaluation was measured using PTO torque sensor (mounted on universal shaft connecting tractor PTO and machine pinion shaft) as mentioned under section 3.5.2.1. Mean PTO torque at different levels of forward speed (S) and depth of operation (D) at 30°, 35° and 40° angle of attack (A) has been shown in Fig. 4.6, 4.7 and 4.8, respectively. It may be observed from the Fig. 4.5, 4.6 and 4.7 that with increase in forward speed (S) and depth of operation (D) the mean PTO torque increased. This increasing trend of PTO torque with forward speed (F) and depth of operation (D) was observed at all three levels (30°, 35° and 40°) of angle of attack (A) of spading machine. The mean PTO torque ranged from 339.07 Nm to 550.78 Nm for 30° angle of attack, 333.54 Nm to 541.71 for 35° angle of attack and 327.67 Nm to 536.33 Nm for 40° angle of attack. Minimum mean PTO torque during the tillage operation was at S1D1A3 (327.66 Nm) and maximum at S3D3A1 (550.78 Nm). This may be attributed to that fact that with increase in forward speed, bite length of the spading machine increased. As bite length increased, greater volume of soil needed to be tilled by blade, thus resulted in more volume of detached soil per bite, resulting in greater energy requirement of machine. Mean PTO torque also increased with increase in depth of operation because as depth of operation increased, blade needed greater power to penetrate at deeper depth and also more volume of soil is needed to be tilled by the machine. This resulted in more PTO torque requirement for deeper operation as compared to shallow operation of the machine.

Analysis of variance (ANOVA) for effect of independent parameters i.e. forward speed (S), depth of operation (D) and angle of attack (A) and their combinations on PTO torque has been provided in Table 4.5. Statistical analysis revealed that the effect of independent parameters i.e. forward speed (S) and depth of operation (D) on PTO torque was statistically significant at 5% level of significance. However, effect of angle of attack (A) was not

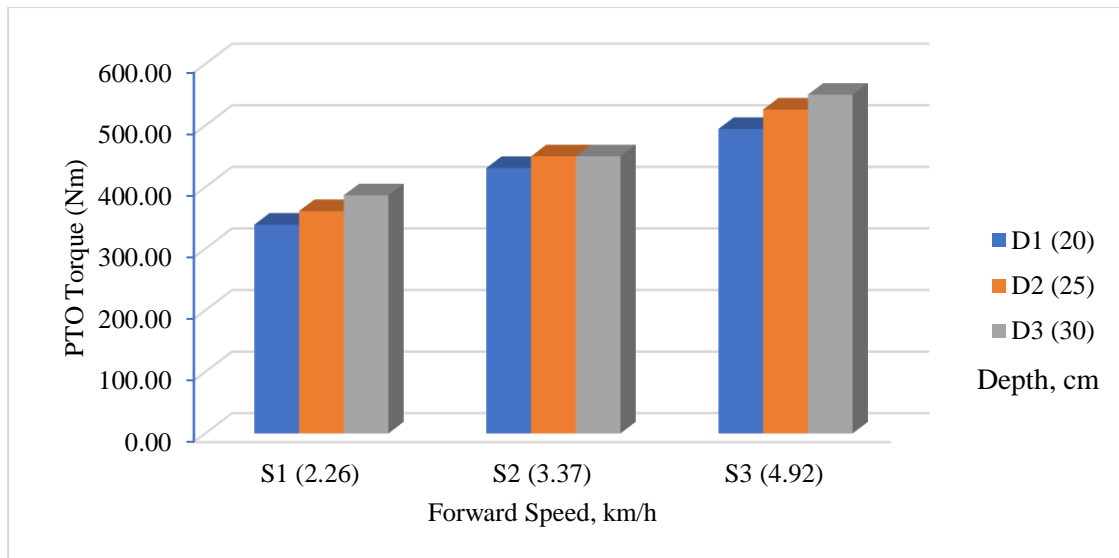


Fig. 4.5 Effect of forward speed and depth of operation at 30° angle of attack on PTO torque

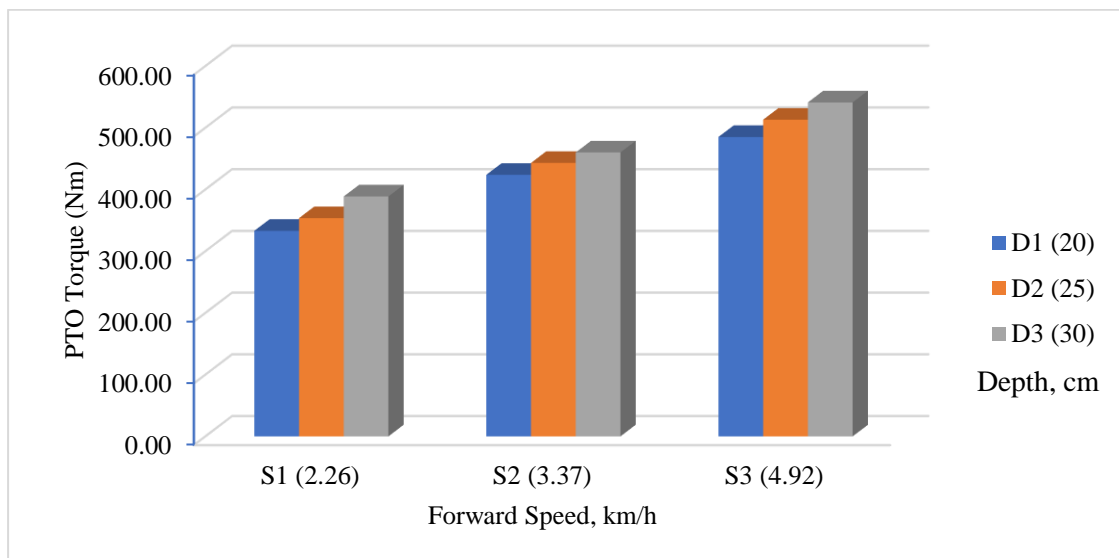


Fig. 4.6 Effect of forward speed and depth of operation at 35° angle of attack on PTO torque

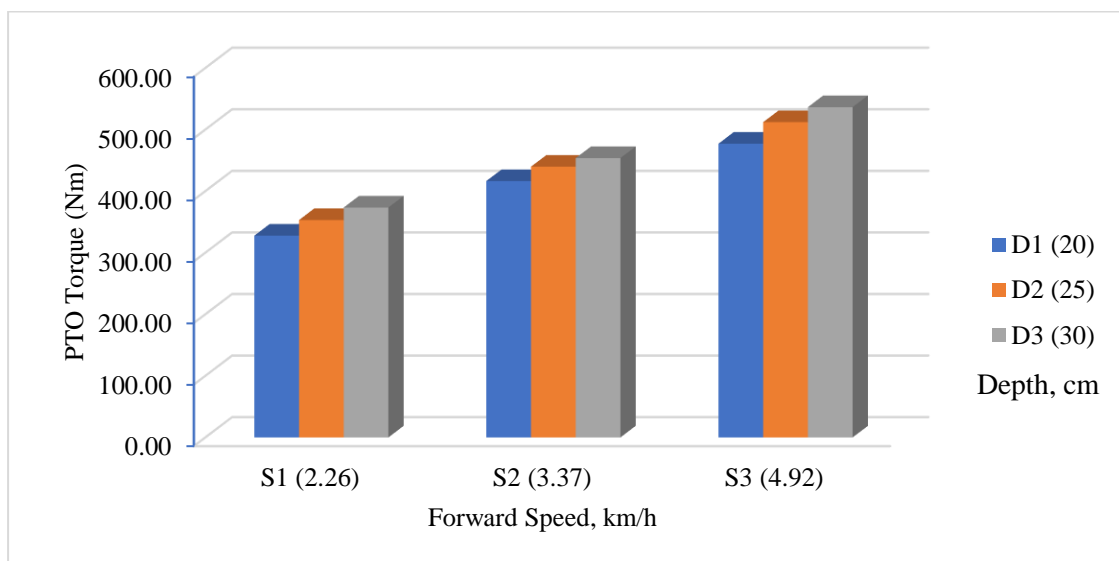


Fig. 4.7 Effect of forward speed and depth of operation at 40° angle of attack on PTO torque

significant at 5% level of significance. First order interaction of forward speed and depth of operation (S x D) was also significant at 5% level of significance, while interaction of forward speed with angle of attack (S x A) and depth of operation with angle of attack (D x A) were non-significant at 5% level of significance. The second order interactions all independent parameters (S x D x A) was non-significant at 5% level of significance for PTO torque.

Table 4.5 ANOVA for effect of forward speed, depth of operation and attack angle on PTO torque of spading machine

Source	DF	SS	Mean Square	F Value	Pr > F
Forward Speed (S)	2	335901.519	167950.760	1172.29	<.0001 (S)
Depth of Operation (D)	2	28452.749	14226.375	99.30	<.0001 (S)
Angle of Attack (A)	2	1634.645	817.322	5.70	0.0768 (NS)
S x D	4	1803.864	450.966	3.15	0.0216 (S)
S x A	4	233.328	58.332	0.41	0.8026 (NS)
D x A	4	328.585	82.146	0.57	0.6831 (NS)
S x D x A	8	283.636	35.454	0.25	0.9793 (NS)

4.2.1 Effect of forward speed on PTO torque

It was observed that PTO torque was affected by the forward speed of the machine during field evaluation as observed from Fig. 4.5, 4.6 and 4.7. Analysis of variance (Table 4.5) shows that the effect of forward speed on PTO torque was significant at 5% level of significance. Mean values of PTO torque for three levels of forward speed (S) are shown in Table 4.6.

Table 4.6 Mean values of PTO torque at different levels of forward speed

Forward Speed	Mean PTO torque (Nm)	Comparison
S3	514.96	A
S2	440.81	B
S1	357.31	C

Note: Mean values with the same letter are not significantly different ($p>0.05$)

As evident in Fig 4.5, Fig 4.6 and Fig 4.7, PTO torque increased with increase in forward speed (S) of spading machine. This was also observed for all three levels of depth of operation D1, D2 and D3 (20 cm, 25 cm and 30 cm), respectively. It was maximum at forward speed 4.92 km/h (S3) for all combination of depth of operation and angle of attack. PTO torque was maximum at forward speed S3 (514.96 Nm) and minimum at forward speed S1 (357.31

Nm). PTO torque was affected more when the forward speed increased from S1 to S2 and S2 to S3. This may be attributed to the fact that at increased forward speed the bite length increased, thus increase in volume of soil tilled by the blade resulted in increased power requirement. Spades required more power to move soil at larger bite length as compared to smaller bite length. This was observed for all treatment combination of forward speed (S), depth of operation (D) and angle of attack (A).

4.2.2 Effect of depth of operation on PTO torque

PTO torque was affected by the depth of operation of spading machine. Analysis of variance (Table 4.5) also shows that the effect of depth of operation on PTO torque was significant at 5% level of significance. Mean values of PTO torque for three levels of depth of operation are shown in Table 4.7.

Table 4.7 Mean values of PTO torque at different levels of depth of operation

Depth of operation	Mean PTO torque (Nm)	Comparison
D3	459.96	A
D2	439.02	B
D1	414.11	C

Note: Mean values with the same letter are not significantly different ($p>0.05$)

As evident from Fig 4.6, Fig 4.7 and Fig 4.8 PTO torque was increased with increase in depth of operation. Mean PTO torque was maximum (459.96 Nm) at 30 cm depth of operation (D3) and minimum (414.11 Nm) at 20 cm depth of operation. This trend was observed for at all three levels of forward speed (S1, S2 and S3) and all three levels of angle of attack (A1, A2 and A3). This may be attributed to the fact that at low depth of operation, the power requirement of the spading arms to penetrate into the soil is less thus resulting in lower PTO torque requirement. Similarly, at for greater depth of operation (D3) the power requirement of machine was higher to penetrate at greater depth and plough larger volume of soil. Thus, resulting in increased PTO torque requirement for depth of operation D3 as compared to depth of operation D2 and D1.

First order interactions of forward speed with depth of operation (S x D) was found to be significant while interaction of depth of operation with angle of attack (D x A) and forward speed with angle of attack (S x A) was found to be non-significant at 5% level of significance (Table 4.5).

Table: 4.8 Mean values of PTO torque for the effect of interaction between forward speed and depth of operation

	S1	S2	S3
D1	333.22 ^h	423.66 ^e	485.44 ^c
D2	355.83 ^g	444.22 ^d	517.00 ^b
D3	382.88 ^f	454.55 ^d	542.44 ^a

Note: Mean values with the same letter are not significantly different ($p>0.05$)

Various interactions between forward speed (S) and depth of operation (D) in descending order for mean PTO torque were: S3 D3, S3 D2, S3 D1, S2 D3, S2 D2 S2 D1, S1 D3, S1 D2 and S1 D1 (Table 4.8 and Fig.4.8). Mean PTO torque shows an increasing trend with increase with forward speed and depth of operation. Maximum mean PTO torque was obtained for treatment S3D3 (542.44 Nm) and is significantly different from all other treatment combination. It may be attributed to the fact that with increase in forward speed (D) and depth of operation (D), machine required more power to plough larger volume of soil (due to increased bite length) and penetrate to greater depth. While minimum mean PTO torque was observed for S1D1(333.22 Nm) and significantly different from all other first order treatment combination for forward speed (S) and depth of operation (D). The reason for can be due to the lower power requirement of the machine due to smaller bite length and lower depth of operation (less power required to penetrate to lower depth). In case of S3D3 the PTO torque was maximum (542.44 Nm) and significantly different from all other combinations. This is due to the increased bite length and increased depth of operation. Machine needed greater power to penetrate at deeper depths and due to increased bite length, the machine has to till greater volume of soil per bite. Further, the mean PTO torque was not significantly different between the combinations S2D3 and S2D2. All the other combinations of forward speed (S) and depth of operation (D) were found to be significantly different from each other. PTO torque show increasing trend with increase in forward speed and depth of operation, thus more PTO power requirement. This was observed for at all three angles of attack (30°, 35° and 40°) but the second order interaction between all three-independent parameter; forward speed (S). depth of operation (D) and angle of attack (A) was non-significant at 5% level of significance.

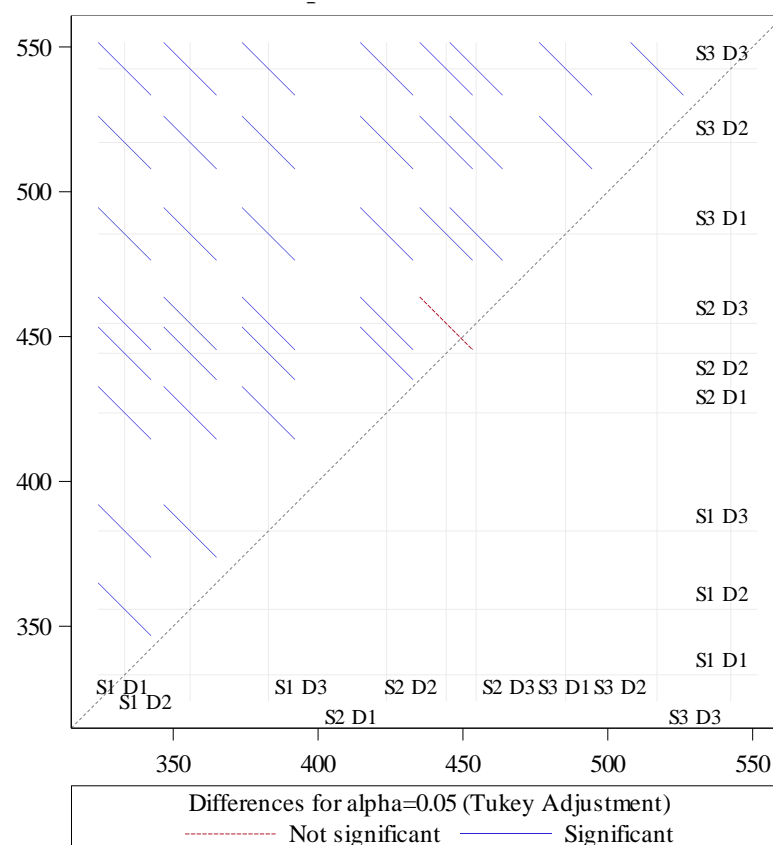


Fig 4.8 Diffogram for the effect of forward speed and depth of operation on PTO torque

4.3 Effect on clod size distribution

The ability of a tillage practice to prevent erosion and runoff control on bare soils may depend upon the clod size distribution at the surface of the ploughed layer. The preparation of seedbed depends on amount of soil pulverization or mean mass diameter (MMD) values. The clod size should be of optimum size required, too fine soil results in soil erosion and unnecessary energy waste and too big clods affect the plant growth and makes other operation difficult. To produce a good seedbed, the clod size must be range from 10 to 25 mm (El-Haddad *et al* 1995). The pulverization index (PI) which is an indicator to the soil pulverization depends on the work conditions in term the ploughing depth, forward speed, tillage method (plough type) and on the soil condition, such as moisture content and bulk density. It increased as the ploughing depth and the moisture content decreased (Yassen *et al* 1992). The Pulverization Index (PI) reduces when secondary tillage equipment is used after primary tillage equipment which further crushes the clods, thus result in finer seed bed.

Pulverization index is based on mean mass diameter (MMD) of clods determined by sieve analysis of soil. Smaller the average clod size (MMD) higher was the pulverization index. Mean weight diameter of soil clods was determined using method given in section 3.5.2.4. Samples were taken randomly at three different spots in one plot for minimum error. The

average values of mean weight diameter of soil clods observed after different treatment were analysed. Mean pulverization index at different levels of forward speed (S) and depth of operation (D) at 30°, 35° and 40° angle of attack (A) has been shown in Fig. 4.9, 4.10 and 4.11, respectively. It is evident from the figure that mean PI increased with increase in forward speed (S) and depth of operation (D). This increasing trend of pulverization index with increase forward speed (F) and depth of operation (D) was observed at all three levels (30°, 35° and 40°) of angle of attack (A) of spading machine. The mean PI ranged from 5.21 mm to 18.20 mm for 30° angle of attack, 4.77 mm to 16.71 mm for 35° angle of attack and 3.68 mm to 15.80 mm for 40° angle of attack. Lowest mean PI was observed at S1D1A3 (3.68 mm) and highest value of mean PI at S3D3A1 (18.20 mm). This may be attributed to the fact that with increased forward speed (S), bite length increased which resulted in bigger sized clods of ploughed soil after tillage. This was observed at all levels of forward speed (2.26 km/hr, 3.37 km/hr and 4.92 km/hr). Similarly, with increase in depth of operation (D), greater volume of soil is tilled, which led to bigger sized clod of ploughed soil and observed at all levels of depth of operation (20 cm, 25 cm and 30 cm). Increase in bigger sized clods, increases the pulverization index value thus showing poor pulverization for tilled soil. Angle of attack A3 had least pulverization index this may be attributed to the fact that with increase in angle the soil above blade decreases. Blade push less soil at increased angle leading to small sized clods and therefore, least pulverization index.

Analysis of variance (ANOVA) for effect of independent parameters i.e. forward speed (S), depth of operation (D) and angle of attack (A) and their combinations on pulverization has been presented in Table 4.9. Statistical analysis revealed that the effect all independent parameters i.e. forward speed (S) and depth of operation (D) were significant at 5% level of significance while angle of attack (A) was not significant at 5% level of significance. The first order interaction between forward speed and depth of operation (S x D) was significant at 5% level of significance, however interaction of forward speed with angle of attack (S x A) and depth of operation with angle of attack (D x A) were non-significant at 5% level of significance. The second order interactions all independent parameters (S x D x A) was non-significant at 5% level of significance for PI.

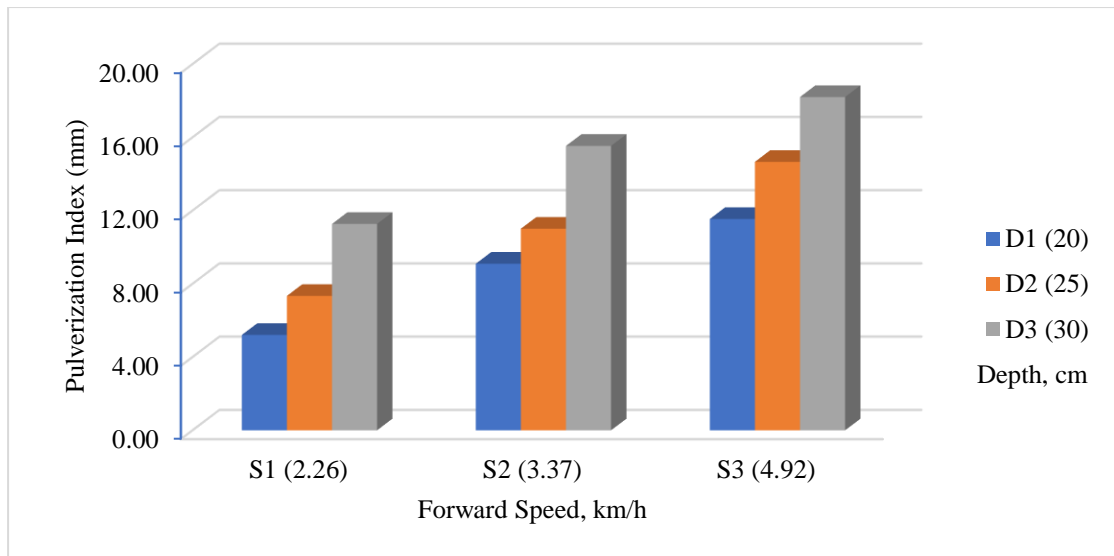


Fig. 4.9 Effect of forward speed and depth of operation at 30° angle of attack on PI

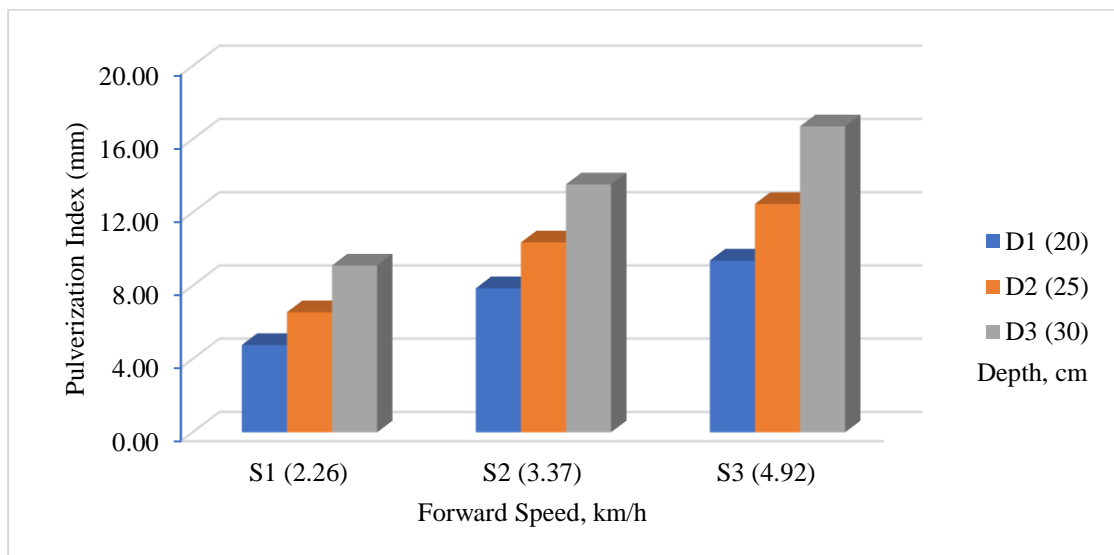


Fig. 4.10 Effect of forward speed and depth of operation at 35° angle of attack on PI

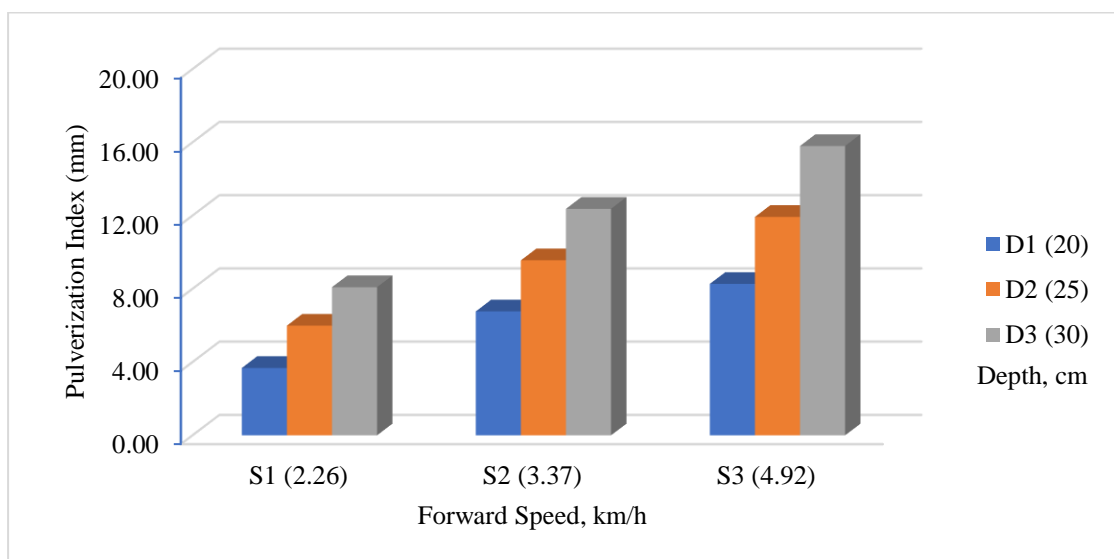


Fig. 4.11 Effect of forward speed and depth of operation at 40° angle of attack on PI

Table 4.9 ANOVA for effect of forward speed, depth of operation and attack angle on pulverization index of soil ploughed by spading machine

Source	DF	SS	Mean Square	F Value	Pr > F
Forward Speed (S)	2	468.234	241.8532	149.36	<.0001 (S)
Depth of Operation (D)	2	461.854	231.673	143.87	<.0001 (S)
Angle of Attack (A)	2	78.653	52.647	37.98	<.1782 (NS)
S x D	4	31.448	8.832	5.63	0.0035 (S)
S x A	4	3.546	0.754	0.64	0.9452 (NS)
D x A	4	8.214	1.598	2.36	0.5214(NS)
S x D x A	8	8.623	0.949	0.87	0.9236 (NS)

4.3.1 Effect of forward speed on PI

Pulverization index was affected by the forward speed of the machine and found statistically significant at 5% level of significance (Table 4.9). Table 4.10 shows mean values of PI at all levels of forward speed (S) in descending order.

Table 4.10 Mean values of pulverization index at different levels of forward speed

Forward Speed	Mean Pulverization Index (mm)	Comparison
S3	13.57	A
S2	11.23	B
S1	7.64	C

Note: Mean values with the same letter are not significantly different ($p>0.05$)

As evident in Fig 4.9, Fig 4.10 and Fig 4.11, PI increased with increase in forward speed (S). This was observed for all combination of depth of operation (D) and angle of attack (A). Maximum PI was observed at S3 (13.57 mm) and minimum at S1 (7.64 mm). This may be attributed to the fact that as forward speed increased, bite length increased, therefore resulting in bigger sized clods left in ploughed soil and pulverization index was increased showing poor pulverization of soil and also at highest forward speed, some portion of soil might have remained untilled therefore resulted in increased pulverization index. On the other hand,

at lower forward speed the bite length is lower which resulted in smaller clod size of tilled soil. Similar finding was observed by Abrougui *et al* (2014) where the Pulverization Index (PI) for tandem disc harrow used after the mouldboard plough decreased from 34.50 to 27.89 mm when forward speed increased from 0.25 to 0.60 m/s. Similar trend was also seen by Sale *et al* (2013) during the performance evaluation of some selected tillage implements during which pulverization index decreased with increase in forward speed of implement.

4.3.2 Effect of depth of operation on PI

Pulverization index was affected by the depth of operation of spading machine. Analysis of variance (Table 4.9) shows that the effect of depth of operation on bulk density was significant at 1% level of significance. As depicted in Table 4.11 mean values of PI for all levels of depth of operation in descending order.

Table 4.11 Mean values of pulverization index at different levels of depth of operation of spading machine

Depth of operation	Mean Pulverization Index (mm)	Comparison
D3	14.47	A
D2	11.87	B
D1	7.89	C

Note: Mean values with the same letter are not significantly different ($p>0.05$)

As evident from Table 4.11 that with increase in depth of operation, mean PI was increased significantly. Also, as evident from Fig 4.9, Fig 4.10 and Fig 4.11 pulverization index increased with increase in depth of operation (D) for all combination of forward speed (S) and angle of attack (A). PI was maximum at D3 (14.47 mm) and minimum at D1 (7.89 mm). PI increased with increase in depth of operation this may be attributed to the fact that with increase in depth, the volume of tilled soil to be moved, increased thereby resulting in bigger clods at higher depths and at low depth of operation, pulverisation of soil was good thus decreased pulverization index. Similar results were found in Aday and Nasser (2009) study where they found that increase in ploughing depth from 15 to 25 cm, the pulverization efficiency decreased from 80 to 75%. Dogra *et al* (2017) also found similar trend of decrease in pulverization index with increase in depth of operation of when studied with prototype of spading machine mounted on a structure on soil bin.

Table 4.12 Mean values of pulverization index the effect of interaction between forward speed and depth of operation

	S1	S2	S3
D1	5.37 ^f	8.34 ^d e	10.99 ^d
D2	6.89 ^{ef}	11.10 ^c	13.64 ^b
D3	10.85 ^{cd}	13.48 ^b	16.85 ^a

Note: Mean values with the same letter are not significantly different ($p>0.05$)

First order interactions of forward speed with depth of operation (S x D) was found to be significant at 5 % level of significance while interaction of depth of operation with angle of attack (D x A) and forward speed with angle of attack (S x A) was found to be non-significant at 5% level of significance. Various interaction between forward speed (S) and depth of operation (D) in descending order for mean pulverization index were: S3D3, S3D2, S3D1, S2D3, S2D2, S2D1, S1D3, S1D2 and S1D1 (Table 4.12 and Fig. 4.12). Mean PI shows an increasing trend with increase in forward speed and depth of operation. The highest mean pulverization index was obtained in treatment combination S3D3 (16.85 mm) and is significantly different from all other treatment combination. While lowest PI was obtained for treatment combination S1D1 (5.37 mm) but does not significantly different from S1D2. This may be attributed to the fact that with increase in forward speed, bite length increased and similarly increase in depth of operation the ploughed soil resulted in bigger clod sizes, thus poor pulverization of soil and higher pulverization index. Both factors (S x D) combined greatly impact the pulverization of tilled soil. The interaction between S1D3, S3D1 and S2D2 was not significantly different at 5% level of significance, which indicated that the mean PI didn't differ much in these treatment combinations even after change of forward speed and depth of operation, same is the case with S2D2, S1D3; S2D1 S1D2 and S1D2, S1D1.

4.4 Effect on soil strength

Tillage is an important agricultural operation. It reduces soil strength and loosens soil (Kumar et al 2012). According to Whalley *et al* (2007) it is generally accepted that at cone index values larger than 2.5 MPa, plant root elongation is significantly restricted. Spading machines prepare the soil prior to making of beds for sowing. Soil strength was based on cone index of soil which gives an indication about the vertical penetration in soil. Harder the soil less is its suitability for root penetration.

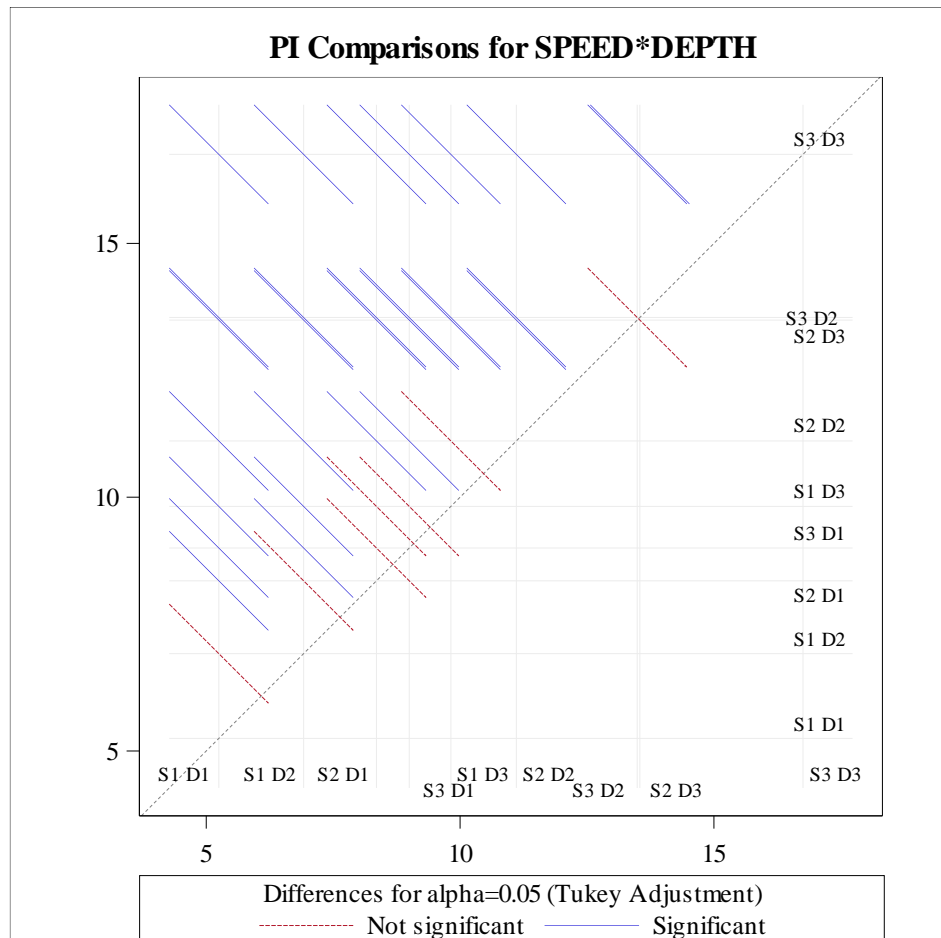


Fig 4.12 Diffiogram for the effect of forward speed and depth of operation on PI

Soil strength was measured using the cone-penetrometer at three random location in each plot as given under section 3.5.2.3. Mean Cone index at different levels of forward speed (S) and depth of operation (D) at 30°, 35° and 40° angle of attack (A) has been shown in Fig. 4.13, 4.14 and 4.15, respectively. It is evident from the figure that mean cone index increased with increase in forward speed (S) and depth of operation (D). This increasing trend of cone index with forward speed (S) and depth of operation (D) was observed at all three levels (30°, 35° and 40°) of angle of attack (A) of spading machine. The mean cone index ranged from 649.45 kPa to 1888.10 kPa for 30° angle of attack, 666.21 kPa to 1759.73 kPa for 35° angle of attack and 624.28 kPa to 1687.67 kPa for 40° angle of attack. Lowest mean cone index was observed at S1D1A1 (624.28 kPa) and highest value of mean cone index at S3D3A3 (1888.09 kPa). This may be attributed to the fact with increased forward speed (S), bite length increased with resulted in bigger sized clods of ploughed soil after tillage, this led to increase of resistance to penetration into the soil. This was observed at all levels of forward speed (2.26 km/hr, 3.37 km/hr and 4.92 km/hr). Similarly, with increase in depth of operation (D), greater volume of soil is tilled which led to bigger sized clod of ploughed soil and observed at all levels of depth of operation (20 cm, 25 cm and 30 cm). Increase in bigger sized clods, increases the force required to insert the probe into the soil thus increase cone index value.

The average values of soil strength (cone index) were measured using cone-penetrometer at different treatments combination and analysed. Analysis of variance (ANOVA) for effect of independent parameters and their combinations on cone index have been presented in Table 4.13. Statistical analysis revealed that the effect of independent parameters i.e. forward speed (S) and depth of operation (D) on cone index was statistically significant at 5% level of significance. However, angle of attack (A) was not significant at 5% level of significance. First order interaction of forward speed and depth of operation (S x D), forward speed with angle of attack (S x A) and depth of operation with angle of attack (D x A) were non-significant at 5% level of significance.

Table 4.14 ANOVA for effect of forward speed, depth of operation and attack angle on cone index of soil ploughed by spading machine.

Source	DF	Type III SS	Mean Square	F Value	Pr > F
Forward Speed (S)	2	5258001.403	2629000.701	96.85	<.0001 (S)
Depth of operation (D)	2	5665833.886	2832916.943	104.36	<.0001 (S)
Angle of attack (A)	2	93923.629	46961.815	1.73	0.1873 (NS)
S x D	4	226319.914	56579.978	2.08	0.0961 (NS)
S x A	4	108852.915	27213.229	1.00	0.4147 (NS)
D x A	4	3585.087	896.272	0.03	0.9978 (NS)
S x D x A	8	54988.634	6873.579	0.25	0.9778 (NS)

4.4.1 Effect of forward speed on soil strength

It was observed that cone index was affected by the forward speed of the machine during field experiments. Analysis of variance (Table 4.13) shows the effect of forward speed on cone index was significant at 5% level of significance. Mean values of cone index for three levels of forward speed are presented in descending order in Table 4.14.

Table 4.14 Mean values of cone index at different levels of forward speed

Forward Speed	Mean Cone index (kPa)	Comparison
S3	1528.37	A
S2	1244.07	B
S1	905.08	C

Note: Mean values with the same letter are not significantly different ($p>0.05$)

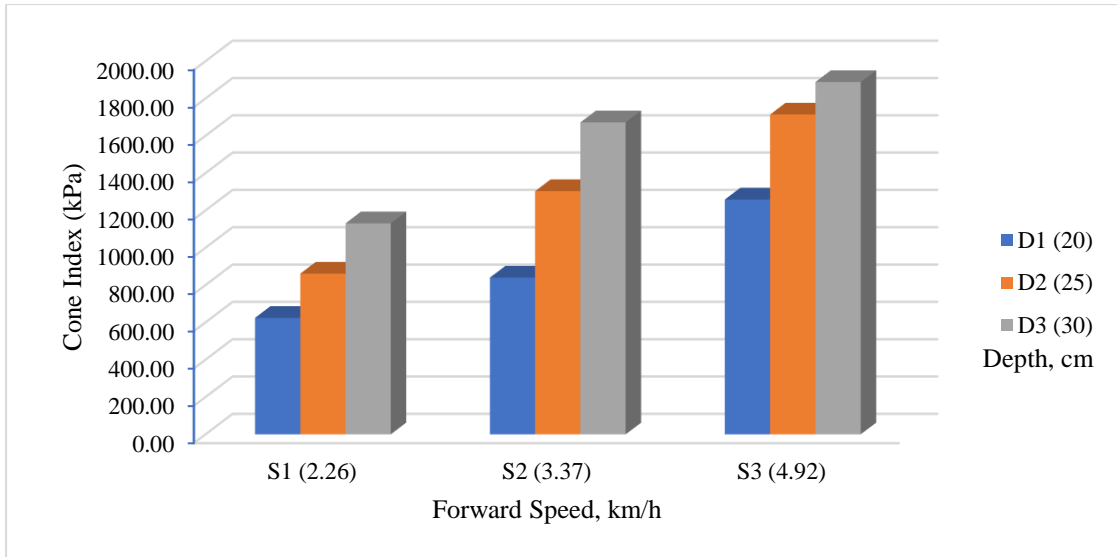


Fig. 4.13 Effect of forward speed and depth of operation at 30° angle of attack on CI

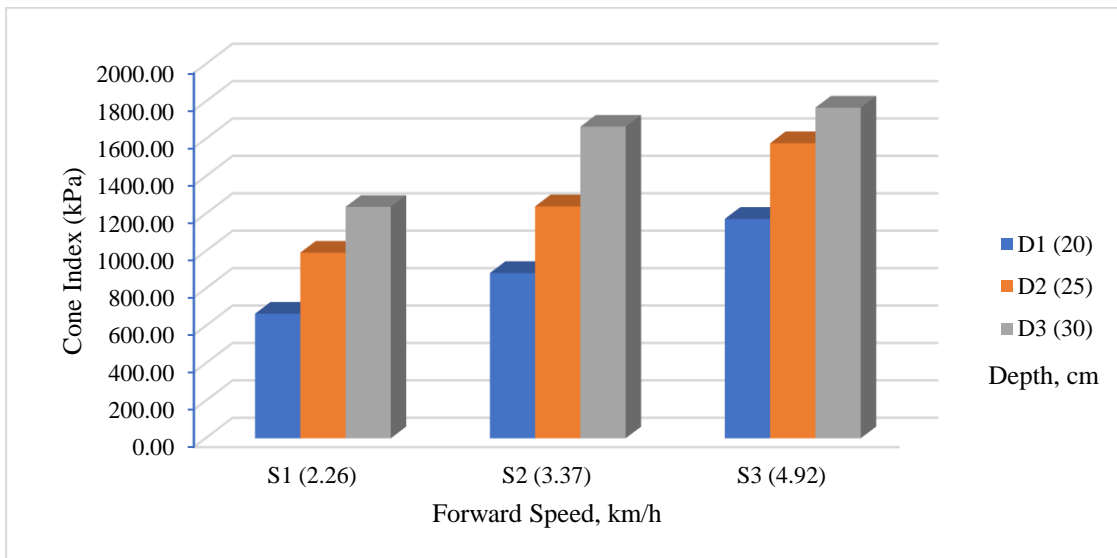


Fig. 4.14 Effect of forward speed and depth of operation at 35° angle of attack on CI

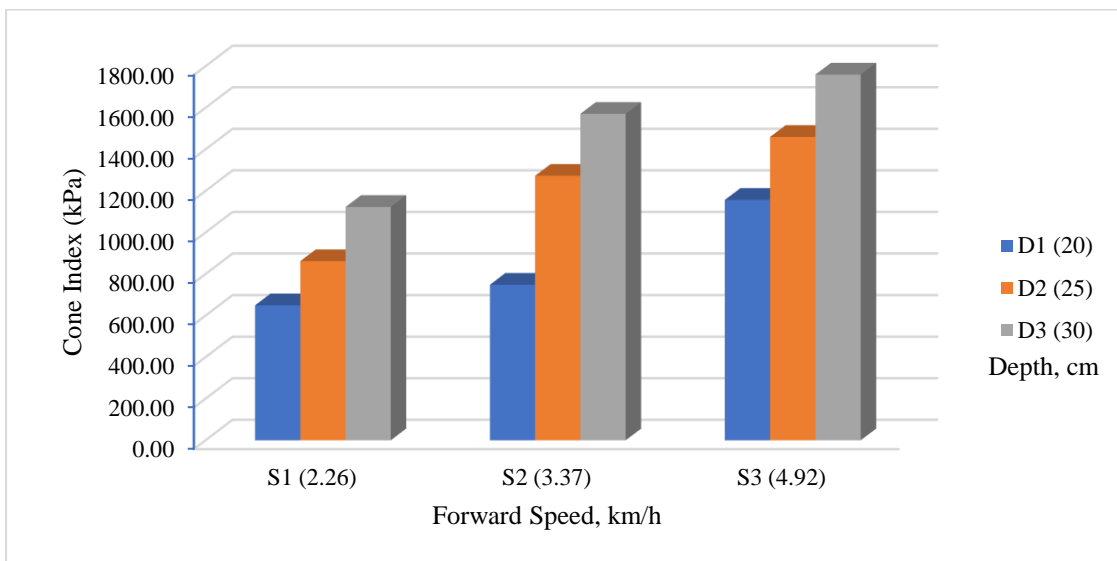


Fig. 4.15 Effect of forward speed and depth of operation at 40° angle of attack on CI

As evident in figure 4.13, 4.14 and 4.15, Cone index increased with increase in forward speed. It was maximum at forward speed S3 (1528.37 kPa) for all combination of depth of operation and angle of attack and minimum at forward speed S1 (905.08 kPa). This may be attributed to the fact that with increase in forward speed, bite length increased which lead to bigger sized clod thus increased value of cone index and also at highest forward speed, some portion of soil might have remained untilled therefore resulted in increased cone index. Similarly, at lower forward speed, bite length was low leading to better soil pulverization and lower cone index value.

4.4.2 Effect of depth of operation on soil strength

Cone index was affected by the depth of operation of spading machine. Analysis of variance (Table 4.13) also shows that the effect of depth of operation on bulk density was significant at 5% level of significance. Mean values of cone index for three levels of depth of operation are presented in Table 4.15.

Table 4.15 Mean values of cone index at different levels of depth of operation

Depth of operation	Mean Cone index (kPa)	Comparison
D3	1534.96	A
D2	1253.64	B
D1	888.92	C

Note: Mean values with the same letter are not significantly different ($p>0.05$)

As evident in figure 4.13, 4.14 and 4.15, mean cone index increased with increase in depth of operation (D). It was observed at all levels of forward speed (S) and angle of attack (A). Maximum value of depth of operation was obtained for depth D3 (1534.96 kPa) and minimum cone index for depth D1 (888.92 kPa). This was attributed to the fact that with increase in depth of operation, the volume of tilled soil increased thereby resulting in bigger clod sizes in ploughed soil. Bigger clod sizes in soil resulted in increases value of penetration resistance thus increase of value of cone index.

4.5 Operational parameters for best field performance of spading machine

Analyzing the results from the study carried out on the performance evaluation of developed tractor operated spading machine on sandy loam soil, while being operated at three forward speeds, three depths of operation and three angles of attack. It has been found that forward speed S1 (2.26 km/h), depth of operation D1 (20cm) and angle of attack A3 (40°) resulted in better soil condition and lower power requirement of the machine. This combination resulted in lowest pulverization index, PTO torque and cone index in comparison to other treatments combinations studied during the research.

CHAPTER V

SUMMARY & CONCLUSION

Crop growth requires preferred environment of soil by achieving good soil structure and air permeability which is accomplished by tillage operation (Canarache 1991). Over last many years, plough is used for this operation but in recent years, to reduce the environmental and economic impact of tillage and to obtain maximum crop production alternate solutions are developed like minimum or zero tillage thus, bringing up alternate machinery, not just plough (Hoffman 1993; Borin *et al* 1997). Tillage practices represent around half of the energy used in agricultural production (Kushwaha and Zhang, 1998) therefore, soil tilth needs to be managed by best management practice in order to reduce energy consumption. The soil failure mainly depends upon the soil properties, tool geometry and cutting speed. Nowadays over pulverisation is also one of the major problems and it influences the soil characteristics, because of which the soil results in soft and finely powdered without structure. It also causes weak soil structure thus result in loss of water holding capacity which greatly affects the soil fertility. Optimizing the design of soil tillage tools will help in improving the energy efficiency of the machine. The three design factors involved in the design of tillage tools are shape, manner of movement and the initial soil condition. Of the above three design factors, the designer has complete control only over shape. The user of a tillage tool may vary the manner of tool movement namely, the depth or speed of operation and may use the tool through a wide range of initial soil conditions. The shape of tillage tools, therefore, has received considerable emphasis since the ideal tillage tool should perform satisfactorily over wide ranges of soil conditions, depths and speeds of operation. There are many studies done on soil-tool interaction and field performance of various implements mooting various parameters like soil condition before and after treatment, tool shape and speed, draft and power take-off (PTO) requirement of the driven implements (Perdok and Kouwenhoven 1994).

Primary advantage of spading machine as compared to the other ploughing methods is that it doesn't create compact layer at the bottom of tilled soil and it has zero draft requirement (Gasparetto 1966). It is attached to 3-point hitch of tractor and operated with tractor PTO. Spading machine mimics the movement of hand digging tool for better soil aeration, mixing of organic matter and deeper operation. As the spades penetrates the soil at an angle to the soil surface, therefore there is no problem of hardpan of soil. Saimbhi (2006) developed a prototype of articulated tillage machine (spading machine) to compare its performance with rotary tillage machine and found that there was 43% of power and 44% of energy saving in soil metal friction resulting in saving in energy requirement but also leave the field with reasonable mechanical impedance for crop production. Study has been done on the performance of different shapes of

spades, thus leads to trapezoidal shape spade giving best results (Dogra *et al* 2017). The spades are attached on the end of connecting rods which form an articulated quadrilateral mechanism. The spades cut slice of soil and launch it behind the machine thus crumbling it.

An 8-spade indigenous spading machine was designed, developed and evaluated for its performance in field. The machine was designed for a 50hp tractor. Analytical analysis of four-bar mechanism was conducted and the link length were optimized using motion simulation software. Theoretical design of the spading machine was completed and its 3-D model was developed in CAD software. The spading machine was fabricated and assembled with the help of a local manufacturer. Field evaluation of the developed spading machine was conducted in sandy loam soil at departmental research farms. There were three independent parameter each at three levels of forward speed (S1= 2.26 km/h, S2= 3.37 km/h and S3= 4.92 km/h), depth of operation (D1= 20 cm, D2 = 25 cm and D3= 30 cm) and angle of attack (A1= 30°, A2= 35° and A3= 40°). Field trial was laid out in a factorial randomized block design with three replications each treatment. The performance was studied on following selected dependent variables: bulk density, PTO torque, clod size distribution, cone index and soil moisture were studied. Data collected for all the dependent variables were subjected for analysis of variance in factorial randomized block design using SAS 9.2 software package. Following conclusions were drawn from these studies:

1. Link lengths of crank-rocker mechanism was optimized using dynamic analysis simulation software. The optimized link length for crank, coupler, rocker and frame are 150 mm, 388 mm, 279 mm and 436 mm, respectively.
2. Bulk density increased with increase in forward speed (S) and depth of operation (D) while there was no effect of angle of attack (A) observed on bulk density of tilled soil. The effect of on forward speed (S) and depth of operation (D) on bulk density were found to be significant at 5% level of significance while angle of attack had no significant effect on bulk density.
3. Maximum mean bulk density for forward speed (S) was 1.49 Mg/m³ at 4.92 km/h (S3) and minimum 1.25 Mg/m³ at 2.26 km/h (S1) whereas, maximum mean bulk density for depth of operation (D) was 1.41 Mg/m³ at 30 cm depth of operation (D3) and minimum 1.32 Mg/m³ at 20 cm depth of operation (D1), respectively.
4. Mean bulk density varied from 1.17 Mg/m³ to 1.51 Mg/m³ for 30° angle of attack, 1.18 Mg/m³ to 1.52 Mg/m³ for 35° angle of attack and 1.20 Mg/m³ to 1.54 Mg/m³ for 40° angle of attack.
5. Treatment combination S3D3A3 generated maximum mean bulk density (1.54 Mg/m³) and it was S1D1A1 minimum mean bulk density (1.17 Mg/m³).

6. PTO torque increased with increase in forward speed (S) and depth of operation (D) while there was no effect of angle of attack (A) observed. The effect of PTO torque for forward speed (S) and depth of operation (D) were found to be significant at 5% level of significance while angle of attack had no significant effect on PTO torque.
7. Maximum mean PTO torque for forward speed (S) was 514.96 Nm at 4.92 km/h (S3) and minimum 357.31 Nm at (S1) whereas, maximum mean PTO torque for depth of operation (D) was 459.96 Nm at 30 cm depth of operation (D3) and minimum 414.11 Nm at 20 cm depth of operation (D1), respectively.
8. Mean PTO torque varied from 339.07 Nm to 550.78 Nm for 30° angle of attack, 333.54 Nm to 541.71 for 35° angle of attack and 327.67 Nm to 536.33 Nm for 40° angle of attack.
9. Treatment combination S3D3A1 gave maximum mean PTO torque 550.78 Nm and S1D1A3 had minimum mean PTO torque 327.67 Nm and also significantly different from all other treatment combination.
10. Pulverization index increased with increase in forward speed (S) and depth of operation (D) while there was no effect of angle of attack (A). The effect of PTO torque for forward speed (S) and depth of operation (D) were found to be significant at 5% level of significance while angle of attack had no significant effect on pulverization index.
11. Maximum mean pulverization index for forward speed (S) was 13.57 mm at 4.92 km/h (S3) and minimum 7.64 mm at 2.26 km/h (S1) whereas, maximum mean pulverization index for depth of operation (D) was 14.47 mm at 30 cm depth of operation (D3) and minimum 7.89 mm at 20 cm depth of operation (D1).
12. Mean pulverization index varied from 5.21 mm to 18.20 mm for 30° angle of attack, 4.77 mm to 16.71 mm for 35° angle of attack and 3.68 mm to 15.80 mm for 40° angle of attack.
13. Treatment combination S3D3A1 gave maximum mean pulverization index 18.20 mm and S1D1A3 gave minimum mean pulverization index 3.68 mm and are significantly different from all other treatment combination.
14. Cone index increased with increase in forward speed (S) and depth of operation (D) for all angle of attacks (A). The effect of PTO torque for forward speed (S) and depth of operation (D) were found to be significant at 5% level of significance while angle of attack had no significant effect on cone index value.
15. Maximum mean cone index for forward speed (S) was 1528.37 kPa at 4.92 km/h (S3) and minimum 905.08 kPa at (S1) whereas, maximum mean cone index for depth of operation (D) was 1534.96 kPa mm at 30 cm depth of operation (D3) and minimum 888.92 kPa at 20 cm depth of operation (D1), respectively.

16. Mean cone index varied from 649.45 kPa to 1888.10 kPa for 30° angle of attack, 666.21 kPa to 1759.73 kPa for 35° angle of attack and 624.28 kPa to 1687.67 kPa for 40° angle of attack.
17. Treatment combination S3D3A1 gave maximum mean cone index 1888.09 kPa and S1D1A3 minimum mean cone index 624.28 kPa and are significantly different from all other treatment combination.
18. Best soil tilth and minimum PTO torque was observed amongst the studied range of operational variables at forward speed S1 (2.26 km/h), depth of operation D1 (20cm) and angle of attack A3 (40°).

Suggestions for future work

There is a scope of examine the machine performance under different conditions and improving the performance in fields under different soil types by incorporating the following suggestions in the present machine

1. A study should be conducted on variable speed gearbox so that the crank revolution can be changed and its effect on the performance.
2. Spading machine field performance comparison on different soil types and different levels of moisture content.
3. Study on analyzing the vibration occurred during the operation under different conditions.
4. Evaluation of different types of blades and its effect on machine performance in field.

REFERENCES

- Abrougui K, Boukhalfa H H , Elaoud A ,Louvet J N , Destain M F and Chehaibi S (2014) Effects of Three Tillage Systems on Physical Properties of a Sandy Loam Soil. *International Journal of Current Engineering and Technology*. 4:3555-3561.
- Aday S H and Nassir A J (2009) Field study of a modified chisel plow performance on the specific and equivalent energy and energy utilization efficiency. *Bassrah J. Agric.* **22**:95-108.
- Ahaneku I E and Ogunjirin O A (2005) Effect of tractor forward speed on sandy loam soil physical conditions during tillage. *Nigerian Journal of Technology* **24**: 51-57.
- Alnahas S A M E (2003) Tillage implements performance and their effects on two types of Soil in Khartoum area. Master's dissertation. University of Khartoum, Sudan.
- Baraldi G and Pezzi F (1987) Technical characteristics and performances of the diggers. *Inf Agr* **40**:45-51.
- Belel M M and Dahab M H (1997) Effect of soil condition on a two – wheel drive tractor performance using three types of tillage implements. *Journal of Agricultural Sciences* **5**:1–20.
- Bishnoi R (2008) *Development and evaluation of blades for spading machine*. Ph.D. Dissertation. Punjab Agricultural University, Ludhiana, India.
- Borin M, Menini C and Sartori L (1997) Effects of tillage systems on energy and carbone balance in north-eastern Italy. *Soil & Tillage Research* **40**:209-26.
- Bronick C J and Lal R (2005) Soil structure and management: a review. *Geoderma* **124**:3-22.
- Brzozko J and Murawski P (2007) Effect of soil loosening depth on power requirement for driving the spading machine “Gramegna”. *Annals of Warsaw University of Life Science – SGGW Agriculture* **51**:59-64.
- Bunemann E K, Bongiorno G, Bai Z, Creamer R E, Deyn G D and Goede R D (2018) Soil quality: a critical review. *Soil Biol Biochem* **120**:105–125.
- Busscher W and Bauer P (2003) Soil strength, cotton root growth and lint yield in a south eastern USA coastal loamy sand. *Soil Tillage Res.* **74**:151–159.
- Canarache A (1991) Factors and indices regarding excessive compactness of agricultural soils. *Soil and Tillage Research* **19**:145–164.
- Choi C H and Nahmgung M J (2000) Load Measurement of Tractor on Field Performance. *Proceedings of the KSAM 2000 summer conference*. **25**:29–34.
- Dahab M H (2011) Effect of selected tillage implements on physical properties of two types of soils in Khartoum area (Sudan). *AMA* **45**:9-13.

- Daraghmeh O, Petersen C, Munkholm L, Znova L A, Obour P B, Nielsen S K and Green O (2019) Impact of tillage intensity on clay loam soil structure. *Soil use and management* **35**:247-248.
- Desbiolles J M A, Godwin R J, Kilgour J and Blackmore B S (1999) Prediction of Tillage Implement Draught using Cone Penetrometer Data. *J. Agric. Engg. Res.* **73**:65-76.
- Dhiman M (2016) *Performance evaluation of tractor operated spading machine*. Master's dissertation. Punjab Agricultural University, Ludhiana, India.
- Dimassia B, Cohan J P, Labreucheb J and Marya B (2013) Changes in soil carbon and nitrogen following tillage conversion in a long-term experiment in Northern France. *Agriculture Ecosystem Environment* **16**:12-20.
- Dogra R, Dogra B, Gupta P K, Sharma B D and Kumar A (2017) Effect of spade angle and spading frequency of spading machine on specific soil resistance and pulverization. *Agricultural Engineering International: CIGR Journal*. **19**:65-73.
- Drewry J J, Cameron K C, and Buchan G D (2008) Pasture yield and soil physical property responses to soil compaction from treading and grazing: a review. *Aust J Soil Res* **46**:237–256.
- El-Haddad Z A, El-Ansary M Y and Tohamey M T M (1995) Identifying a proper seedbed preparation system using locally manufactured machinery. *Misr. J. Agric. Eng.* **12**:36-45.
- Fechete L V T, Gaspar F and Gyorgy Z (2019) Soil-tool interaction of a simple tillage tool in sand. *Sustainable Solutions for Energy and Environment* **85**:1-6.
- Gasparetto E (1966) Kinematics and dynamics of articulated quadrilateral digging machines. *ISMA* **17**:3-33.
- Gill W R and Vandenberg G E (1968) *Soil dynamics in tillage and traction*. Pp. 211-297 Agricultural Research Service. USDA, Washington, USA.
- Giordano D M, Facchinetti D and Pessina D (2015) The spading machine as an alternative to the plough for the primary tillage. *Journal of Agricultural Engineering* **46**: 36-40.
- Hoffman M (1993) The spading machine A substitute for the plough in ecological farming. *Landtechnik* **48**:29-31.
- Hu W, Tableya F, Bearea M, Tregurtha C, Gillespie R, Qiu W and Gosden P (2018) Short-term dynamics of soil physical properties as affected by compaction and tillage in a silt loam soil. *Vadose Zone Journal* **17**:0-13.
- Hunt D (2013) *Farm Power and Machinery Management*. Waveland Press, Dublin
- Hunt N and Gilkes B (1992) *Farm Monitoring Handbook*. The University of Western Australia. Nedlands, WA.
- Jeavons J C (2001) Biointensive mini-farming. *Journal of Sustainable Agriculture* **19**:81-83.

- Jian S (2015) Analysis and Optimization of the Transmission Angle of Crank Rocker Mechanism. *Proceedings of the 2015 International Conference on Mechatronics, Electronic, Industrial and Control Engineering*. Atlantis Press.
- Khorami S S, Kazemeini S A, Afzalnia S and Gathala M K, (2018) Changes in soil properties and productivity under different tillage practices and wheat genotypes: a short-term study in Iran. *MDPI Open Access Journal* **10**:1-17.
- Khurmi R S and Gupta J K (2005) *A Textbook of Machine Design*. Eurasia Publishing House, New Delhi.
- Kim D C, Nam J S, Kim M H, Choe J S, Inoue E, Okayasu T and Kim D C (2013) Analysis of the tillage and power consumption characteristics of a crank-type rotavator according to the tillage blade shape. *J Fac Agr* **58**:319–328.
- Kim D C, Park Y J and Lee G H (2015) Fatigue life prediction of crank-type rotavator. *Journal of Biosystems Engineering* **40**:305-313.
- Kim Y J, S O Chung, C H Choi and D H Lee (2011) Evaluation of tractor PTO severances during rotary tillage operation. *Jl of Biosystems Engineering* **36**:163–170.
- Kumar A (2017) *Evaluation of soil compaction as affected by different tillage practices*. Master's Dissertation. Punjab Agricultural University, Ludhiana, India.
- Kumar A, Chen Y, Sadek A and Rahman S (2012) Soil cone index in relation to soil texture, moisture content, and bulk density for no-tillage and conventional tillage. *Agric Eng Int: CIGR* **14**:26-37
- Kushwaha R L and Zhang Z X (1998) Evaluation of factors and current approaches related to computerized design of tillage tools: a review. *J Terramechanics* **35**:69–86.
- Kwon T H, Araghi A A, Lee C, Kang T G, Lee B M and Rhee J Y (2014) Evaluation of a crank-type walking cultivator for upland farming. *Journal of Biosystems Engineering* **39**:1-10.
- Lal R (1995) *Tillage Systems in the Tropics: Management Options and Sustainability Implications*. FAO, Rome, Italy.
- Lamande M, and P Schjønning (2018) Soil mechanical stresses in high wheel load agricultural field traffic: a case study. *Soil Res* **56**:129–135.
- Logsdon S E and Kaspar T C (1995) Tillage influences as measured by ponded and tension infiltration. *Journal of Soil and Water Conservation* **50**:571-575.
- McKyes E (1985) *Soil Cutting and Tillage*. 217-237. Elsevier.
- Moeenifar A, Mousavi-Seyedi S R and Kalantari D (2014) Influence of tillage depth, penetration angle and forward speed on the soil/thin-blade interaction force. *Agric Eng Int* **16**:69-73.
- Mohler C L, Frisch J C and McCulloch C E (2006) Vertical movement of weed seed by tillage implements and natural processes. *Soil and Tillage Research* **86**:110-22.

- Myszka D H (2012) *Machines and mechanisms: Applied kinematic analysis*. Prentice Hall, New Jersey.
- Naderloo L, R Alimadani, A Akram, P Javadikia and H Zeinali Khanghah (2009) Tillage depth and forward speed effects on draft of their primary tillage implements in clay loam soil. *Journal of Food, Agriculture & Environment* **7**:382–385.
- Nam J S, Kim D C, Kim M H and Kim D C (2012) Tillage Characteristics Estimation of Crank-type and Rotary-type Rotavators by Motion Analysis of Tillage Blades. *Journal of Biosystems Engineering* **37**:279-286.
- Nam Ju-Seok, Kang Dae-Sig, Kang Young-Sun , Kim Kyeong-Uk and Dae-Cheol Kim (2012) Comparison of Work Performance of Crank-type and Rotary-type Rotavators in Korean Farmland Conditions. *Journal of Biosystems Engineering* **37**:140-147.
- National Institute of Agricultural Engineering (2004) *Experimental and research report Suwan*: National Institute of Agricultural Engineering.
- Oduma O, Oluka S I and Eze P C (2018) Effect of soil physical properties on performance of agricultural field machinery in south eastern Nigeria. *Agricultural Engineering International: CIGR Journal* **20**:25-31.
- Okyere R G, Moon B E, Qasim W, Basak J K, Kahn F, Kang D S, Yoon Y C and Kim H T (2018) Tillage operational analysis based on soil moisture content, machine speed, and disc space of compact disc harrow. *Journal of Biosystems Engineering* **43**:161-172.
- Olatunji O M, Burubai W I and Davies R M (2009) Effect of weight and draught on the performance of disc plough on sandy loam soil. *Journal of Applied Sciences, Engineering and Technology*.**1**:22- 26.
- Perdok U D and Kouwenhoven J K (1994) Soil-tool interactions and field performance of implements. *Soil & Tillage Research* **30**:283-326.
- Pezzi F (2005) Traditional and new deep soil tillage techniques in Italy. *Transactions of the ASAE* **48**:13-17.
- Reynolds W D, Drury, C F Yang X M, Fox C A, Tan C S and Zhang T Q (2007) Land management effects on the near-surface physical quality of a clay loam soil. *Soil & Tillage Research* **96**:316–330.
- Rider J M (2015) *Design and Analysis of Mechanisms*. Wiley, UK.
- Saimbhi V S (2006) *Computer based development and field evaluation of articulated tillage machine*. Punjab Agricultural University, Ludhiana, India.
- Sale N A, Gwarzo M A, Felix O G and Idris S I (2013) Performance evaluation of some selected tillage implements. *Proceeding of Nigeria Institution of Agricultural Engineers (NIAE)*. **34**: 71-77.
- Sharma D N and Mukesh S (2018) *Farm Machinery Design (Principles and Problems)*. Jain Brothers, New Delhi.

- Shmulevich I (2010) State of the modelling of soil–tool interaction using discrete element method. *Soil and Tillage research* **111**:41-53.
- Shmulevich I, Asaf Z and Rubinstein D (2007) Interaction between soil and a wide cutting blade using the discrete element method. *Soil & Tillage Research* **97**:37–50.
- Singh J, Salaria A and Kaul A (2015) Impact of soil compaction on soil physical properties and root growth: a review *International Journal of Food, Agriculture and Veterinary Sciences* **5**:3-32.
- Singh R, Serawat M, Singh A and Babli (2018) Effect of tillage and crop residue management on soil physical properties. *Journal of Soil Salinity and Water Quality* **10**:200-206.
- Taniguchi T, Makanga J T, Ohtomo K and Kishimoto T (1999) Draft and soil manipulation by a moldboard plow under different forward speed and body attachments. *Transactions of ASABE*. **42**:1517-1521.
- Varsa E C, S K Chong, J O Aboaji, D A Farquhar and F J Olsen (1997) Effect of deep tillage on soil physical characteristics and corn (*Zea mays* L) root growth and production. *Soil and Tillage Research* **43**:219–228.
- Whalley W R, To J, Kay B D and Whitmore A P (2007) Prediction of the penetrometer resistance of soils with models with few parameters. *Geoderma*. **137**:370–377.
- Yassen H A, Hassan H M and Hammadi I A (1992) Effects of plowing depth using different plow types on some physical properties of soil. *AMA* **23**:21-24.
- Ye X, Ye Y, Chai R, Li J, Ma C, Li H, Xiong Q and Gao H (2019) The influence of a year-round tillage and residue management model on soil N fractions in a wheat-maize cropping system in central China. *Scientific Reports (Nature)* **9**:47-67.
- Yoo C H, J H Ryu, C H Yang, T K Kim, S W Kang, J D Kim and K Y Jung (2006) Influence of diagnostic fertilization and subsoil breaking on soil physico–chemical properties in direct seeding of rice on flooded paddy surface. *Journal of Korean Society of Soil Science and Fertilizer* **39**:334–338.

APPENDIX B

Detail and specification of Torque transducer instrument used

Appendix B1: Detail Torque transducer (Torque Trak)

Torque Telemetry System

The TorqueTrak Torque Telemetry System utilizes digital RF technology to transmit a single data signal a distance of 6 meters or more depending on the environment. The TorqueTrak is a robust, precision strain measurement instrument ideal for short-term data collection and diagnostic testing. The system, comprised of three main components:

1. RX10K Receiver

The RX10K Receiver features a simple keypad on the front panel for user configuration and adjustment. A two-line display indicates the operational status of the RX10K. The RX10K outputs the signal received from the TX10K-S Transmitter in three ways: a) as text and graphics on the display, b) as an analog voltage signal and c) as a digital data signal.

2. TX10K-S Transmitter

The TX10K-S transmitter is encased in a tough nylon housing. The TX10K-S also features a status indicator light, an infrared receiver lens, a transmitter antenna connector, and a screw terminal block for making power and sensor input connections. The TX10K-S can be configured even while it is installed (but not rotating) using the RM10K Remote Control. The TX10K-S has sixteen RF Channel settings and six Gain settings (500, 1000, 2000, 4000, 8000, and 16000). It can send low and high reference signals to the RX10K: internal precision shunt resistors simulate strain values that can be used to check calibration (refer to Appendix A for specifications). The TX10K-S will operate at short distances from the Receiver Antenna without the Transmitter Antenna installed if space around the shaft is limited.

3. RM10K Remote Control (for TX10K-S Transmitter)

It is used to change transmitter setup without tools or removal from shaft. Infrared signal transmits up to 6 meters. The RM10K keypad operates similar to a common TV remote control, emitting an infrared signal through the window on the front of the unit.

Appendix B2: Specification of Torque transducer used

Sr. No.	Part/ Features	Specification
TorqueTrak 10K Telemetry System		
1.	Resolution	14 bits
2.	Sample transmission rate	2400 Hz
3.	Signal bandwidth	500 Hz (-3dB)
4.	Signal to noise ratio	67 dB (min)
5.	Signal delay	4.2 mS
6.	RF transmission distance	6 m line-of-sight
TT10K-S Transmitter		
7.	Power supply voltage	7 to 18 V dc
8.	Power supply current Transmit mode Standby mode	40 mA (nom), 50 mA (max) 4 mA (nom), 5 mA (max)
9.	Bridge excitation voltage	2.50 VDC ($\pm 0.1\%$, 10ppm/ $^{\circ}\text{C}$)
10.	Available output current	20 mA (max) to sensor
11.	Input voltage range ($\pm S$ to $-E$)	0.2 to 3.9 V
12.	Antenna connection	Reverse SMA
13.	G-force	3000 G's (max continuous)
14.	Operating temperature range	-30 to 85 $^{\circ}\text{C}$
RM10K Remote Control		
15.	Power supply	9 V battery
16.	Pulsed infrared frequency	38 KHz
17.	Transmission distance (line-of-sight) Normal mode High power mode	15 mm 3 m
18.	Operating temperature range	20 to 60 $^{\circ}\text{C}$
19.	Size	22 mm x 63 mm x 112 mm

RX10K Receiver		
20.	Analog voltage output signal Nominal range Maximum range	± 10 V ± 12 V
21.	Display	2-line x 20 character high contrast LCD with backlight
22.	Power input	10 to 18 VDC @ 300mA (max)
23.	Antenna input connection	SMA
24.	Power input connector	2.1 mm jack (5.5 mm x 2.1 mm plug)
25.	Operating temperature range	-20 to 70°C (- 4 to 158°F)
26.	Size	73 mm x 146 mm x 216 mm

APPENDIX C

Specification of Cone Penetrometer used

Sr. No.	Part/ Feature	Specification
1.	Model	Rimik CP II
2.	Type	Load Cell
3.	Weight (assembled without GPS), kg	3.9
4.	Dimensions (assembled without GPS), mm	560 x 1073 x 130
5.	Maximum Small Cone Index (kPa,kg)	5600, 75
6.	Maximum Large Cone Index (kPa,kg)	2200, 75
7.	Resolution, kg	0.03
8.	Maximum Insertion Depth, mm	750
9.	Interval Spacing, mm	10, 15, 20, 25
10.	Memory Capacity (no. of insertions)	2047
11.	Battery Life, mAh	3000
12.	Small Cone Size (dia.mm, area,mm ²)	12.83, 130
13.	Large Cone Size (dia.mm, area,mm ²)	20.27, 323
14.	Shaft Diameter, mm	9.53
15.	Cone angle, degree	30

VITA

Name of the student : Nitin Karwasra
Father's name : Dr. Jagdish Chander Karwasra
Mother's name : Smt. Saroj Karwasra
Nationality : Indian
Date of birth : 7th May, 1990
Permanent home address : 800, Sector-15a, Hisar, Haryana

EDUCATIONAL QUALIFICATIONS

Bachelor degree : B.Tech. (Agriculture Engineering)
University : CCS Haryana Agricultural University, Hisar
Year of award : 2012
OCPA : 6.93/10.00
Master's degree : M.Tech. (Farm Machinery and Power Engineering)
University : CCS Haryana Agricultural University, Hisar
Year of award : 2014
OCPA : 8.02/10.00
Title of Master's Thesis : Application of Artificial Neural Network for
Prediction of Tractor Performance
Doctoral degree : Ph.D. (Farm Machinery and Power Engineering)
University : Punjab Agricultural University, Ludhiana
Year of award : 2020
OCPA : 7.81
Title of Doctoral Dissertation : Design, Development and Evaluation of Tractor
Operated Spading Machine